DESIGN AND IMPROVEMENT OF UNDERRUN PROTECTION DEVICE FOR TRUCK

NARONGRIT SUEBNUNTA

A THESIS SUBMITTED IN PARTIAL FULFILLMENT

OF THE REQUIREMENT FOR THE DEGREE OF

MASTER OF ENGINEERING IN AUTOMOTIVE ENGINEERING

SCHOOL OF ENGINEERING

KING MONGKUT'S INSTITUTE OF TECHNOLOGY LADKRABANG

2023

KMITL-2023-EN-M-037-094

หัวข้อวิทยานิพนธ์	การออกแบบและปรับปรุงอุปกรณ์ป้องกันการมุดสำหรับรถบรรทุก
นักศึกษา	นาย ณรงค์ฤทธิ์ สืบนันตา
รหัสประจำตัว	61610003
ปริญญา	วิศวกรรมศาสตร์มหาบัณฑิต
สาขาวิชา	วิศวกรรมยานยนต์ (หลักสูตรนานาชาติ)
อาจารย์ที่ปรึกษาวิทยานิพนธ์	รศ. ดร. ปรีชา การินทร์
อาจารย์ที่ปรึกษาวิทยานิพนธ์ร่วม	ดร. ศราวุธ เลิศพลังสันติ
อาจารย์ที่ปรึกษาวิทยานิพนธ์ร่วม	Prof.Dr. Masaki Okuma

บทคัดย่อ

หนึ่งในอุบัติเหตุที่ร้ายแรงที่สุดบนท้องถนนซึ่งเกิดขึ้นเนื่องจากรถชนท้ายคือรถยนต์นั่งส่วนบุคคลชนท้ายรถบรรทุก วิธีหนึ่งในการลดการบาดเจ็บและเสียชีวิตจากอุบัติเหตุประเภทนี้คือการติดตั้งอุปกรณ์ป้องกันด้านท้ายรถ (RUPD) บนรถบรรทุก งานวิจัยนี้มีวัตถุประสงค์เพื่อสร้างแนวทางการออกแบบและการตรวจสอบความถูกต้องของการวิเคราะห์ความแข็งแรงของโครงสร้างของอุปกรณ์ป้องกันใต้ทางด้านหลัง (RUPD) โดยใช้การทดสอบกึ่งสถิตและการวิเคราะห์องค์ประกอบไฟไนต์เอลิเมนต์ตามมาตรฐาน UN regulation No.58 แนวทางการออกแบบที่คาดหวังจะศึกษาพารามิเตอร์การออกแบบที่สำคัญ เช่น ประเภทของหน้าตัดและความหนาของส่วนประกอบของ RUPD เป็นต้น การตรวจสอบความถูกต้องของแบบจำลองคานป้องกัน การศึกษาเกณฑ์มาตรฐานของ RUPD เชิงพาณิชย์สองรุ่นเป็นไปตามระเบียบข้อบังคับของ UN regulation No.58 และการออกแบบ RUPD ที่คาดหวังได้ดำเนินการตามแนวทางการออกแบบที่นำเสนอ การวิเคราะห์ไฟไนต์เอลิเมนต์เพื่อแสดงให้เห็นถึงความแข็งแรงทางโครงสร้างของโมเดล RUPD ทั้งหมดได้ใช้การวิเคราะห์ไดนามิกไฟไนต์เอลิเมนต์ที่ไม่เป็นเชิงเส้นอย่างชัดเจนใน RADIOSS การศึกษาพบว่าการเสียรูปและประสิทธิภาพการรับน้ำหนักของโมเดล RUPD แบบพับได้หลายรุ่นผ่านตามข้อกำหนด ท้ายที่สุดเลือกแบบจำลอง RUPD ที่มีประสิทธิภาพสูงสุดในแง่ของอัตราส่วนแรงต่อน้ำหนักปฏิกิริยาและน้ำหนักต่ำสุด การค้นพบนี้ให้ข้อมูลเชิงลึกเกี่ยวกับประสิทธิภาพของโมเดลทั้งหมดและสามารถใช้เป็นแนวทางสำหรับ RUPD ประเภทอื่นๆ ได้

Thesis	Design and Improvement of Underrun Protection Device for Truck
Student	Mr. Narongrit Suebnunta
Student ID.	61610003
Degree	Master of Engineering
Program	Automotive Engineering (International Program)
Year	2023
Thesis Advisor	Assoc.Prof.Dr. Preechar Karin
Co-Thesis Advisor	Dr.-Ing. Sarawut Lerspalungsanti
Co-Thesis Advisor	Prof.Dr. Masaki Okuma

ABSTRACT

One of the most fatal accidents on the road that occurs due to a rear underrun is a passenger car crashing into the rear of a truck. One solution to reduce injury and death from this type of accident is installing a rear underrun protective device (RUPD) on the truck. This research aims to establish a design guideline and validate the structural strength analysis method of a rear underrun protective device (RUPD) using a quasi-static test and finite element analysis according to the UN regulation No.58 standard. The proposed design guidelines investigate significant design parameters, such as the type of cross-section and component thickness of the RUPD. Validating of protective beam model, A benchmark study of two models of commercial RUPDs satisfied the UN regulation No.58 regulation and the proposed RUPD design was carried out following the presented design guideline. The finite element analysis to demonstrate the structural strength of all RUPD models is achieved using non-linear explicit dynamic finite element analysis in RADIOSS. The study found the deformations and load-bearing performance of several foldable RUPD models met the requirements. Finally, the RUPD model with the highest performance in terms of reaction force-to-weight ratio and lowest weight was selected. These findings provide insight into the performance of all models and can serve as guidelines for other types of RUPDs.

ACKNOWLEDGEMENT

I would like to express my sincere thank you to my NSTDA advisor, Dr.-Ing. Sarawut Lerspalungsanti and KMITL advisor, Assoc.Prof.Dr. Preechar Karin, for allowing me to do research and providing invaluable guidance throughout this research. Their vision, advice, and knowledge have intensely inspired me. This thesis would not have been completed without all the support that I have always received from them.

I would like to thank Thailand Advance Institute of Science and Technology, Tokyo Institute of Technology (TAIST-Tokyo Tech), and National Science and Technology Development Agency (NSTDA) for providing full scholarship and financial support. I would like to thank Vehicle and Driving Technology Laboratory, National Metal and Material Technology Center (MTEC) for instruments and materials used for this research success.

Finally, I am most grateful to my family and my friends for all their support throughout the period of this research.

Narongrit Suebnunta

TABLE OF CONTENTS

TABLE OF CONTENTS (CONT.)

LIST OF TABLES

Table **Page**

LIST OF FIGURES

Figures **Page**

LIST OF FIGURES (CONT.)

Figures **Page**

LIST OF FIGURES (CONT.)

Figures **Page**

LIST OF FIGURES (CONT.)

Figures **Page**

CHAPTER 1

INTRODUCTION

1.1 Research Background

Between 2004 and 2008 in the United States, truck traffic accidents accounted for 16.5% of fatalities, with 74.7% of deaths involving other vehicles [1]. In 2016, the World Health Organization reported that Thailand had a staggering 32.7 deaths per 100,000 population resulting from road accidents, totaling 22,491 deaths [2]. One of the most severe types of road accidents involves passenger vehicles colliding into the rear of trucks due to factors such as driver fatigue, emergency lane changes, and nighttime truck parking. This type of accident is particularly severe due to the vast differences in geometry, size, and mass between the two vehicles. In such incidents, the height of a passenger car is lower than that of a truck, causing the former to potentially slide underneath the latter during a rear-end collision. Moreover, the A-pillar of the passenger car typically serves as the first point of contact with the rear of the truck but is generally not designed to withstand the significant impact forces generated during such collisions. As a result, the height of the rear of the truck is often level with the head of the passenger car driver, leading to direct and potentially fatal impacts between the driver's head and the truck's rear body. As a result, drivers of passenger vehicles stand a significantly increased risk of death in such accidents.

An effective solution to mitigate the risk of injury and fatality resulting from rear-end collisions between passenger cars and trucks is the installation of a rear underrun protective device (RUPD) on the rear end of the truck. The RUPD serves to prevent the cabin space of the passenger car from directly colliding with the rear of the truck. This device is engineered to interact with the crumple zone of the passenger car, which is designed to absorb a significant amount of impact energy during a collision. To effectively absorb the energy of a collision and stop the passenger car, the RUPD must be sufficiently strong. When combined with the crumple zone, airbag, and seatbelt of the passenger car,

the RUPD functions to significantly reduce the severity of a collision and minimize the potential for injury or fatality. However, the RUPD must meet safety standards to effectively prevent accidents and minimize the occurrence of injuries and fatalities.

The widely used standard concerning rear underrun protective devices, which is relevant to the accident, is the UN regulation No.58 standard. It includes requirements for static testing load in each position, cross-sectional height, and device location. These tests can be conducted through actual testing or finite element analysis, depending on the factory's requirements [3]. However, actual testing requires a suitable test site, prototyping costs, and testing expenses, making it a significant investment. On the other hand, finite element analysis can reduce both time and costs while allowing for testing on various designs. Several researchers have conducted simulation tests on fixed RUPDs using techniques like trial and error, Pareto optimization, and morphological analysis. Some have used LS-DYNA, while others have used RADIOSS [4-6]. One researcher investigated the process of designing foldable RUPDs to address issues such as interference during tripping and varying departure angles for trucks [7]. Another researcher conducted a quasi-static test on five RUPD models attached to the trailer chassis [8], while another tested sedan cars at a speed of 48 km/h crashing into RUPDs attached to a fixed barrier [9].

The UN regulation No.58 standard has not been enforced in Thailand yet. Although some trucks have already installed Rear Under-Run Protection Devices (RUPD), their characteristics do not meet the standard criteria. Dump trucks face limitations in installing RUPD due to small installation space and obstructing material pouring, resulting in almost no installation of this device on these trucks in Thailand. As the law has not been enforced, truck manufacturers and users are reluctant to add equipment that would increase the weight by more than a hundred kilograms, leading to higher shipping costs. However, the implementation of the UN regulation No.58 standard can significantly improve road safety in Thailand.

1.2 Research Objectives

- To design a Foldable RUPD for dump trucks to overcome the limitations of dump trucks and can be fabricated and utilized with domestic materials.
- To design a foldable RUPD that is lightweight and strong to pass UN regulation No. 58.

1.3 Scope of Work

This study focuses on developing a foldable RUPD for dump trucks, which following to UN regulation No. 58 and considers the available materials in Thailand, while also avoiding material flow out and departure angle concerns. The strength analysis is conducted using the finite element method, specifically using quasi-static in RADIOSS. The cross-section type and component thickness are significant parameters considered for the study. The selection of the most significant parameters in this study is based on two criteria: achieving the lightest weight and the highest force-to-weight ratio.

CHAPTER 2

LITERATURE REVIEW

2.1 UN regulation No.58 for dump truck and constraints

2.1.1 Dimension requirements

- The cross-member is required to meet a minimum section height of 120 mm and must not exhibit any bending towards the rear or sharp outer edges. Moreover, the cross-member must have a curvature radius of not less than 2.5 mm.
- The vehicle's ground clearance must not surpass 500 mm, and its departure angle should not be less than 8°.
- The width of the rear protective device should not exceed the outermost points of the wheels, excluding the bulging of the tires close to the ground, at any given point. Additionally, the Rear Underrun Protection Device (RUPD) should not be shorter than 100 mm on either side.
- The horizontal distance should not exceed 300 mm before applying the test forces. The same requirements mentioned above apply.

2.1.2 Test procedure requirements

- The test mandrels must be used to verify compliance with the Regulation on a test surface no more than 250 mm in height and 200 mm wide, with a 5 ± 1 mm curvature radius at the vertical edges. The RUP must resist forces parallel to the vehicle's longitudinal axis, and the test surface must be articulated in all directions.
- A 180 kN horizontal force must be applied consecutively to two points symmetrically located about the center line of the RUPD or the vehicle, as applicable, spaced between 700 mm and 1 m apart.
- For horizontal force tests of 100 kN two points should be located 300 ± 25 mm from the longitudinal planes tangential to the outer edges of the wheels on the rear axle

or of the RUPD. A third point should be located on the line joining these two points, in the median vertical plane of the vehicle.

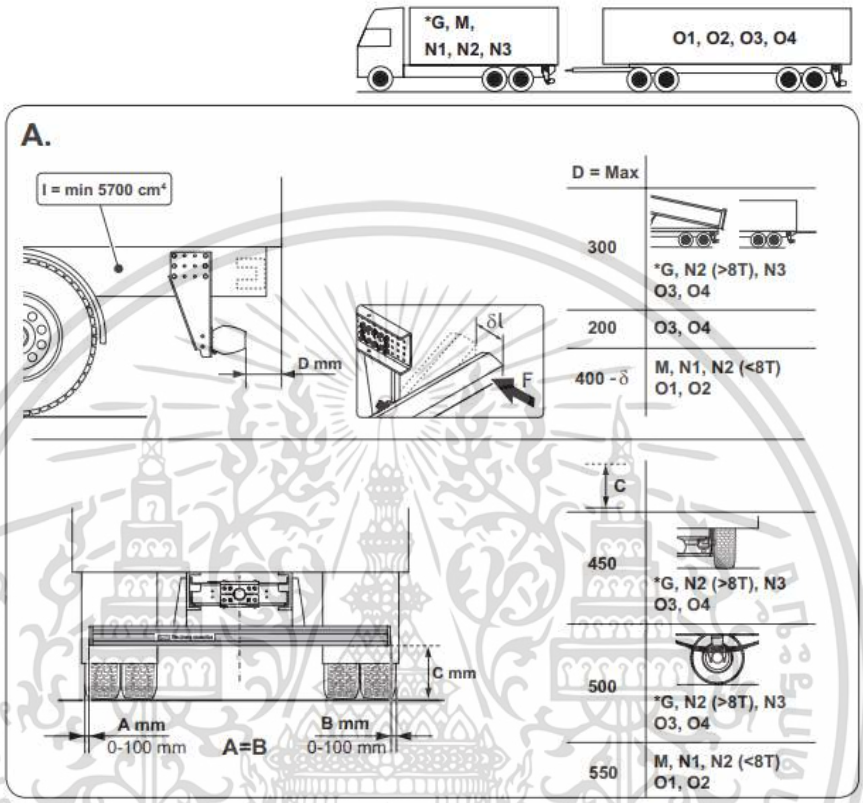

Figure 2.1 Requirement for the dimension of UN regulation No.58 rev 3 [11].

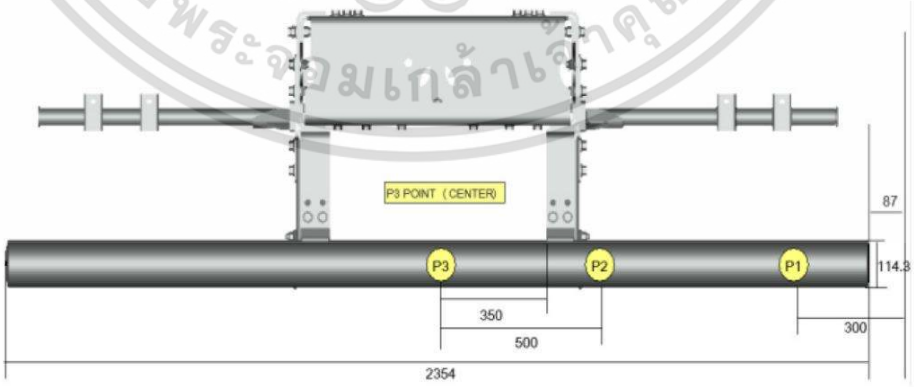

Figure 2.2 RUPD loading condition and position [5].

2.1.3 RUPD constraints

Dump trucks are commonly used to transport and unload a variety of materials, such as soil, sand, gravel, and other loose materials. The unloading process involves lifting the truck bed using hydraulic systems, allowing the materials to flow out in a triangular pile at an angle of approximately 90 degrees. One of the major challenges of installing a rear underrun protective device on dump trucks is the potential damage caused by the materials during unloading. When the truck bed is raised, the materials may flow down onto the RUPD, potentially causing significant damage. In addition, the RUPD must avoid the materials during the unloading process, which can be challenging given the weight and volume of the materials being transported. Another significant challenge when installing a rear underrun protective device on dump trucks is its susceptibility to scratches and damage while driving on steep roads or surfaces with high departure angles, such as piers, mountains, or truck weighbridge weighing scales. When the vehicle encounters a slope, the RUPD may contact the road surface, causing scratches or other types of damage, As shown in Figure 2.3 [7].

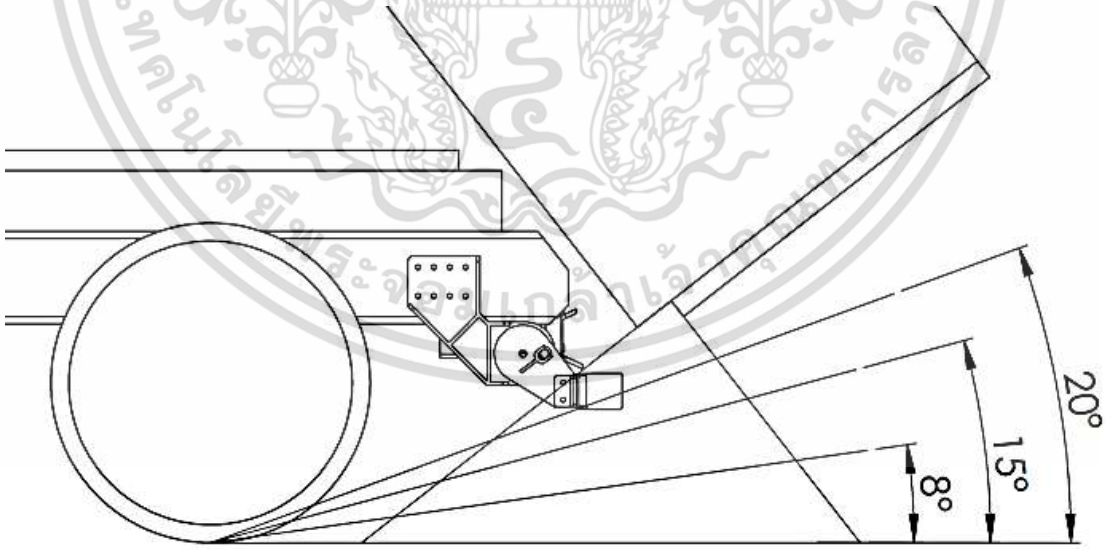

Figure 2.3 The constraints of installing RUPD on the dump truck.

2.2 Overview of RUPD

Research has shown that a significant percentage of accidents involving passenger vehicles and trucks were rear-ended collisions. In fact, out of all such collisions, 45 percent were rear-ended accidents, 33 percent were frontal impacts, and 22 percent were side impacts. Rear-end collisions are particularly concerning because they can result in severe injuries or fatalities, especially for the occupants of smaller, lighter personal vehicles. One of the primary issues leading to these collisions is the difference in height between trucks and personal vehicles. Personal cars can be divided into zones based on their height, which include the bumper, grill, and pillar. The design of the rear bumper of trucks aims to align its height with that of the bumper of personal cars. However, in the absence of Rear Underride Protection Devices (RUPD), the pillar of a personal car can collide directly with the rear of the truck, leading to catastrophic consequences.

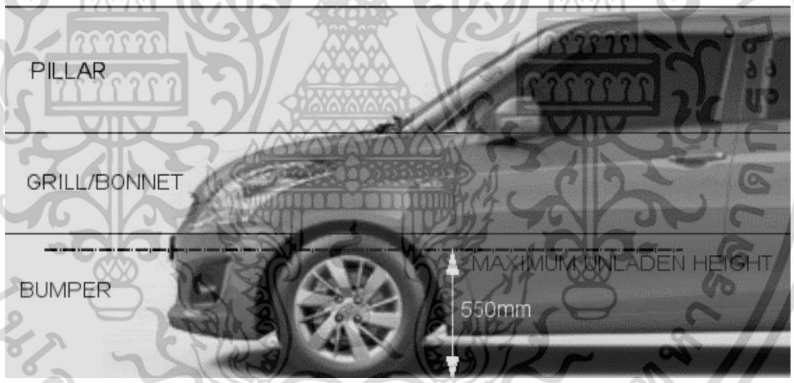

Figure 2.4 Sections of the height of initial contact of RUPD with the car [15].

Studies have revealed that the installation of RUPDs in personal vehicles can significantly reduce the likelihood of severe injuries or fatalities resulting from rear-end collisions. These devices are designed to prevent or minimize the impact of a collision between the front of a personal car and the rear of a truck by creating a physical barrier between the two vehicles. RUPDs are installed at the rear of the truck and are designed to align with the bumper of personal cars, providing a buffer that absorbs the impact and helps prevent the car from sliding under the truck.

In addition to the installation of RUPDs, wearing seat belts can also contribute to reducing the fatality rate in rear-end collisions. Seat belts provide an additional layer of protection by preventing occupants from being thrown forward and colliding with the interior of the vehicle or being ejected from the car in the event of an accident. Research has shown that the combined use of RUPDs and seat belts in personal vehicles can reduce the fatality rate in rear-end collisions by up to 20 percent. These findings highlight the importance of investing in safety measures that can protect motorists from severe injuries or fatalities resulting from rear-end collisions involving trucks and personal vehicles [15].

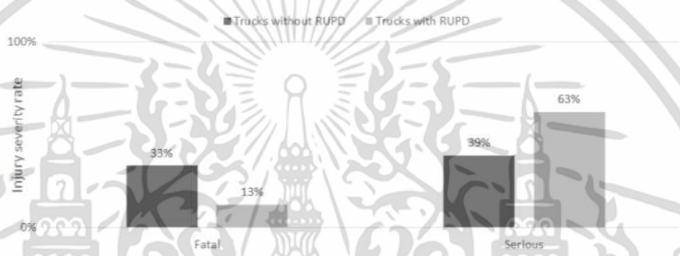

Figure 2.5 Fatality and Serious injury rates for belted car drivers in crashes with and without RUPD fitment in trucks [15].

In terms of rear-end collisions, two types are typically distinguished: center collisions and offset collisions. A study was undertaken to explore the efficacy of Rear Underride Protection Devices (RUPD) in reducing the severity of rear-end collisions. Specifically, the study involved a sedan weighing 1700 kg traveling at a velocity of 48 km/h colliding with the RUPD mounted on the rear end of a truck.

Figure 2.6 Test crash without the RUPD system in offset crash event [9].

The study revealed that in the absence of a rear offset bumper, the cabin of the passenger car collided directly with the rear of the truck, leading to significant damage to the driver. However, when an RUPD was installed, both center and offset collisions showed that the damage to the passenger car occurred primarily at the front bumper, with no harm to the passenger compartment.

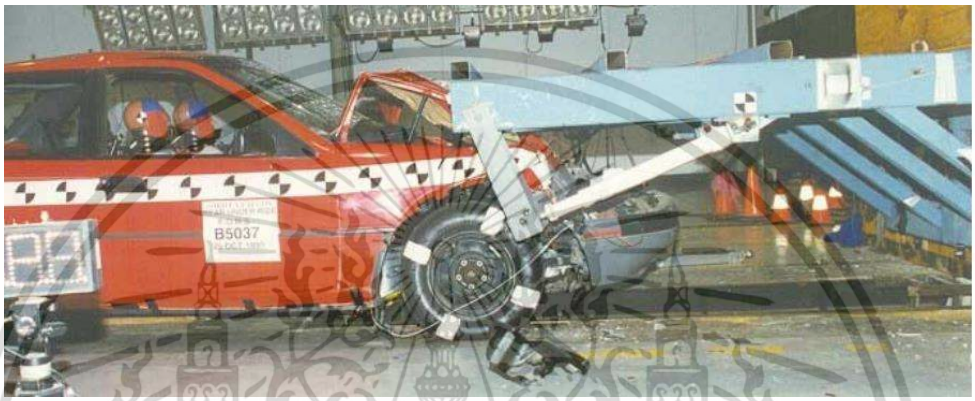

Figure 2.7 Test crash with the RUPD system in the center crash event [9].

Figure 2.8 Test crash with the RUPD system in offset crash event [9].

The experimental findings indicate that the standard used to define RUPD is a specification capable of stopping a 1700 kg passenger car traveling at 48 kilometers per hour. Moreover, the minimum force required for designing RUPD was found to be close to this standard. Thus, the results of the study support the effectiveness of RUPDs in mitigating the severity of rear-end collisions involving trucks and passenger vehicles.

2.3 Conceptual design process

Morphological analysis has emerged as a useful tool for studying and evaluating RUPD designs for different trucks. This method involves the systematic generation of a wide range of conceptual designs, by breaking down the design problem into constituent parts and exploring various possible combinations of these parts. This approach enables designers to explore a vast design space and consider many alternatives, which may not have been possible with other methods.

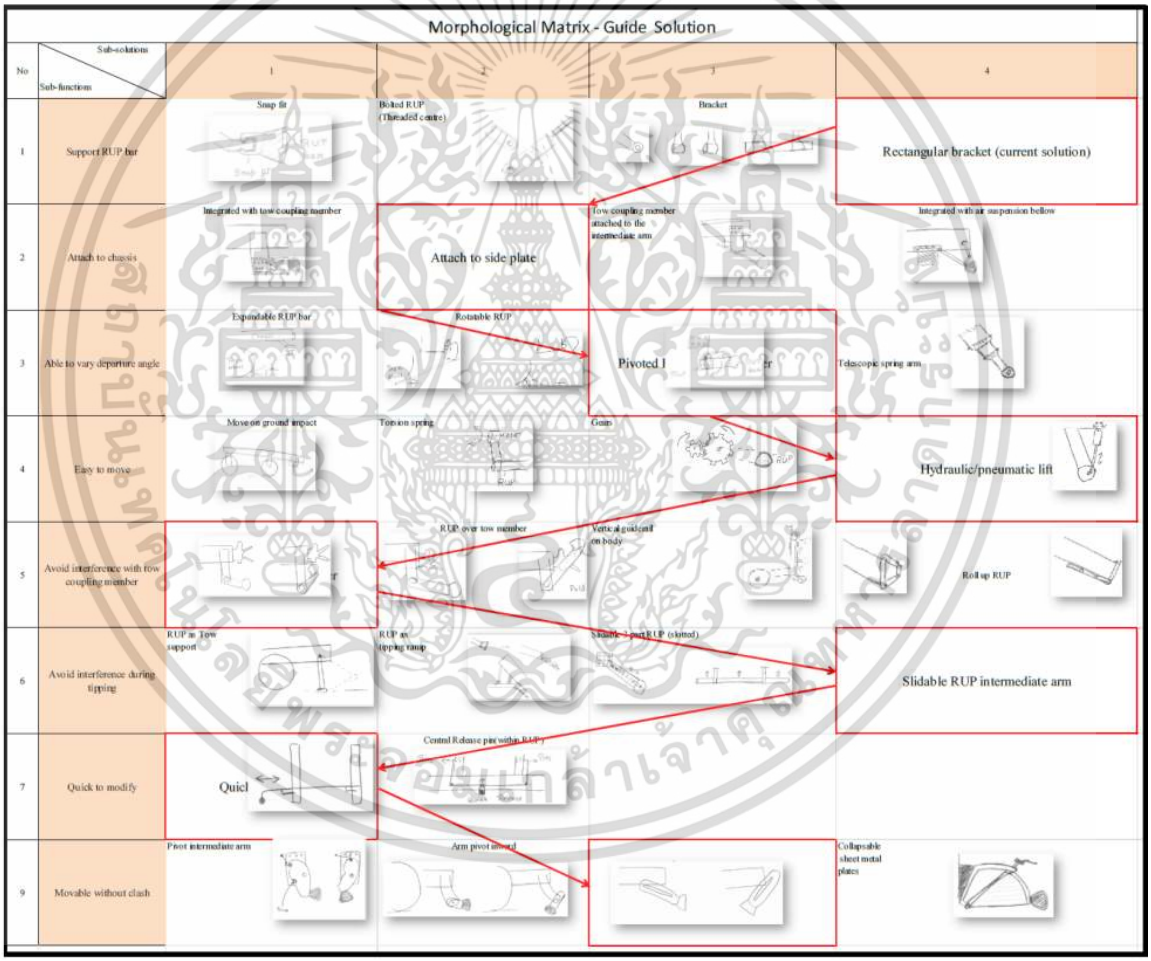

Figure 2.9 Morphological Matrix guide solution [7].

Kesselring Matrix

Sr. No	Criteria	Weights (1-10)	Ideal	Alternative Concepts: The Plug-Stopper	C-Arm	Limb	Threaded telescopic	Ring	Lever	Guide Profile	Van Damme	Two way foldable	Triple RUP
1	Avoid clash during operation	10	10	7	9	8	8	6	6	8	9	6	6
2	Withstand impact loads	8	10	8	9	6	7	6	5	8	4	4	7
3	Compactness	6	10	6	8	6	7	7	7	7	9	6	5
4	Assembly	7	10	7	7	7	7	7	7	7	7	7	7
5	Cost effeciency	5	10	8	7	5	6	7	7	8	3	7	6
6	Easy to operate	8	10	7	7	8	8	8	7	6	8	6	7
7	Aesthetics	5	10	7	7	6	8	5	5	8	7	5	5
8	Change in departure angle	7	10	7	7	8	7	8	8	8	6	8	3
9	Simplicity in design	8	10	7	8	6	6	7	6	8	6	7	5
10	Ease of Maintenance	6	10	7	7	6	7	6	6	8	5	7	6
	Final score		700	497	540	472	500	471	447	531	459	439	403
	Percentage		100	71	77,1429	67,4286	71,428571	67,28571	63,86	75,857	65,571	62,714	57,5714
	Comments												

Figure 2.10 Kesselring matrix method [7].

Once a range of RUPD design options is generated, the Kesselring matrix method can be used to assess and rank the designs based on a range of factors, such as weight, cost, ease of manufacturing, and effectiveness in preventing rear-end collisions. The Kesselring matrix is a tool for structuring and evaluating design alternatives that allow the identification of the most promising design options based on their scores across multiple criteria. The use of this method enables designers to select the most suitable design for further development and refinement.

2.4 Finite element analysis and experimental testing of RUPD

This study employs UN regulation No.58 as the design criterion, one of several standards related to RUPD. The standard stipulates that the RUPD can be tested using either the finite element method or the experimental method, with the manufacturer having the option to select the testing method. The study investigated the RUPD design for trucks and analyzed its ability to withstand collision loads following UN regulation No.58. The FE model analysis was conducted using RADIOSS or LS-DYNA program depending on each

researcher. The bumper was constructed with a tube cross-section, while most of the other components were made from sheet steel. The FE model analysis uses non-linear material parts made of sheet metal with Shell Element and 1D Beam Element bolt type. The researchers established a quasi-static load and applied a revolute joint with a fixed in all directions at the chassis ends. in preparation for analysis [4-6].

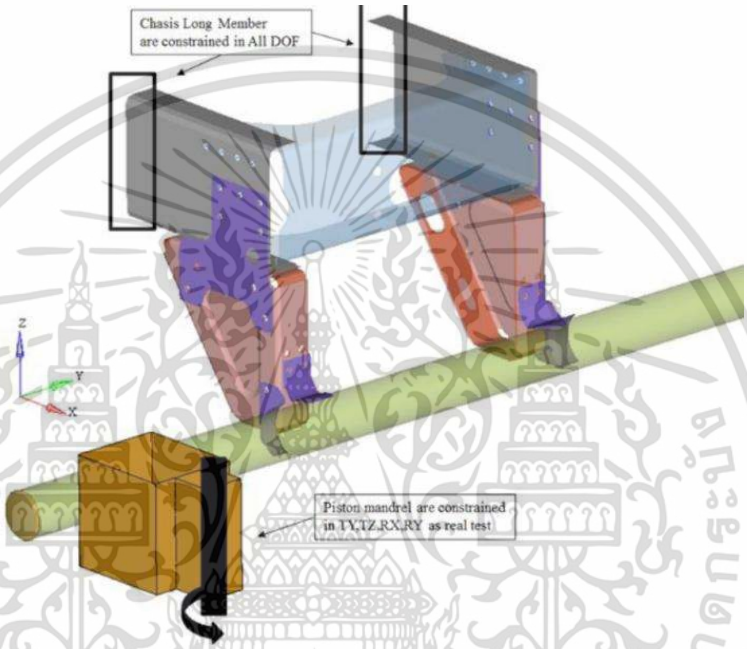

Figure 2.11 FE model boundary conditions and loading [5].

Based on the results of the analysis conducted, it was discovered that each load test had varying effects on different components of the bumper system. Specifically, the P1 load test demonstrated the greatest impact on the bumper cross-section, indicating that it is the most suitable position for evaluating the strength of the bumper cross-section. Conversely, the P2 load test revealed the most significant influence on the mounting bracket. Thus, this position can be utilized as a location for assessing the strength of the mounting bracket. The P3 load test was damaged in the middle of the bumper cross-section. It was found that this test has a load capacity much higher than the standard, indicating that it is not a particularly severe test [4-6].

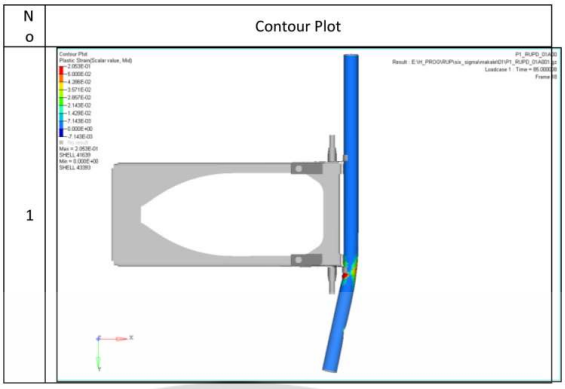

Figure 2.12 Von Mises stress regarding load testing P1 [5].

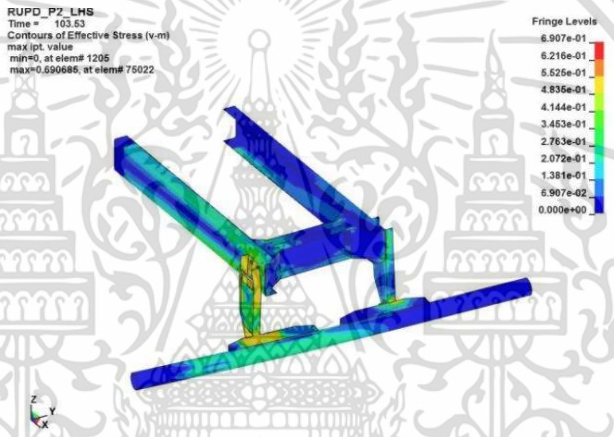

Figure 2.13 Von Mises stress regarding load testing P2 [4].

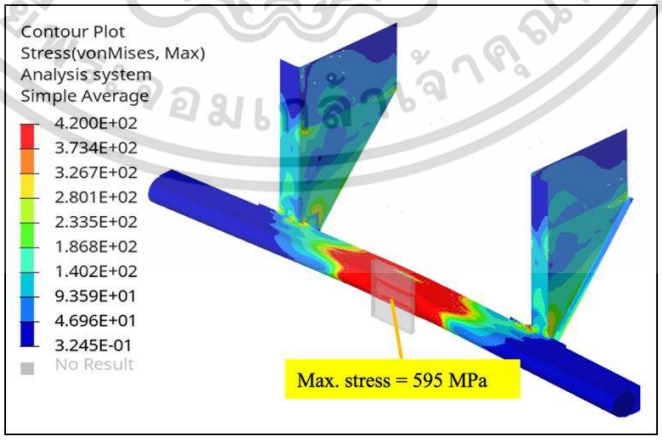

Figure 2.14 Von Mises stress load testing P3 [6].

The Rear Under-run Protection Device (RUPD) is an essential safety feature that is installed on the back of a truck to protect other vehicles from under-riding in the event of a collision. However, the weight of the RUPD can have a significant impact on the overall weight of the truck, affecting its fuel efficiency, handling, and load capacity. Therefore, minimizing the weight distribution around the RUPD system is a crucial consideration during its design and installation. To achieve optimal weight distribution of the RUPD system. First, the use of stronger materials can enhance the strength and durability of the RUPD while minimizing its weight. Secondly, selecting the right material thickness can ensure that the RUPD provides adequate protection without adding excessive weight. Additionally, the design of the blanket support can be optimized for strength, and the installation site can be strategically located to reduce the weight impact [4-6]. Several methods can be employed to determine the most appropriate RUPD selection for a specific truck model. One such approach is the trial-and-error design method, where multiple iterations of design and testing are conducted to determine the optimal RUPD configuration [4]. Another approach is the multi-interpreter design technique that utilizes statistical tools to analyze various design options based on multiple parameters, such as material, thickness, and position support. The strength-to-weight ratio evaluation is yet another approach that assesses the RUPD's ability to provide adequate protection while minimizing its weight impact [6].

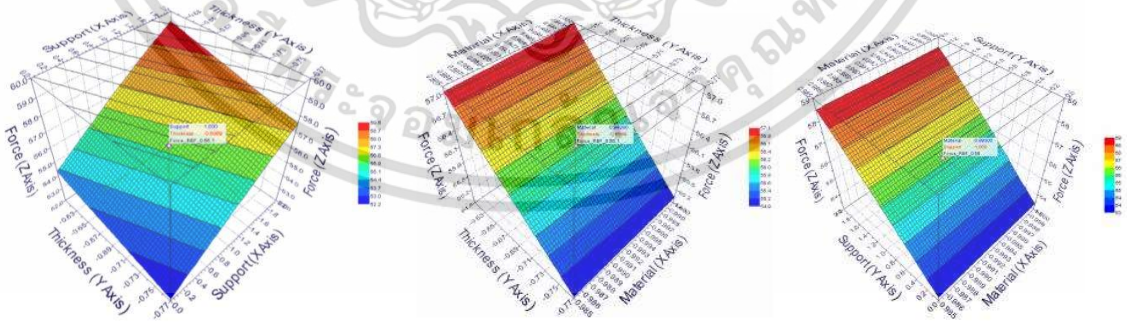

Figure 2.15 Contour Plot: Material, Thickness, Support, and Force [5].

To conduct an experimental test of RUPD, two possible methods can be employed. The first involves fixing the chassis to a test bench and attaching the RUPD to the chassis. Next, a hydraulic actuator equipped with a revolute joint can be used to load the RUPD, ensuring that the hydraulic axis remains unbent and that the loading plate is continuously in contact with the bumper section. The second method is to mount the RUPD onto an actual truck and press the load with a hydraulic actuator that also features a revolute joint [6].

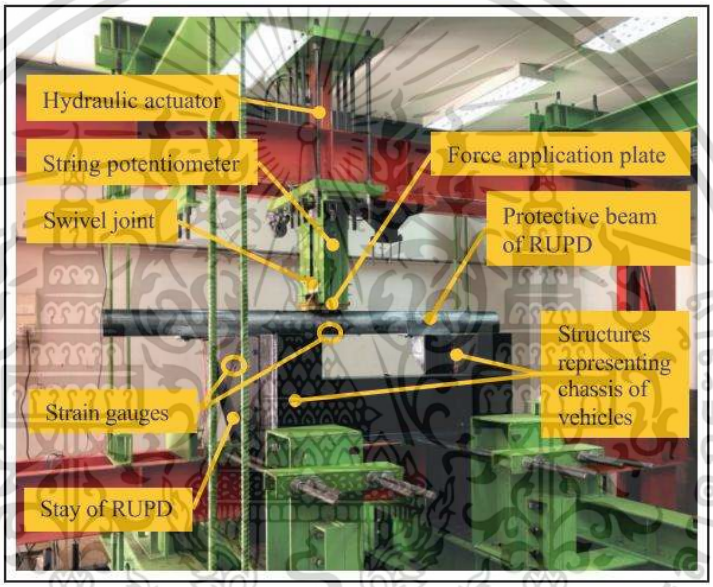

Figure 2.16 RUPD test bench and measure equipment [6].

Once the test has been completed, force measurements can be obtained using a load cell. Meanwhile, displacement measurements can be derived from a sling plot. The data obtained through these methods can then be compared to the results obtained from a finite element method. The goal of this comparison is to assess whether the force-to-displacement curve is consistent and within acceptable tolerances. It is worth noting that these tests are critical for verifying the safety and effectiveness of RUPDs. In recent years, there has been a growing concern over the safety of trucks and the potential hazards they pose to other road users. Therefore, it is essential to ensure that RUPDs can perform their intended function effectively and without fail. These tests also provide valuable insights

into the structural behavior of RUPDs under different loads and scenarios, allowing manufacturers to fine-tune their designs to improve safety and performance [6].

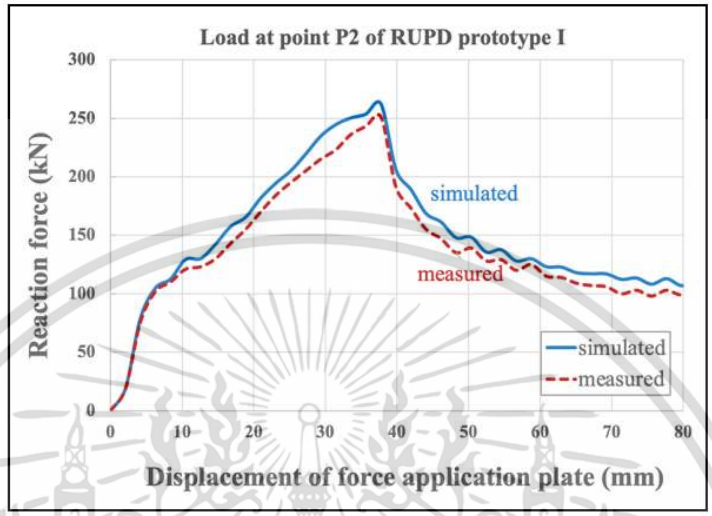

Figure 2.17 Comparison of FE result and experimental result [6].

2.5 Material

2.5.1 TIS 107-2561 carbon steel pipes

TIS 107-2561 is a crucial product standard for carbon steel pipes that are extensively utilized in structural applications across Thailand. This standard governs the production requirements for three types of carbon steel pipes - round, square, and rectangular - that are employed in a variety of engineering, architectural, and general structural works. The standard outlines stringent manufacturing guidelines that specify the chemical composition, mechanical properties, dimensions, and tolerances of the pipes. Compliance with these guidelines is critical to ensuring the pipes' high quality and safety standards. The standard mandates a low carbon content of no more than 0.25% and typically includes a maximum of 0.35% silicon, 1.30% manganese, and 0.040% phosphorus and sulfur. Additionally, the yield stress of the pipes must be at least 245 MPa, with a minimum tensile strength of 400 MPa. According to the standard, the minimum height for the pipes is set at 120 mm. The round pipes that are closest to this standard are OD114.3 mm and

139.8 mm, while the nearest square pipe dimension is 125 x 125 mm. The appropriate thickness range for these pipes is between 3.2 and 6 mm. In summary, TIS 107-2561 is a crucial product standard that ensures the production of high-quality carbon steel pipes that meet the necessary safety standards for structural applications in Thailand [13].

Figure 2.18 Carbon square steel tube and round tube.

2.5.2 SS400 carbon steel plate

SS400 is a Japanese structural steel material that is commonly used for a wide range of applications. The "SS" in its name stands for "structural steel," and the number 400 denotes its yield strength in megapascals (MPa). SS400 steel is highly favored for its excellent mechanical properties and cost-effectiveness, making it one of the world's most widely used structural steels. SS400 steel is a commonly used type of black steel sheet that is known for its high durability and versatility. It is typically produced through hot-rolling and is available in two types: thick steel sheets with a thickness of 3 millimeters or more, and thin steel sheets with a thickness of fewer than 3 millimeters. The composition of SS400 steel typically include carbon (C) content of no more than 0.22%, silicon (Si) content of no more than 0.50%, manganese (Mn) content of no more than 1.40%, phosphorus (P)

content of no more than 0.050%, sulfur (S) content of no more than 0.050%, and iron (Fe) as the remaining balance. The yield stress must be at least 245 MPa and the tensile strength must be between 400 and 510 MPa. The minimum elongation is 21%. This type of steel plate is available in a range of thicknesses, with popular options including 3, 4.5, 6, 9, 12, 16, and 20 millimeters. Standard sizes for black steel sheets include 4x8 feet and 5x10 feet. This type of steel plate is often used in construction, buildings, and industrial plants. This type of steel plate is often used for connecting structures, vehicles, and machinery due to its strength, durability, and versatility [14].

Figure 2.19 Structural steel sheet (SS400).

2.5.3 ASTM E8 Standard test methods for tension testing of metallic materials

The ASTM E8 standard is a widely recognized and essential test method for evaluating the tensile properties of metallic materials. It is published by ASTM International, a global leader in the development of voluntary consensus standards. This standard provides comprehensive guidelines for preparing and testing various metallic materials, including metals, alloys, and metallic-coated materials. Tensile testing, a fundamental mechanical test, is used to determine the strength and ductility of a material by applying a controlled pulling force until it fails.

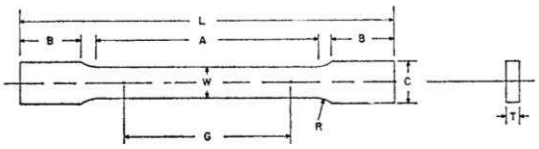

	Dimensions		
	Standard Specimens		Subsize Specimen
	Plate-Type, 40 mm [1.500 in.] Wide	Sheet-Type, 12.5 mm [0.500 in.] Wide	6 mm [0.250 in.] Wide
	mm [in.]	mm [in.]	mm [in.]
G—Gauge length (Note 1 and Note 2)	200.0 ± 0.2 [8.00 ± 0.01]	50.0 ± 0.1 [2.000 ± 0.005]	25.0 ± 0.1 [1.000 ± 0.003]
W—Width (Note 3 and Note 4)	40.0 ± 2.0 [1.500 ± 0.125, -0.250]	12.5 ± 0.2 [0.500 ± 0.010]	6.0 ± 0.1 [0.250 ± 0.005]
T—Thickness (Note 5)		thickness of material	
R—Radius of fillet, min (Note 6)	25 [1]	12.5 [0.500]	6 [0.250]
L—Overall length, min (Note 2, Note 7, and Note 8)	450 [18]	200 [8]	100 [4]
A—Length of reduced section, min	225 [9]	57 [2.25]	32 [1.25]
B—Length of grip section, min (Note 9)	75 [3]	50 [2]	30 [1.25]
C—Width of grip section, approximate (Note 4 and Note 9)	50 [2]	20 [0.750]	10 [0.375]

Figure 2.20 Plate type and sheet type specimen dimensions [10].

The ASTM E8 standard specifies different types of specimens, such as round, flat, and rectangular, and provides guidelines for preparing them for testing. Additionally, the standard defines the testing conditions, including the testing speed, temperature, and other factors that must be controlled to ensure consistent and accurate results. During the tensile test, the material specimen is clamped into the testing machine and subjected to a gradually increasing force until it reaches its ultimate tensile strength or breaks. The testing machine measures the load and elongation of the specimen, which is used to calculate various mechanical properties such as yield strength, ultimate tensile strength, and elongation.

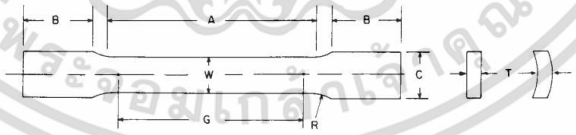

	Dimensions						
	Specimen 1	Specimen 2	Specimen 3	Specimen 4	Specimen 5	Specimen 6	Specimen 7
	mm [in.]	mm [in.]	mm [in.]	mm [in.]	mm [in.]	mm [in.]	mm [in.]
G—Gauge length	50.0 ± 0.1 [2.000 ± 0.005]	50.0 ± 0.1 [2.000 ± 0.005]	200.0 ± 0.2 [8.00 ± 0.01]	50.0 ± 0.1 [2.000 ± 0.005]	100.0 ± 0.1 [4.000 ± 0.005]	50.0 ± 0.1 [2.000 ± 0.005]	100.0 ± 0.1 [4.000 ± 0.005]
W—Width (Note 1)	12.5 ± 0.2 [0.500 ± 0.010]	40.0 ± 2.0 [1.5 ± 0.125-0.25]	40.0 ± 0.2 [1.5 ± 0.125,-0.25]	20.0 ± 0.7 [0.750 ± 0.031]	20.0 ± 0.7 [0.750 ± 0.031]	25.0 ± 1.5 [1.000 ± 0.062]	25.0 ± 1.5 [1.000 ± 0.062]
T—Thickness	measured thickness of specimen						
R—Radius of fillet, min	12.5 [0.5]	25 [1]	25 [1]	25 [1]	25 [1]	25 [1]	25 [1]
A—Length of reduced section, min	60 [2.25]	60 [2.25]	230 [9]	60 [2.25]	120 [4.5]	60 [2.25]	120 [4.5]
B—Length of grip section, min (Note 2)	75 [3]	75 [3]	75 [3]	75 [3]	75 [3]	75 [3]	75 [3]
C—Width of grip section, approximate (Note 3)	20 [0.75]	50 [2]	50 [2]	25 [1]	25 [1]	40 [1.5]	40 [1.5]

Figure 2.21 Tube specimen dimensions [10].

Moreover, the ASTM E8 standard provides guidelines for reporting the test results, including the type of specimen, testing conditions, and mechanical properties. This information is crucial for comparing the mechanical properties of different materials and ensuring consistency in the testing process. Overall, the ASTM E8 standard plays a crucial role in the manufacturing and testing of metallic materials for various applications, including aerospace, automotive, construction, and medical industries, and helps ensure the safety and reliability of metallic materials used in critical applications [10].

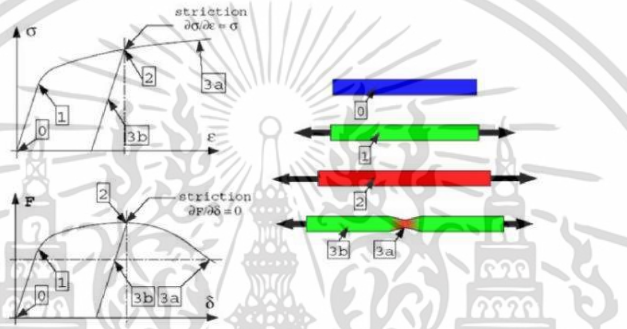

Material Property	Generic Equation
Engineering stress	$\sigma_e = \frac{F}{S_0}$
Engineering strain	$\varepsilon_e = \frac{\Delta l}{l_0}$
True stress	$\sigma_{tr} = \sigma_e \exp(\varepsilon_{tr})$
True strain	$\varepsilon_{tr} = \ln(1+\varepsilon_e)$
True strain rate	$\dot{\varepsilon}_{pl} = \frac{\Delta \varepsilon_{pl}}{\Delta t}$

Figure 2.22 Engineering stress-strain and true stress-strain equations [16].

Raw data obtained from material testing cannot be used directly for analysis in this study. The experimental data, which are typically expressed as engineering stress and engineering strain, do not provide an accurate representation of the true material behavior because of elastic deformation. To overcome this issue, the engineering stress and engineering strain data must be converted to true stress and true strain using the appropriate equations, as shown in Figure 2.22.

Once the data has been converted, a graph like the one in Figure 2.23 can be obtained, which accurately represents the material properties of interest. This graph can then be used to determine key material properties, such as the yield strength, ultimate strength, and modulus of elasticity, that are necessary for subsequent analysis. It is worth noting that accurate material characterization is critical for ensuring the reliability and safety of structures and components. Therefore, it is important to carefully analyze and interpret experimental data to obtain the most accurate representation of material behavior possible [16].

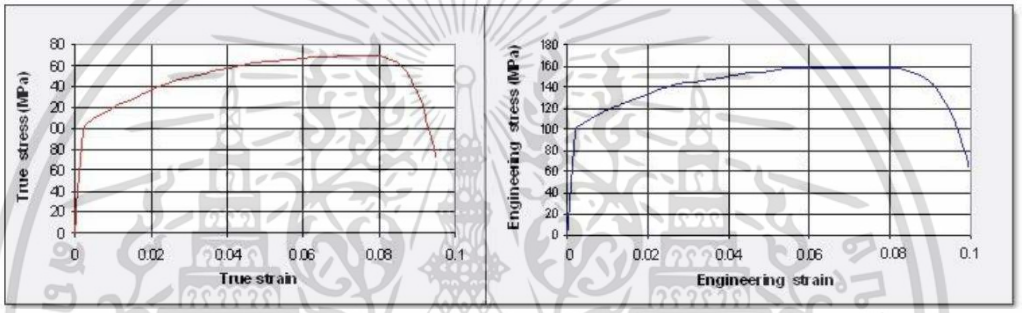

Figure 2.23 Engineering stress-strain curve and true stress-strain curve [16].

2.6 Foldable RUPD available in market

The limitations of RUPD for dump trucks have been a topic of concern in the transportation industry. Several strategies have been proposed to overcome these limitations, including the use of foldable RUPD. An international market survey has identified both passed standard and non-passed standard models of folding RUPD. These designs are primarily intended for trailers. However, their potential application in dump trucks is limited due to the varying chassis heights. In the context of dump trucks, direct application of these folding RUPD models may not be feasible, and customization may be required to ensure compatibility. Customization of folding RUPD can be done by modifying the design to suit the specific requirements of dump trucks. This modification can be achieved by using a custom-made design approach that considers the design requirements of the dump truck, such as the chassis height and width, as well as the intended use of the RUPD [11-12].

2.6.1 Passed standard foldable RUPD

This comprehensive solution comprises a protective beam with a steel, cylindrical profile, which enables the effortless and convenient lifting and lowering of the beam whenever necessary [11].

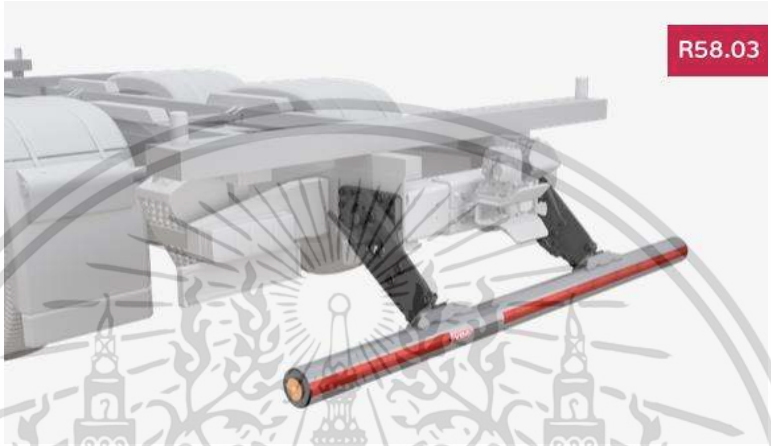

Figure 2.24 VBG foldable RUPD system with cylindrical steel profile [11].

The WAP lift-up RUPD is designed to comply with the updated UN regulation No.58 REV3 approval standards and square-tube profile. Furthermore, it offers the flexibility of mounting bolts, ensuring a customized solution for each application [12].

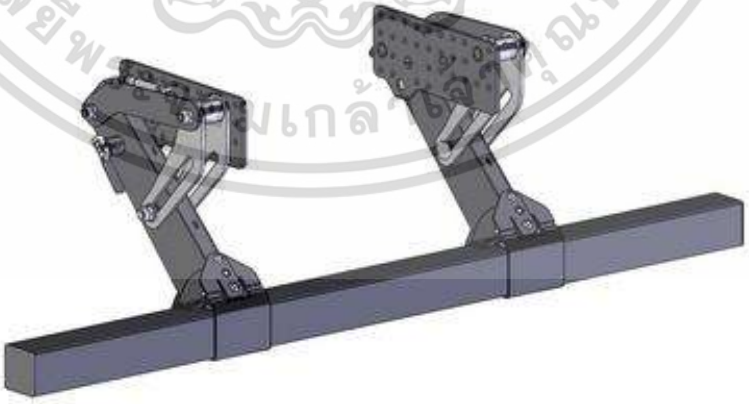

Figure 2.25 WAP lift-Up RUPD meeting UN regulation No.58 REV3 [12].

2.6.2 non-passed standard foldable RUPD

The Endplate Underrun Protection, which is foldable and adjustable, represents a versatile and ergonomic design that allows for easy folding and length adjustment. This protection system offers a practical and convenient solution for individuals who value simplicity and flexibility [11].

Figure 2.26 VBG foldable and adjustable RUPD system with cylindrical steel profile [11].

The WAP Lift-Up Rear RUPD, equipped with gas strut-assisted lift-up, is available in a standard universal version and can be ordered with other leg lengths and mounting bolt options to suit specific requirements [12].

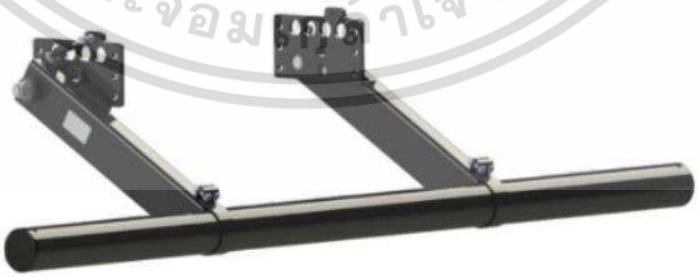

Figure 2.27 WAP Lift-Up RUPD with gas strut assisted lift [12].

The WAP Lift-Up Rear RUPD features adjustable-length legs and a gas strut-assisted lift-up mechanism. It is offered in a standard universal version and can be ordered with alternative leg lengths and mounting bolt options to accommodate various needs [12].

Figure 2.28 WAP Lift-up RUPD with adjustable length legs [12].

The WAP Parallelogram Lift-Up Rear Underrun Protection Device (RUPD) incorporates a light charring bar that remains operational when the RUPD is lifted. Moreover, the bar can be utilized separately on fixed brackets, enhancing its versatility [12].

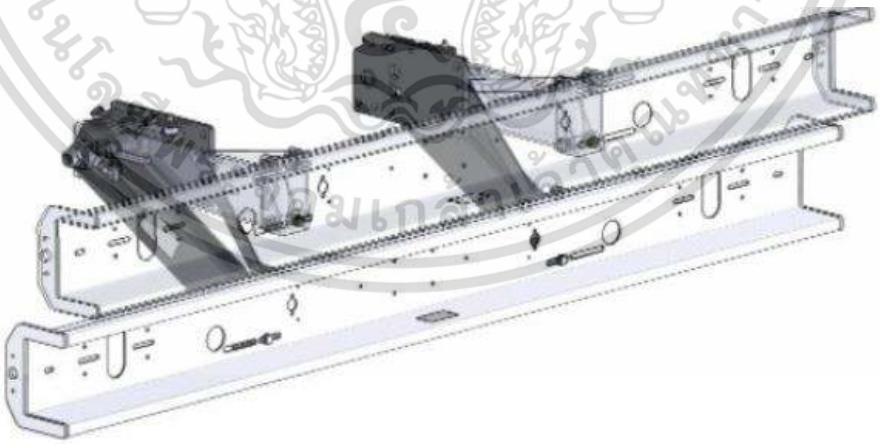

Figure 2.29 WAP parallelogram Lift-Up RUPD [12].

Rear-end collision accidents are a matter of utmost concern due to their severe implications for road safety. In Thailand, the authorities have not enacted legislation focused on rear-end collision protection devices. However, the current state of research on finite element rear collision studies focuses on fixed rear bumpers, with some studies still adhering to outdated standards. Consequently, there is a need to critically assess their relevance and effectiveness in contemporary scenarios.

A particular challenge arises when considering dump trucks, as the conventional fixed rear bumper design proves inadequate for these vehicles. Furthermore, international markets offer folding rear bumpers that hold potential solutions, but these are primarily designed for trailer trucks. Regrettably, these bumpers are unsuitable for dump trucks in Thailand due to disparities in mounting heights, widths, and the prohibitively high costs associated with importing components.

Hence, there exists a pressing necessity for innovative research and development efforts aimed at rear-end collision protection specifically for dump trucks in Thailand. The primary objective of this research endeavor is to conceive and modify a standard folding rear bumper, custom-fitted to meet the safety requirements and practical constraints unique to dump trucks in the country.

In conclusion, this research project endeavors to bridge the current gap in rear-end collision protection for dump trucks in Thailand. Through the application of advanced engineering techniques and innovative design methodologies, we aspire to introduce a reliable, efficient, and cost-effective folding rear bumper solution that will significantly contribute to road safety and potentially set new industry standards.

CHAPTER 3

RESEARCH METHODOLOGY

3.1 Design Guideline

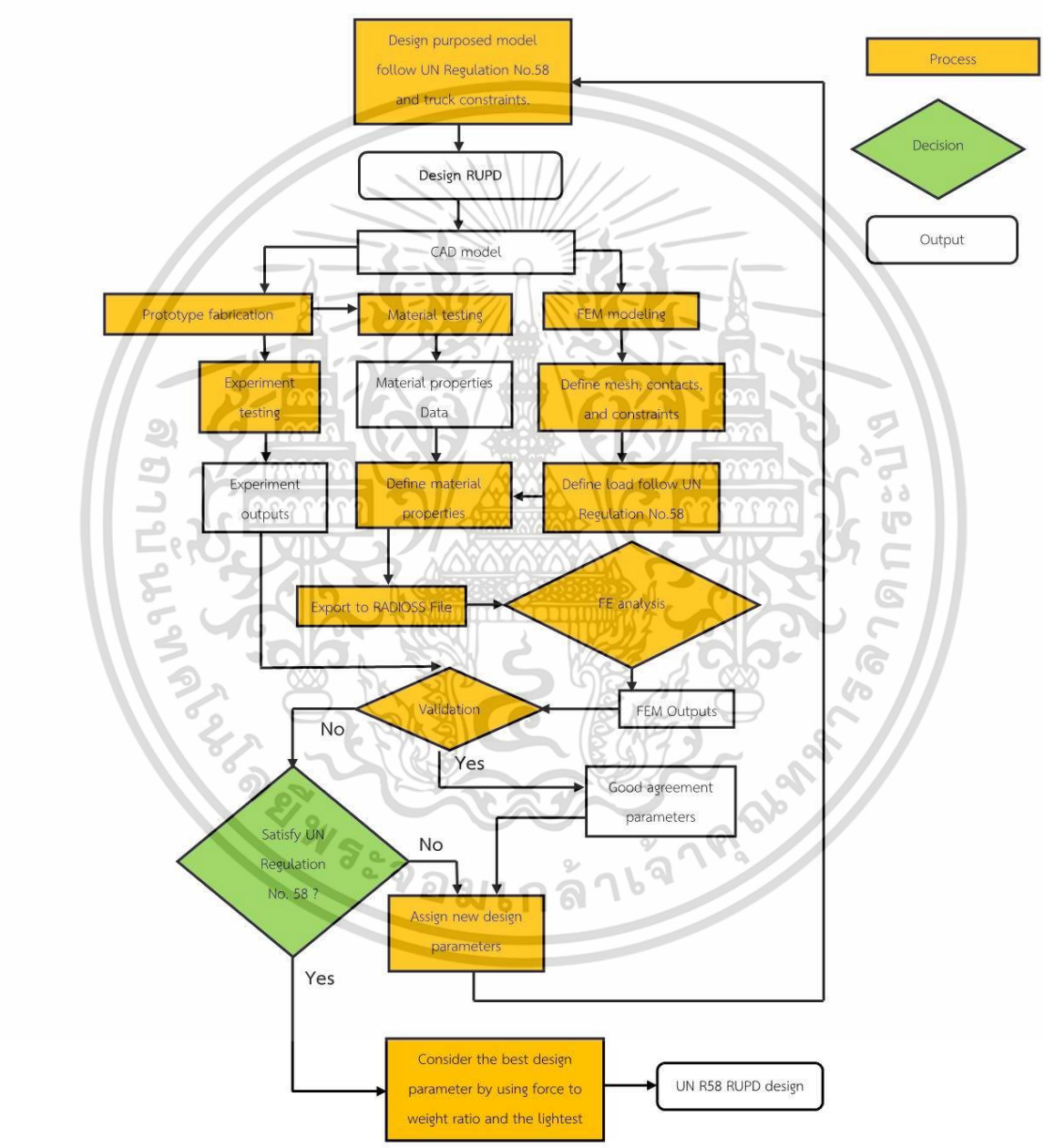

Figure 3.1 Guidelines for designing a study workflow.

This study consisted of three distinct groups. The first group utilized a protective beam model to compare the finite element analysis and the empirical test results. The second group studied two standardized commercial RUPDs to increase confidence in the finite element analysis. Finally, the third group is the proposed design model to meet the limitations and pass the requirements of the standard. All three models were utilized to analyze the flow, as shown in Figure 3.1. A detailed exposition of each group is explained in the next section.

3.2 Test procedure

The tests conducted on the surface must meet certain requirements to ensure accuracy and consistency. Specifically, the force applied during the testing process must not exceed 250 mm in height and 200 mm in width, with a radius of 5 mm at the vertical edge. This ensures that the surface is not damaged during the testing process and that the results obtained are reliable. Three testing points, namely P1, P2, and P3, are identified to conduct the tests. Testing points P1 should be applied to two points that are 300 mm away from the outer edges of the rear axial wheel, with a horizontal force of 100kN. Testing points P2 should be applied to two points along the symmetrical line of the RUPD, at 700-1000 mm from another point, with a horizontal force of 180kN. Finally, testing point P3 should be applied at the center of the vehicle, with a horizontal force of 100kN [3].

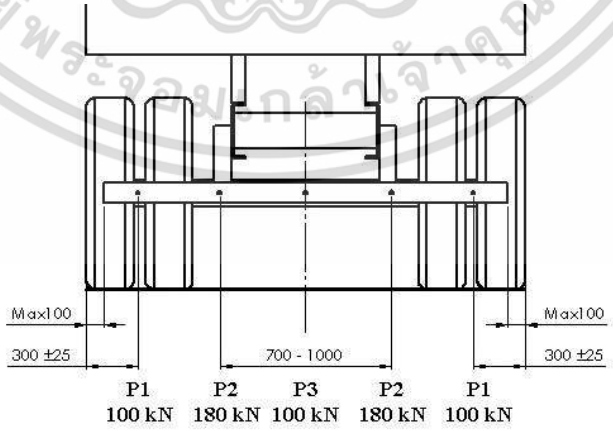

Figure 3.2 Requirement on strength of RUPD according to UN Regulation No.58.

3.3 Materials

The study utilizes TIS 107-2561 carbon steel tubes, TIS 107-2561 carbon square steel tubes, TIS 1479-2558 hot-rolled steel plate (SS400), TIS 1228-2561 lip channel steel, bolts, and nuts with a grade of 10.9. To obtain material properties similar to those from general metal shops, specimens are created by cutting a piece of material with a wire-cut machine, referring to the ASTM E8 standard, five times each. The standard tensile testing machine is used to determine the engineering stress-strain curve of each material, as shown in Figure 3.3. This procedure increases confidence in the consistency of these materials with those available from a general material store. For finite element analysis, all engineering stress-strain data points of the materials are converted to true stress-strain and reduced to smooth data curves, as required by RADIOSS. The material card in RADIOSS M36_PLAS_TAB is utilized, which provides a density of 7,850 kg per cubic meter, Poisson ratio of 0.3, Young modulus, yield stress, and plasticity table curve. According to this function, the elastic material stress-strain curve is defined by Poisson's ratio and Young's modulus, and the material properties switch to nonlinear material when stress exceeds the yield stress. All material properties are defined for all models in this study.

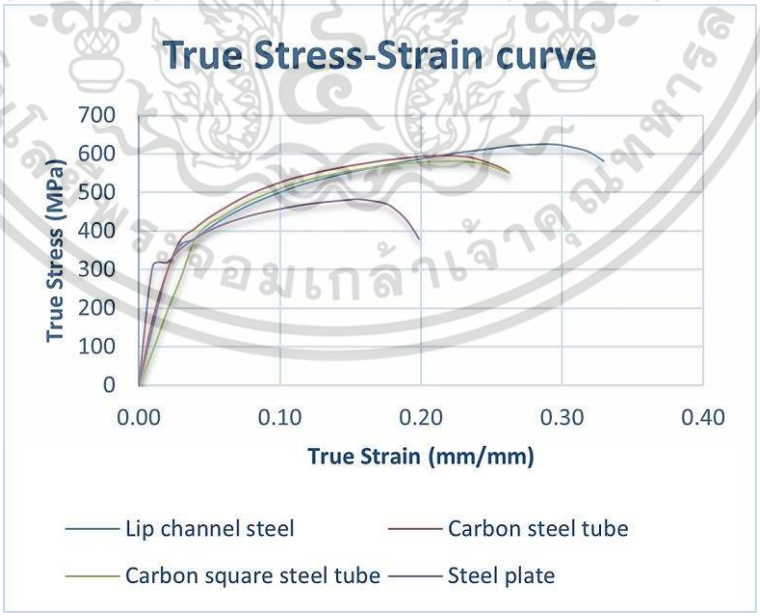

Figure 3.3 True Stress-Strain curves of the material.

3.4 Finite element analysis and experimental testing

In this study, the finite element meshing was performed using Hypermesh, and the analysis was carried out with explicit non-linear dynamics in RADIOSS. Post-processing of the finite element analysis was done using Hyperview. A mixed meshing approach was used, where the finite element mesh for parts made from steel plate was modeled to the shell surface by mid-surface and defined as a 4-node shell element. For parts made from thick steel plates and machined processes, a 3D solid 8-node element was defined. Bolts and nuts were modeled to a simple 3D model and defined as a 3D solid 8-node element. A mesh size of 10 mm was defined for all deformable components, except for the chassis, which was defined as 20 mm.

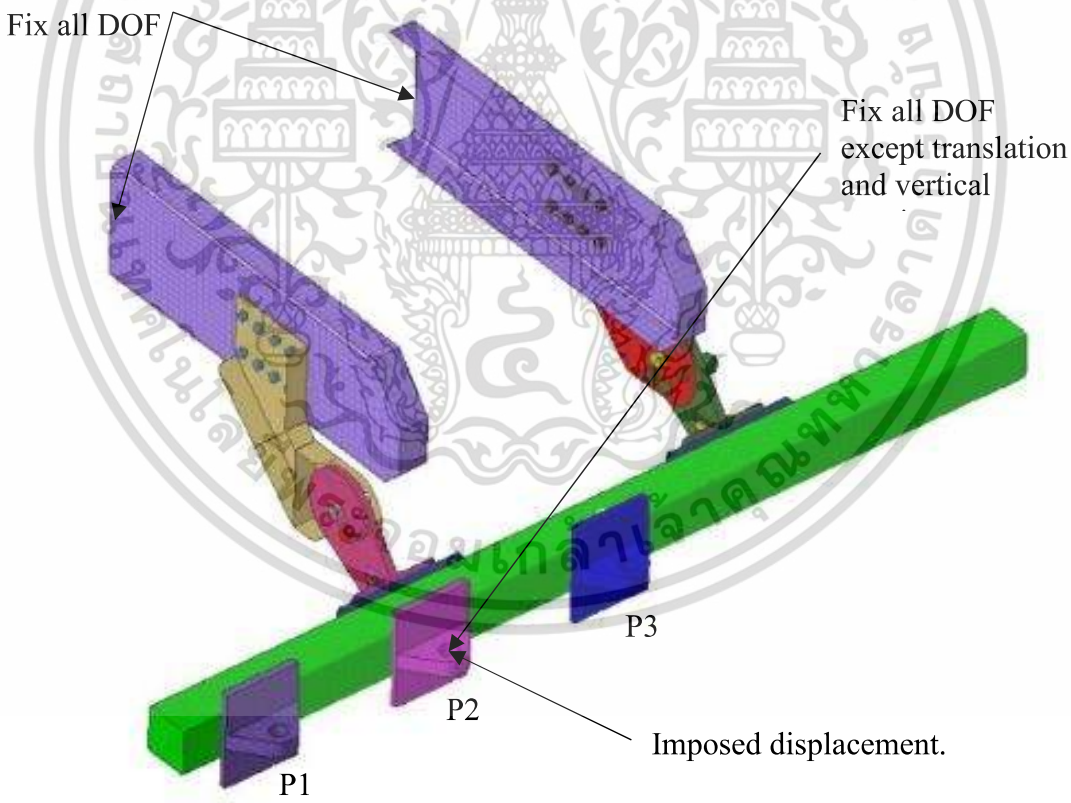

Figure 3.4 Boundary conditions.

The interaction between contracting surfaces was defined as a type7 of the multi-purpose interface, which is a node-to-surface contract. A friction coefficient of 0.2 was used between each part. The chassis was cut at 1000 mm from the rear end and fixed with constraints in all translations and rotations. The loading plate was defined as rigid using a 1D rigid element and fixed with constraints in all directions and rotations, except for the translation direction and vertical rotation at the center point of the 1D rigid element. This allowed the loading plate to move in a normal direction, rotate around the center point, and always be in contact with the protective beam during the loading process. The loading condition was defined using the displacement-time function to represent the quasi-static loading test. The mass scaling of analysis was limited to around 5%. The outputs of the finite element analysis were the reaction force of RUPD, displacement of the loading plate, and the von-mises stress contour plot.

3.4.1 Protective beam model

The protective beam model is an integral component of the validation process for comparing finite element analysis (FEA) results with experimental test results. Its purpose is to accurately represent the physical behavior of the beam during testing by utilizing steel plates, steel tubes, and lip channels made from materials commonly used in Thailand, as shown in Figure 3.5.

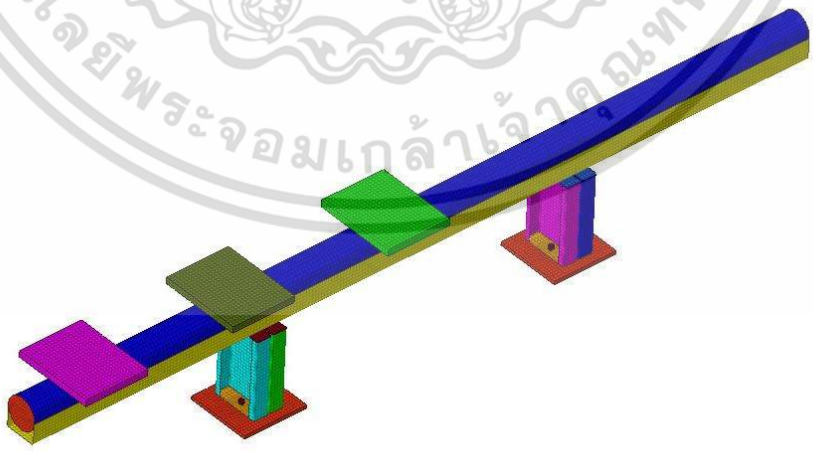

Figure 3.5 Finite element model of the protective beam model.

It is essential to use the correct material thickness and properties to ensure the accuracy and reliability of the FEA and experimental tests. To achieve this, structural and plate steel pieces are carefully cut and tested to determine the material properties, including tensile strength and Young's modulus, and the actual thickness of the steel components used in the model. The obtained material properties and thickness measurements are then incorporated into the finite element analysis model to ensure that it accurately represents the physical behavior of the protective beam during testing. The results obtained from the FEA and experimental tests can be compared, leading to more accurate predictions and a better understanding of the behavior of the protective beam under various loading conditions.

3.4.2 The prototype of the protective beam model

The prototype of the protective beam model is a crucial element in the validation process for comparing FEA results with experimental test results. Installed on the test bench and fastened by bolts and nuts, the protective beam model prototype is subjected to loading tests using a hydraulic actuator that applies pressure on the loading plate. The reaction force and displacement of the beam are accurately measured using a load cell and string potentiometer, as shown in Figure 3.6.

Figure 3.6 Experimental testing of the protective beam model.

During the test, the loading distance is carefully controlled, and the test is terminated when the protective beam can no longer withstand the loading force applied to the RUPD. The careful measurement of the reaction force and displacement ensures that the data obtained from the test is accurate and reliable to make more informed decisions about the behavior of the protective beam model under various loading conditions.

3.4.3 Commercial Models I and II

To enhance the confidence of the finite element analysis method, the present study focuses on the analysis of two commercially available foldable RUPD models. These models claim to meet the UN Regulation No.58 standards and are currently available in the market. Commercial models I and II are meticulously modeled to closely resemble the two market models. The resulting finite element analysis outcomes are expected to conform to the standards, further strengthening confidence in the analysis method. The protective beam of the commercial model I is fabricated using a tube with an outer diameter of 120 mm and a thickness of 6 mm, as shown in Figure 3.7.

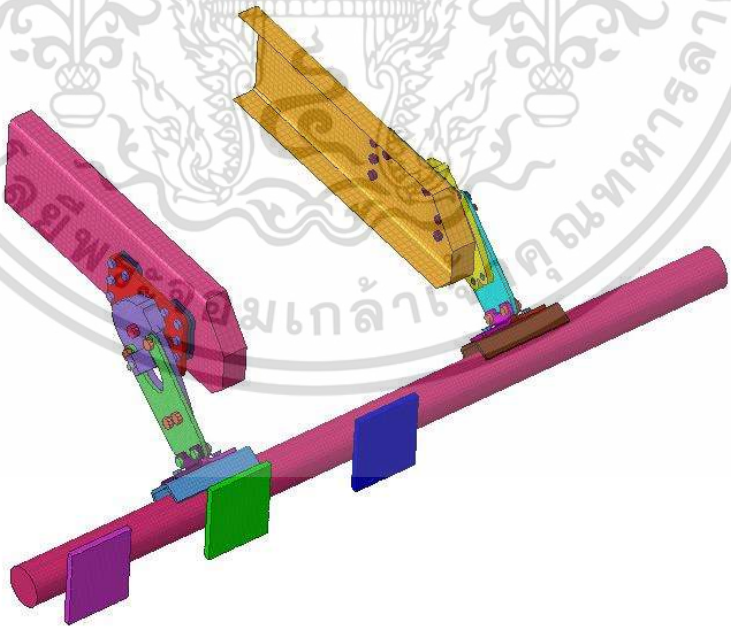

Figure 3.7 Finite element model of the commercial model I [11].

On the other hand, the protective beam thickness of commercial model II is made of a square tube cross-section of 125 x 125 mm with a thickness of 6 mm. Fasteners and mechanisms are modeled using 3D simple models. The same chassis is utilized for both models, as shown in Figure 3.8.

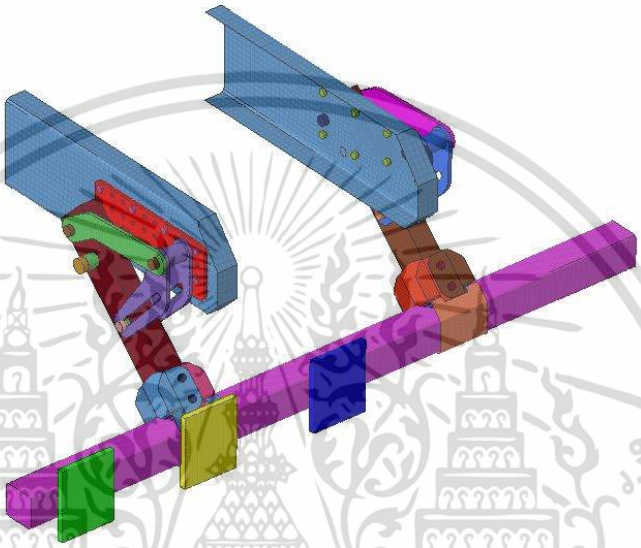

Figure 3.8 Finite element model of the commercial model II [12].

3.4.4 The purposed RUPD design model

The proposed design of the RUPD is specifically intended for use with dump trucks and can be folded up to prevent materials from sliding out during the dumping process, even on steeply inclined roads where previous designs may not be effective. The design process was informed by the results of finite element analyses of two previous models, serving as a guideline for the development of this iteration. The protective beam of the proposed model utilizes a square tube with a thickness of 4.5 mm, while the mounting brackets for the chassis are composed of plates with a thickness of 12 mm. The swing arms, on the other hand, use plates with a thickness of 20 mm. The mechanisms and fasteners are modeled using 3D simple models. The chassis used in the proposed design is identical to that of the previous model.

The foldable RUPD comprises three main components: mounting brackets, swing arms, and a protective beam. The mounting brackets are used to fasten the RUPD to the chassis. The swing arms enable the protective beam to fold up, prevent material from sliding out during the dumping process, and accommodate the departure angle of the road. The position of the swing arms can be adjusted manually and locked in place using a pin-lock system. The protective beam serves to protect against underrun cases, as shown in Figure 3.9.

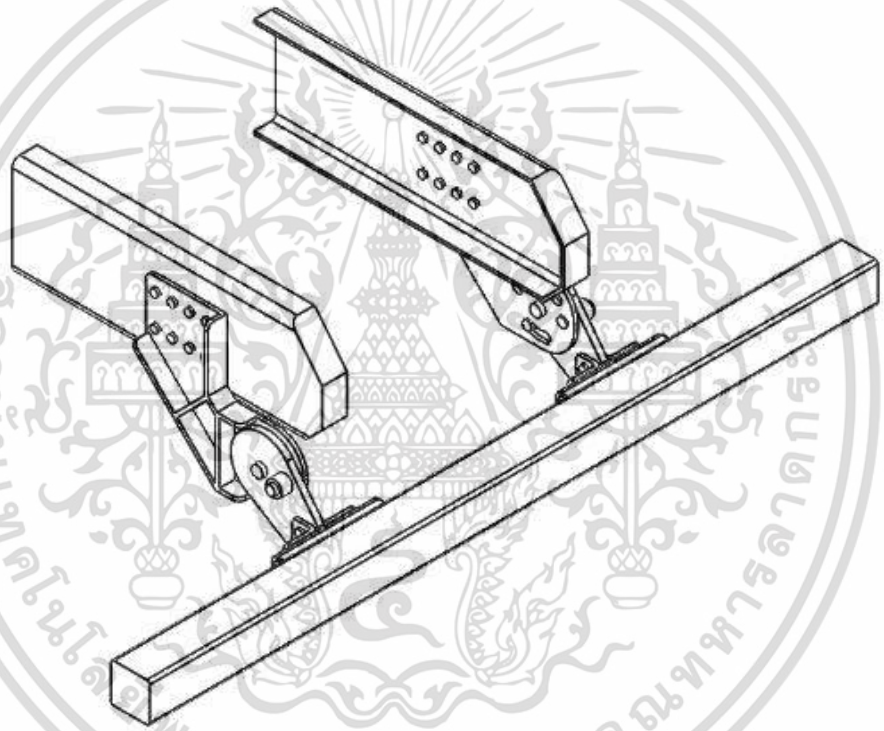

Figure 3.9 The purposed RUPD design model.

Two main constraints exist for installing the rear underrun protective device (RUPD). Firstly, when materials are dumped from the truck in a triangular pile at a 90-degree angle onto the RUPD, it may cause damage. Secondly, when the truck travels on steep inclines such as piers, mountains, and truck weighbridge weighing scales, the RUPD may scrape against the road surface, as shown in Figure 3.10.

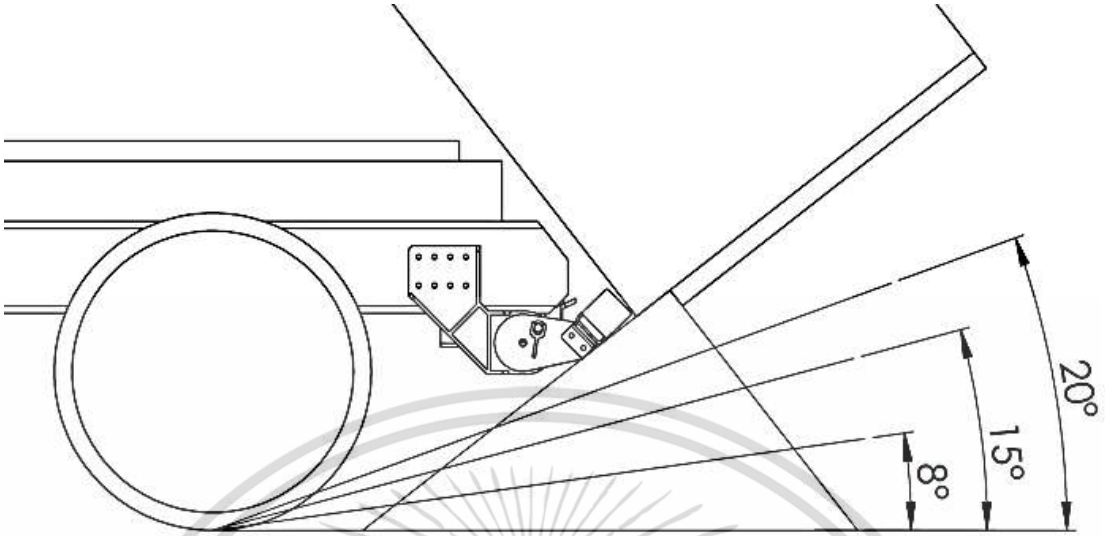

Figure 3.10 The constraints of installing RUPD on the dump truck.

Table 3.1 Requirements for the proposed design model

No.	Description	Requirements
1	Ground clearance	500 mm
2	The horizontal distance	not exceed 300 mm
3	Cross section height	Not less than 120 mm
4	The width of the protective beam	Not shorter than 100 mm on either side.
5	Departure angle	Not be less than 8°
6	Avoid dumped material	Fold to avoid dumped material
7	Structural strength at P1	100 kN
8	Structural strength at P2	180 kN
9	Structural strength at P3	100 kN
10	Max. weight	Not over 120 kg

The proposed design model follows the geometry requirements set by UN Regulation No. 58. The ground clearance in this design is 464 mm, which is within the maximum limit of 500 mm. The distance between the endpoint of the vehicle and the

end of the RUPD is 288 mm, which is within the permissible limit of 300 mm. The protective beam cross-section is a square tube measuring 125 x 125 mm, which is larger than the previous design's 120 mm. The length of the protective beam is also shorter than the distance between each outside wheel by 100 mm, ensuring that the proposed foldable RUPD design meets the geometry requirements of UN Regulation No. 58, as shown in Figure 3.11.

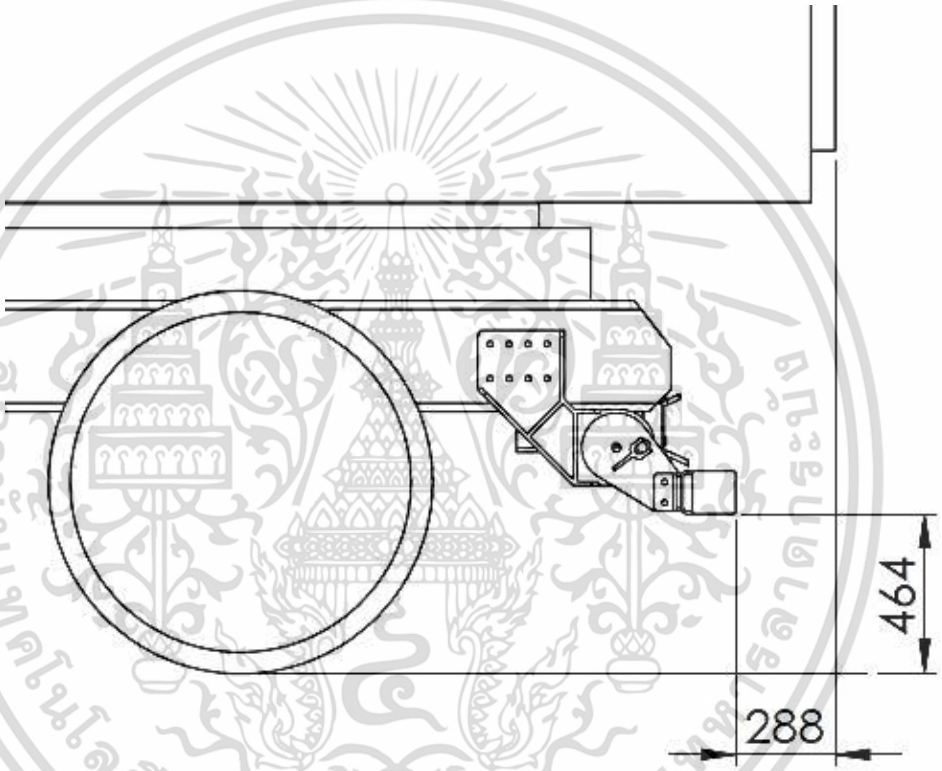

Figure 3.11 Protective beam position.

The weight of a foldable RUPD is a critical design factor, as it affects the allowable payload and power consumption. Therefore, designing a lightweight foldable RUPD that meets the necessary standards while utilizing locally available materials is preferable. This study examines various parameters that impact the strength and weight of the RUPD, including the protective beam cross-sections, mounting brackets, and swingarms. The protective beam cross-sections are of three types: round tube OD 139.8 mm, square tube 125 x 125

mm, and round tube OD114.3 mm mixed with C-folded steel plates of 4.5 mm thickness and cross-section thicknesses of 3.2mm, 4.5mm, and 6mm. There are two types of mounting brackets, one with center ribs and another without, having thicknesses of 12 mm and 9 mm, respectively. The swingarm comes in thicknesses of 20 mm, 15 mm, and 12 mm, as shown in Figures 3.12 – 3.13. The selection criteria for the best foldable RUPD in this study are the lightest weight, strength close to the minimum requirement of UN Regulation No. 58, and strength-to-weight ratio. The strength evaluation of the foldable RUPD is based on the maximum reaction force observed in each test case.

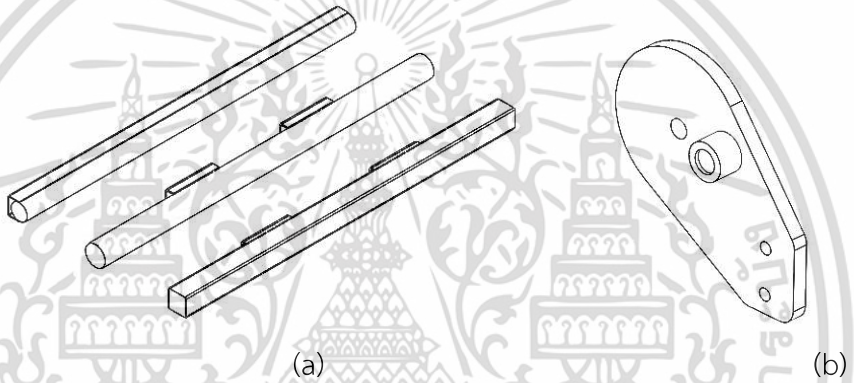

Figure 3.12 (a) Protective beam type, (b) Moving arm.

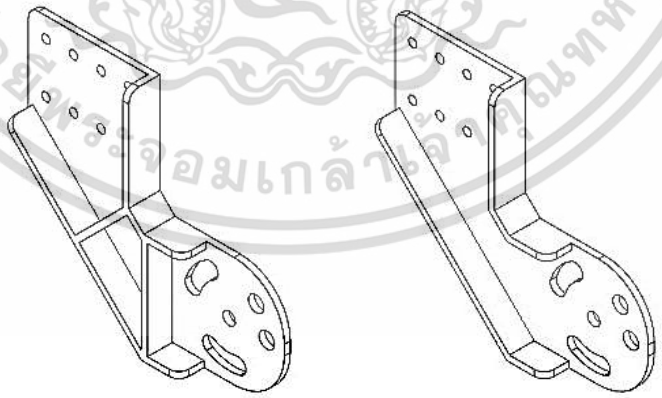

Figure 3.13 (a) Mounting bracket, (b) Mounting bracket without center rib.

CHAPTER 4

RESULTS AND DISCUSSIONS

4.1 Validation of the protective beam model

It is important to validate the results by comparing the reaction force and displacement curves to ensure the accuracy of experimental testing and finite element analysis. Among these two parameters, the reaction force is of primary interest, as it provides a measure of the load-bearing capacity of the structure under test. In the present study, three testing points (P1, P2, and P3) were selected to evaluate the accuracy of the experimental testing and finite element analysis results.

For testing point P1, the maximum reaction forces obtained from experimental testing and finite element analysis were found to be 59kN and 60kN, respectively. The difference between the two values was only 1.8%, indicating a high level of agreement between the two methods.

Similarly, for testing point P2, the maximum reaction forces obtained from experimental testing and finite element analysis were 224kN and 215kN, respectively, resulting in a difference of 4.0%. Although the error was slightly larger than that for testing point P1, it still fell within an acceptable range, indicating that the experimental testing and finite element analysis were in good agreement.

However, for testing point P3, the maximum reaction forces obtained from experimental testing and finite element analysis were 93kN and 102kN, respectively, with a difference of 10.0%. This larger discrepancy suggests that there may be some systematic errors in the experimental testing or finite element analysis, or both, for this testing point. Further investigation is required to identify the cause of this discrepancy and improve the accuracy of the results.

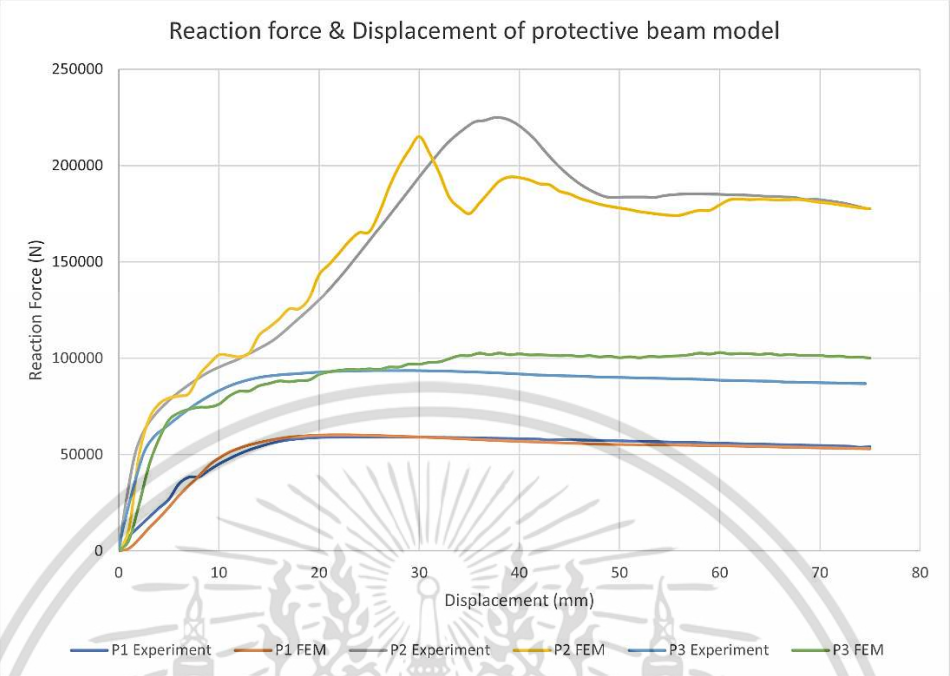

Figure 4.1 Comparison of the experimental testing and the finite element analysis of a simple model.

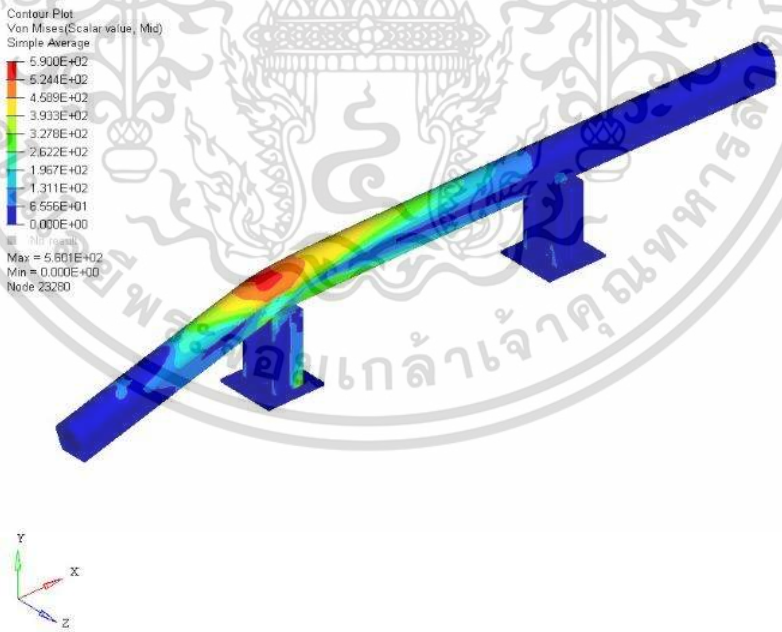

Figure 4.2 Finite element analysis of protective beam model result regarding load applied at point P1.

Figure 4.3 Experimental testing of protective beam model result regarding load applied at point P1.

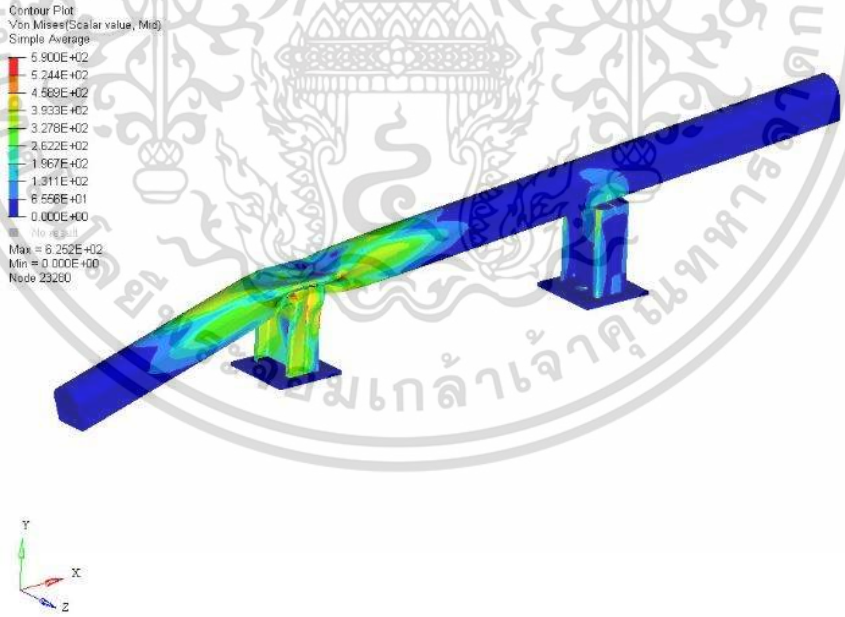

Figure 4.4 Finite element analysis of protective beam model result regarding load applied at point P2.

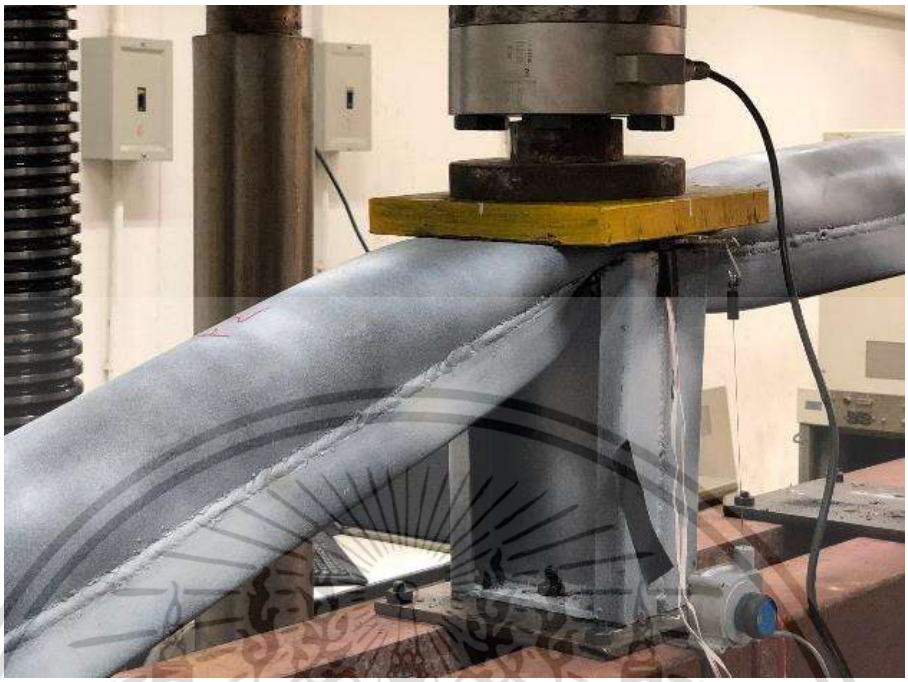

Figure 4.5 Experimental testing of protective beam model result regarding load applied at point P2.

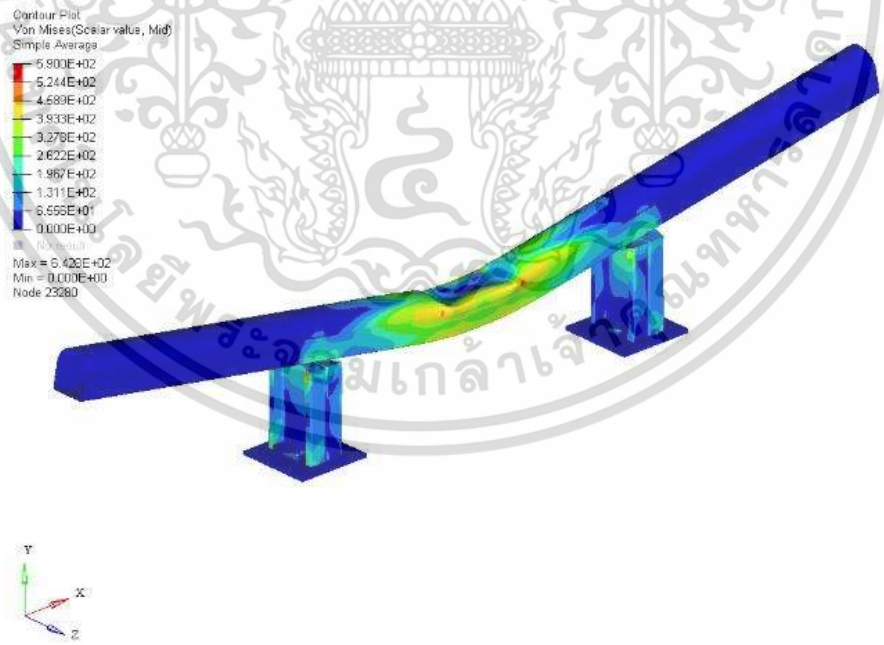

Figure 4.6 Finite element analysis of protective beam model result regarding load applied at point P3.

Figure 4.7 Experimental testing of protective beam model result regarding load applied at point P3.

Based on findings from various academic studies conducted by different researchers, it has been observed that there exists a consistent trend in the results obtained from finite element analysis and experiment tests. The level of disparity between these two sets of data is typically below 10%, and importantly, their trends tend to align closely. Such a discrepancy of less than 10% is generally regarded as a favorable error in the context of their relationship [5, 6, 17, 18].

Despite the good correlation between the maximum reaction force obtained from experimental testing and finite element analysis, the protective beam model failed to meet the requirements of the standard for testing points P1 and P3. The average deviation from the standard across all testing points was 5.4%. Nevertheless, it is worth noting that the trend of the reaction force curve from both experimental testing and finite element analysis was consistent. This suggests that the finite element analysis method, which utilized a non-linear explicit dynamic in RADIOSS with quasi-static loading, is a valid and acceptable means of representing the experimental testing results.

Therefore, while the current protective beam model may not fully meet the requirements of the standard, the finite element analysis method employed in this study is a valuable tool for predicting the performance of the protective beam under different loading conditions. Further modifications and improvements to the protective beam model can be made using this method to optimize its design and enhance its overall effectiveness.

4.2 Strength analysis results of the commercial models I and II

In the case of testing at point, P1, the maximum reaction forces of commercial models I and II are 114kN and 114kN, respectively, as shown in Figures 4.8 and 4.9. The performance of both models in this testing meets the minimum requirement of the standard of 100kN, indicating that both models can withstand a significant amount of force. However, the test did result in some deformation of the protective beam, particularly around the front of the beam close to the left swing arm. This deformation is likely due to the high amount of force applied to that specific area during the test. As shown in Figures 4.10 – 4.11. Despite the damage to the protective beam, the testing point at P1 is important because it represents the worst-case scenario for this component. By subjecting the protective beam to such high forces, the test can help engineers determine the strength and durability of this critical component. By understanding the failure point of the protective beam, engineers can work to improve its design or choose a different material that can better withstand these types of forces.

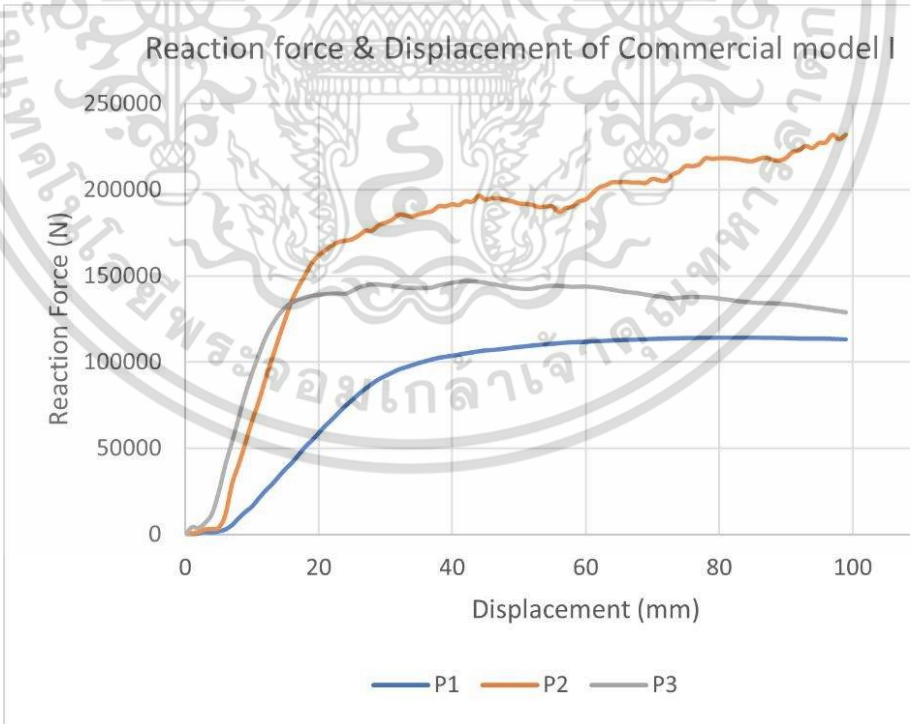

Figure 4.8 Reaction force and displacement of the commercial model I.

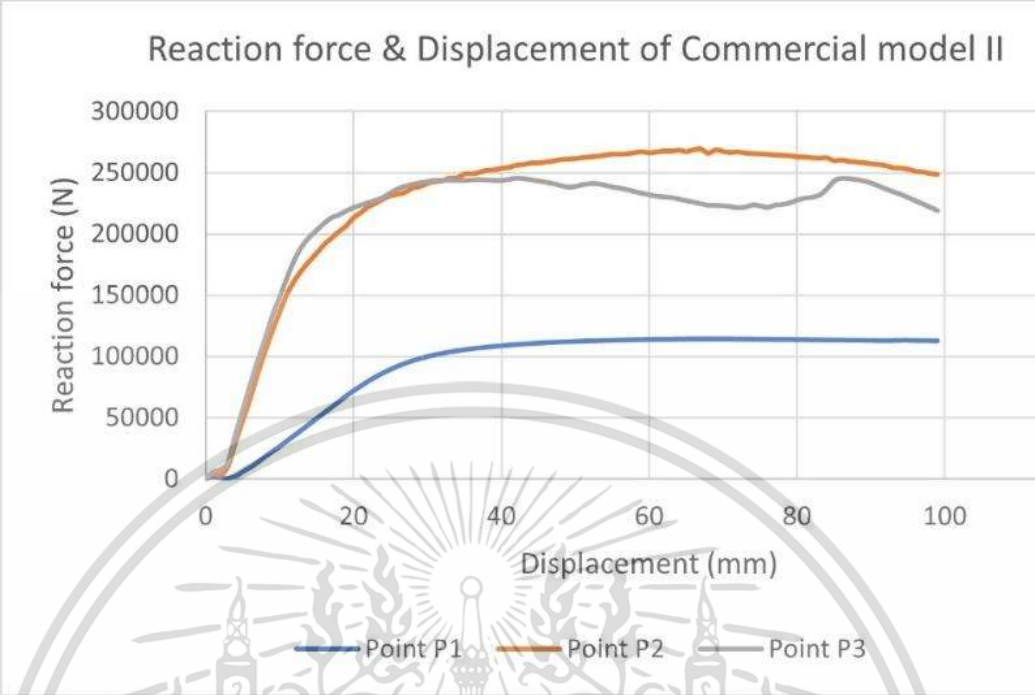

Figure 4.9 Reaction force and displacement of the commercial model II.

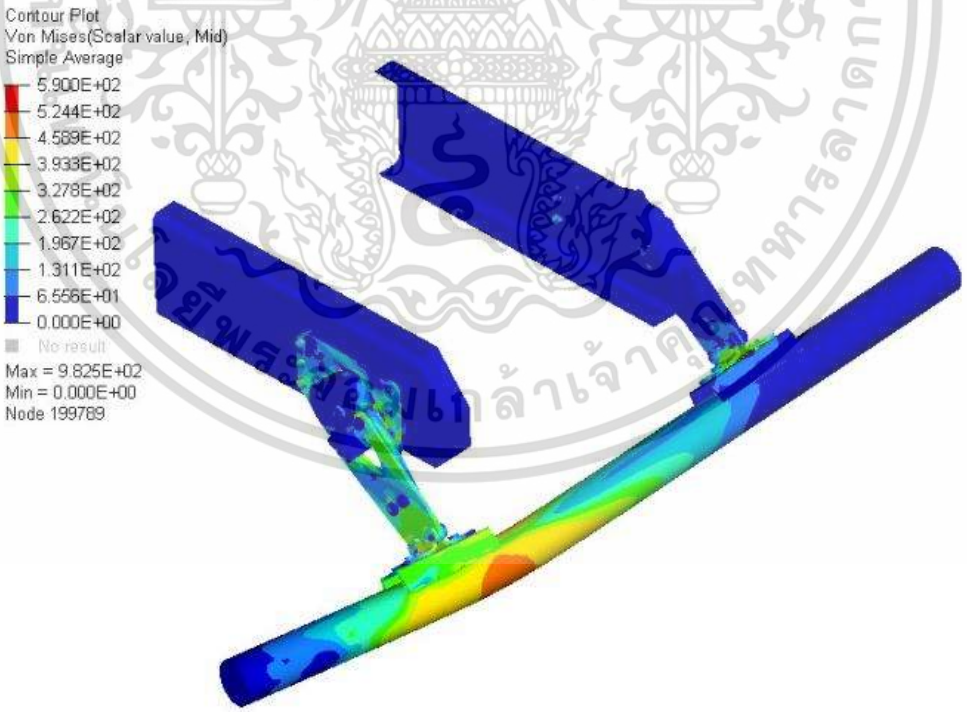

Figure 4.10 Finite of the commercial model I result regarding load applied at point P1.

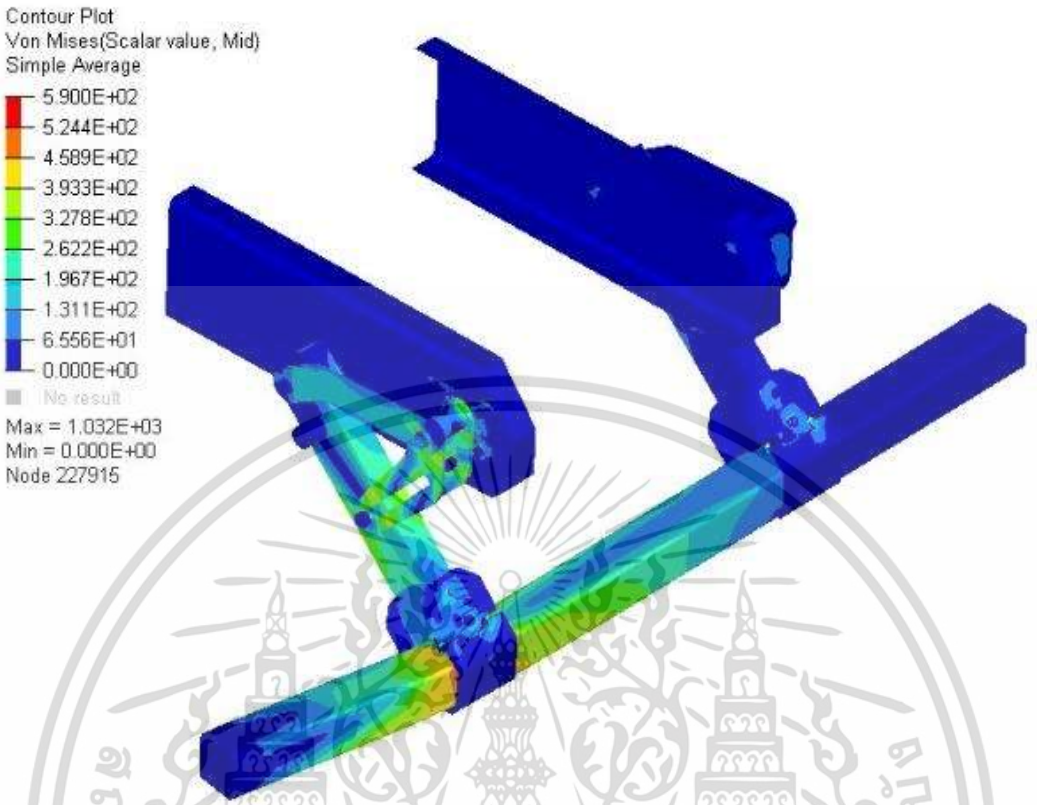

Figure 4.11 Finite of the commercial model II result regarding load applied at point P1.

Moving on to testing at point P2, the maximum reaction force of commercial models I and II are 232kN and 269kN, respectively, as shown in Figures 4.8 and 4.9. This testing point is particularly important because it directly affects the fasteners used to attach the chassis, mounting bracket, and swingarms. As shown in Figures 4.12 – 4.13, the high forces applied during the test caused some deformation in the fasteners. Despite the severe deformation of the swingarm during this test, it was still able to withstand the high loads. This indicates that the design of the swingarm is strong enough to withstand the forces that it is likely to encounter during normal use. Additionally, this testing point may be useful in determining the strength of other components, such as the mounting brackets and other fasteners.

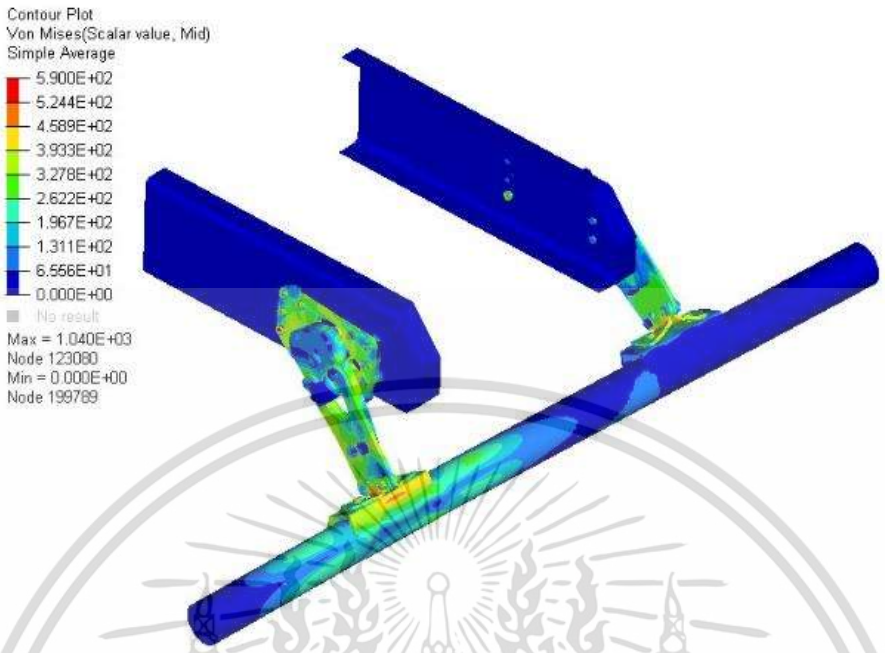

Figure 4.12 Finite of the commercial model I result regarding load applied at point P2.

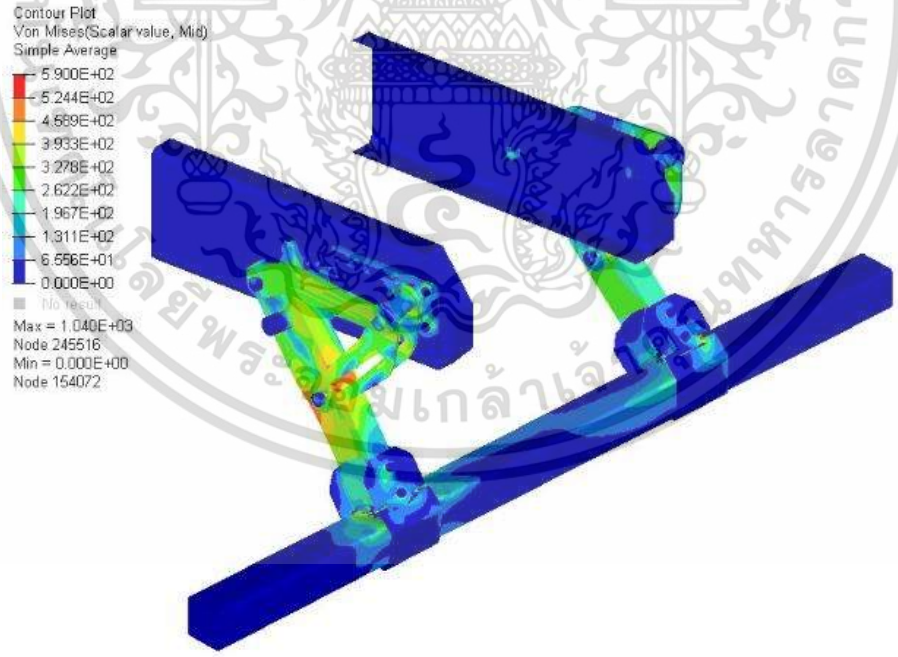

Figure 4.13 Finite of the commercial model II result regarding load applied at point P2.

Finally, testing at point P3 resulted in maximum reaction forces of 147kN and 245kN for commercial models I and II, respectively, as shown in Figures 4.8 and 4.9. Like the other testing points, the performance of both models in this test met the minimum requirement of the standard of 100kN. However, the protective beam and swing arm in this test were both directly affected, with significant deformation occurring in the center of the protective beam and little deformation around both swing arms. As shown in Figures 4.14 – 4.15, the results of this test were much higher than the standard, indicating that this testing point is less harmful to the RUPD compared to other points.

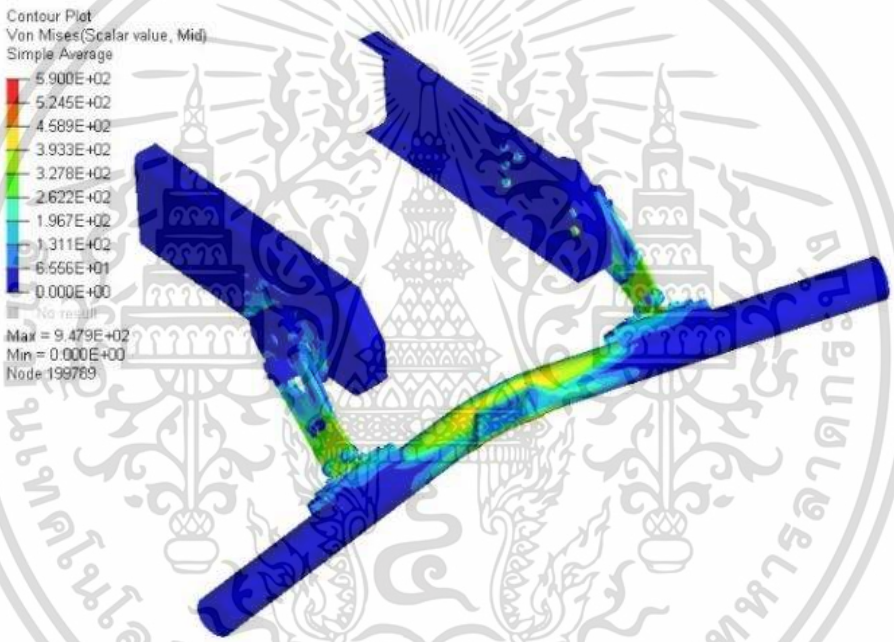

Figure 4.14 Finite of the commercial model I result regarding load applied at point P3.

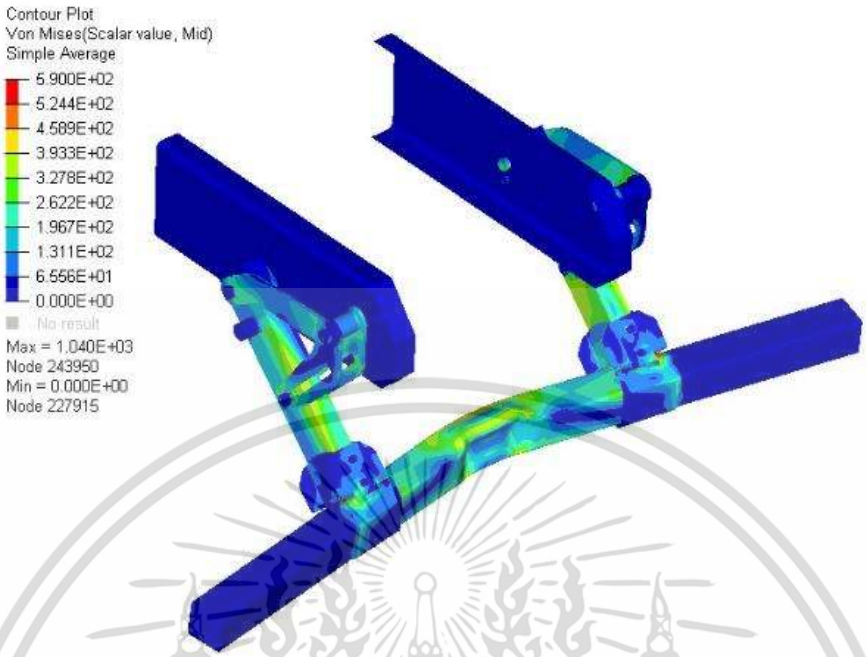

Figure 4.15 Finite of the commercial model II result regarding load applied at point P3.

4.3 Strength analysis results of the purposed design model.

Design case 1 represents the use of the maximum thickness of materials specified in Table 4.1. This design case is aimed at understanding the behavior of the RUPD at each testing point. The results obtained from testing point P1 showed that it had the most impact on the protective beam and a minor impact on the mounting brackets and swing arms. The maximum stress experienced during testing was found to be 459 MPa. Testing point P2, on the other hand, had the most impact on the mounting brackets and swing arms, with a maximum stress of 393 MPa. Finally, testing point P3 had the most significant effect on the center of the protective beam, with a minor impact on the pair of swing arms, with a maximum stress of 393 MPa, as shown in Figures 4.16 to 4.18.

Table 4.1 Properties of foldable RUPD design case 1.

Design case	Protective beam type	Mounting brackets thickness	Swing arms thickness	weight
		mm	mm	kg
1	Square tube 125 x 125 t = 6 mm	12	20	121

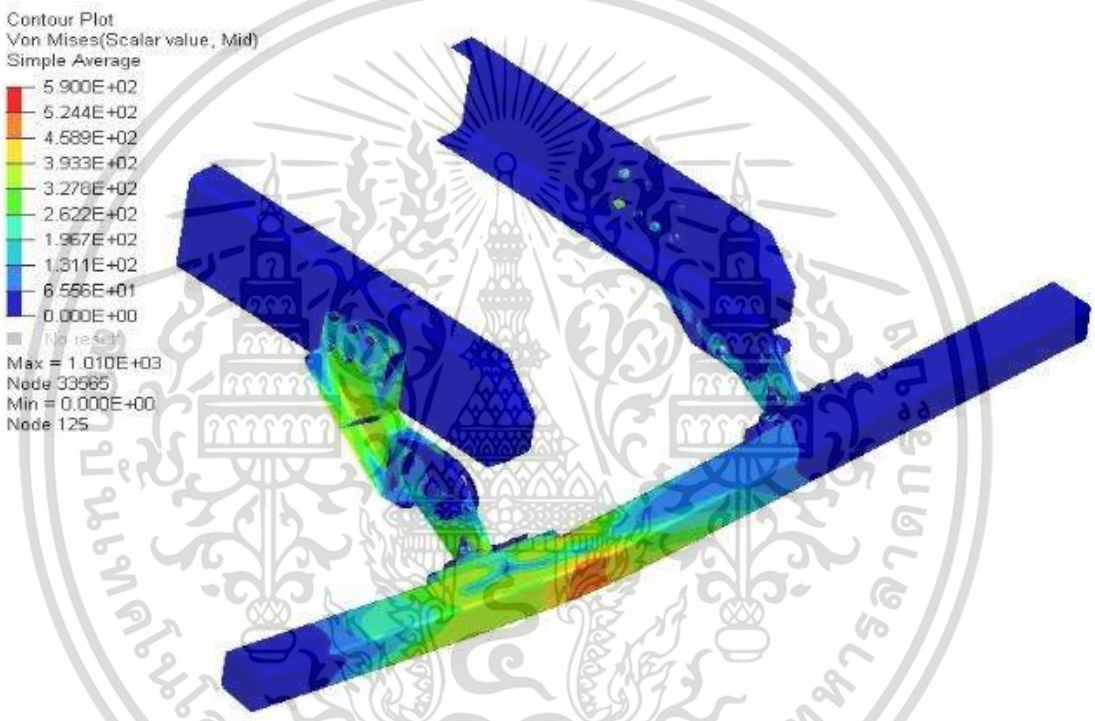

Figure 4.16 Result of design case 1 testing points P1.

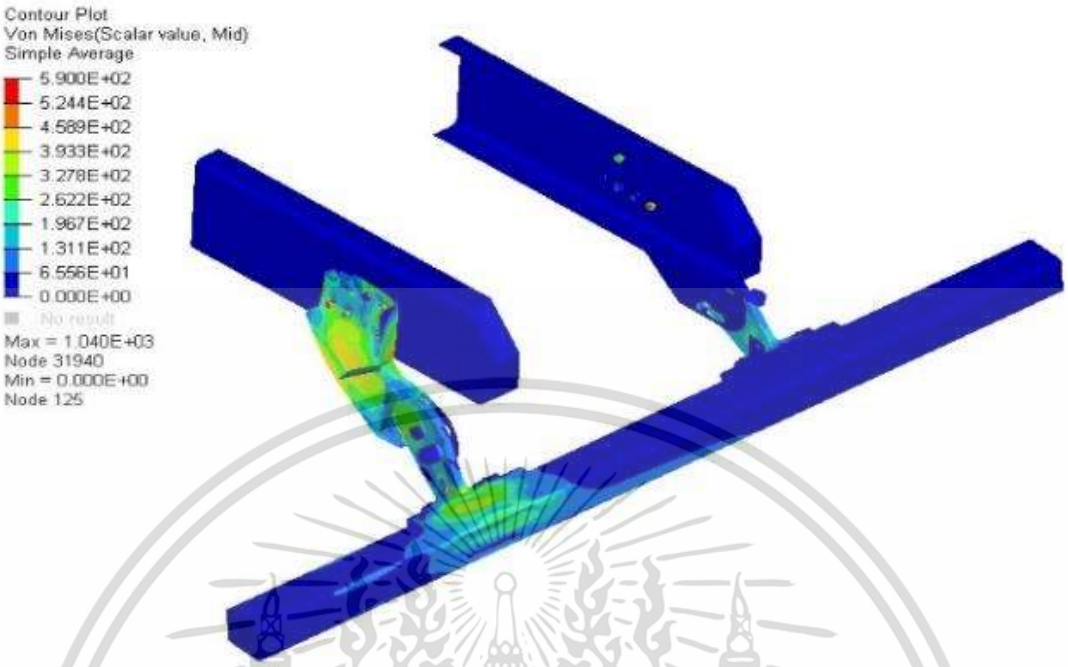

Figure 4.17 Result of design case 1 testing points P2.

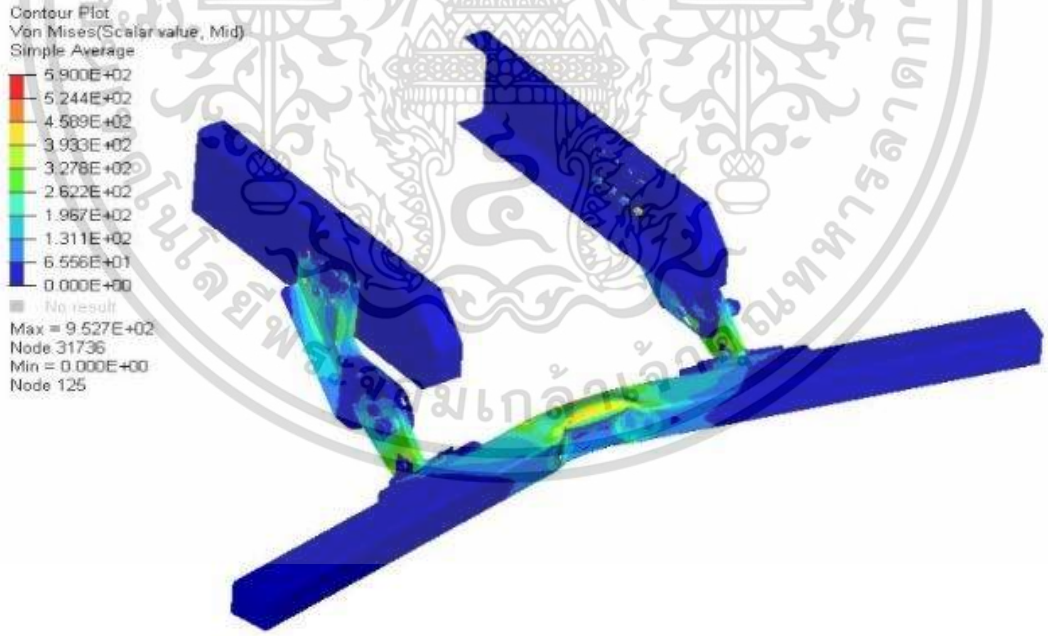

Figure 4.18 Result of design case 1 testing points P3.

Figure 4.19 shows the reaction force versus displacement of design case 1 at testing points P1, P2, and P3. It is noteworthy that the maximum reaction forces of testing point P1 and P3 were higher than the required value of 100 kN specified in UN Regulation No.58. The reaction force of testing point P2, however, was found to be greater than the required value of 180 kN. Table 4.2 shows that all testing points passed the requirements of UN Regulation No. 58 for maximum reaction force, while the result of displacement at the maximum reaction force of all testing points did not exceed the specified value of 300 mm.

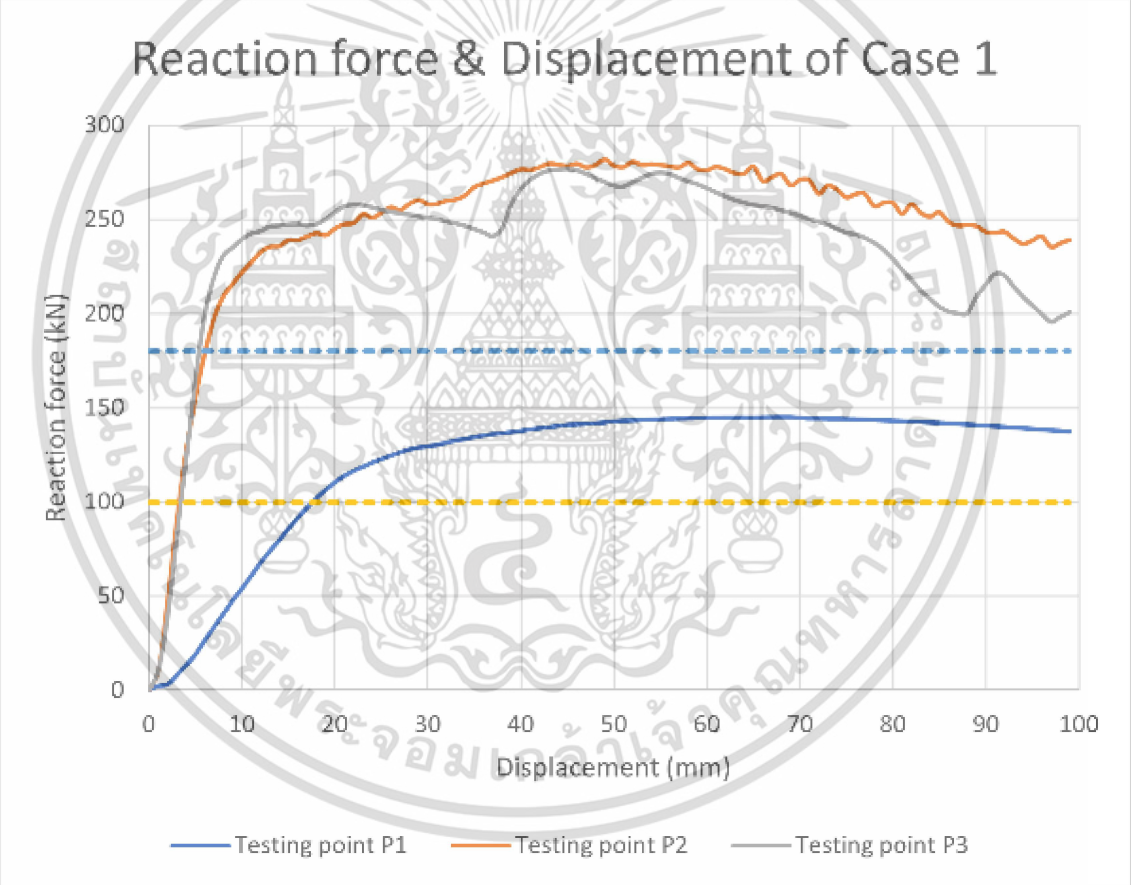

Figure 4.19 Reaction force & displacement of case 1.

Table 4.2 Foldable RUPD design case 1 finite element analysis result.

Design case	Maximum reaction force P1	Maximum reaction force P2	Maximum reaction force P3	UN Regulation No.58
	kN	kN	kN	
1	145	282	277	pass

Based on the results obtained from Design Case 1, it is evident that the design is overdesigned, resulting in a weight of 121 kg. This weight is still too high and indicates that there is a need to optimize the design. The optimization process involves minimizing the thickness of the materials used in the design without compromising the RUPD's performance.

To achieve this goal, the testing points that had the most impact on the protective beam were analyzed. Testing point P1 was found to have the most effect on the protective beam, with a maximum stress of 459 MPa. Therefore, this testing point was selected to identify the appropriate protective beam cross-section type and thickness to achieve the lightest weight and pass UN Regulation No.58.

To achieve this objective, nine test cases were designed with different protective beam cross-sections and tube thicknesses, as shown in Table 4.3. The goal of these tests was to find the optimal combination of cross-section type and thickness that would meet the UN Regulation No.58 requirements while minimizing the weight of the RUPD.

It should be noted that testing point P3 can handle a much higher load than the value given by the regulation. Therefore, this study is not the primary focus at this point. The testing point P2 had the most impact on mounting brackets and swing arms, with a maximum stress of 393 MPa. However, the results showed that all testing points passed much higher than the regulation.

Table 4.3 Properties of foldable RUPD design case 1-9.

Case	Protective beam type	Thickness	weight
		mm	kg
1	Square tube	6	121
2	Round tube	6	119
3	Round tube & C plate	6	125
4	Square tube	4.5	109
5	Round tube	4.5	108
6	Round tube & C plate	4.5	116
7	Square tube	3.2	98
8	Round tube	3.2	98
9	Round tube & C plate	3.2	108

Based on the results obtained from the tests conducted on Design cases 1-9, it is evident that the displacement at the maximum reaction force for each of the design cases ranges between 50-60 mm, which meets the regulatory requirements, as shown in Figure 4.29. After analyzing the results of the tests and considering the weight of the materials used, it was concluded that a tube thickness of 6 mm is too heavy to withstand the load. On the other hand, a tube thickness of 3.2 mm cannot resist the standard load. Therefore, a tube thickness of 4.5 mm is found to be the most suitable for the foldable RUPD design.

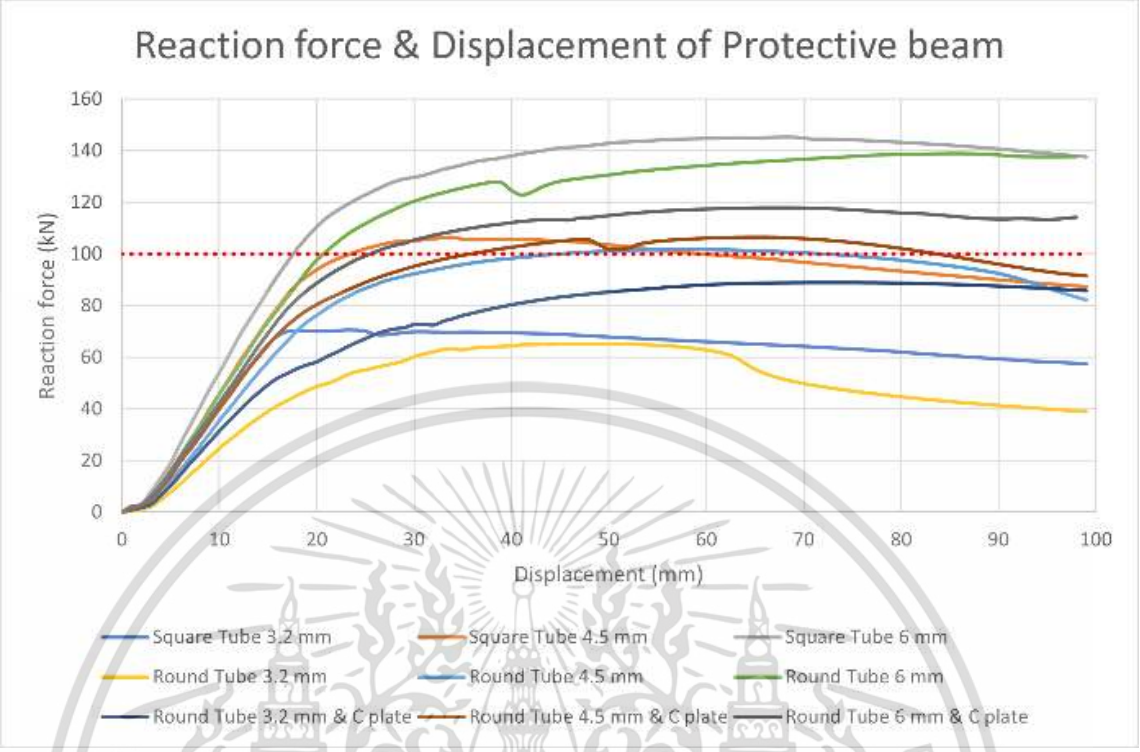

Figure 4.20 Reaction force & displacement of cases 1-9.

Nine different test cases were conducted using different protective beam cross-sections and tube thicknesses, as shown in Table 4.3. Among the cross-sections, the round tube mixed with a C-folded plate cross-section was found to be the heaviest, followed by the square tube cross-section, and the round tube cross-section was the lightest. The maximum stress was observed on the front surface of the protective beam near the support point, and it was found to be around 459 MPa. Most of the stresses observed in this study were found to be greater than the yield stress of materials but lower than the ultimate strength of materials, indicating nonlinear material behavior. Consequently, the deformation after these tests is permanent.

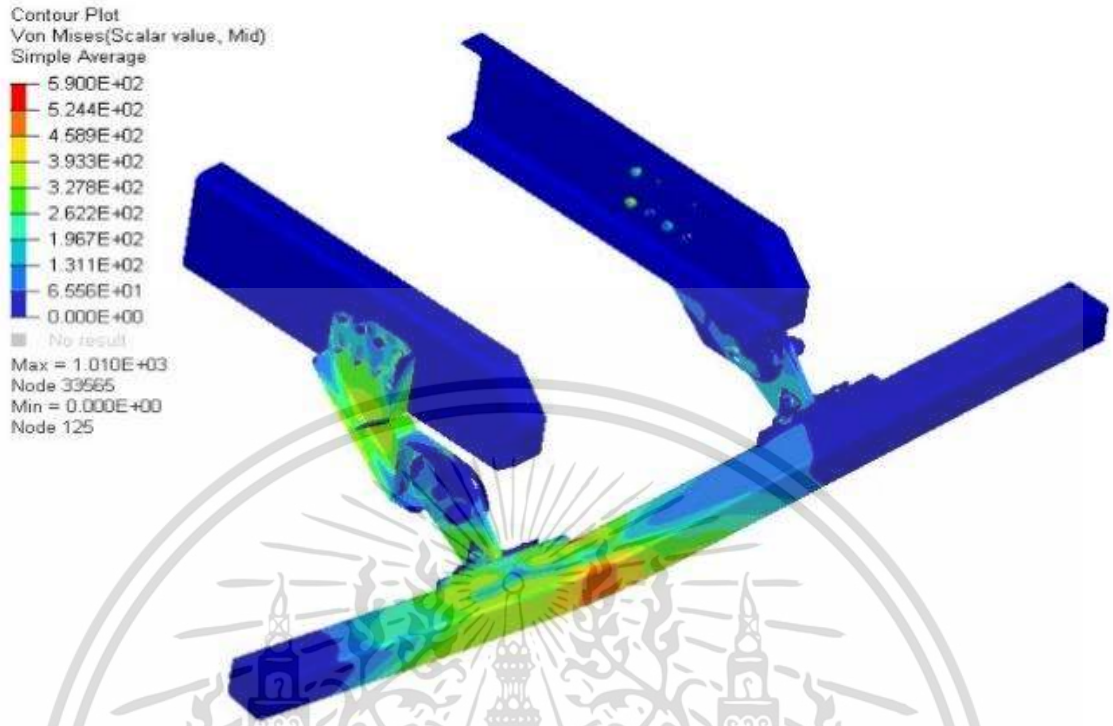

Figure 4.21 Result of design case 1 testing point P1.

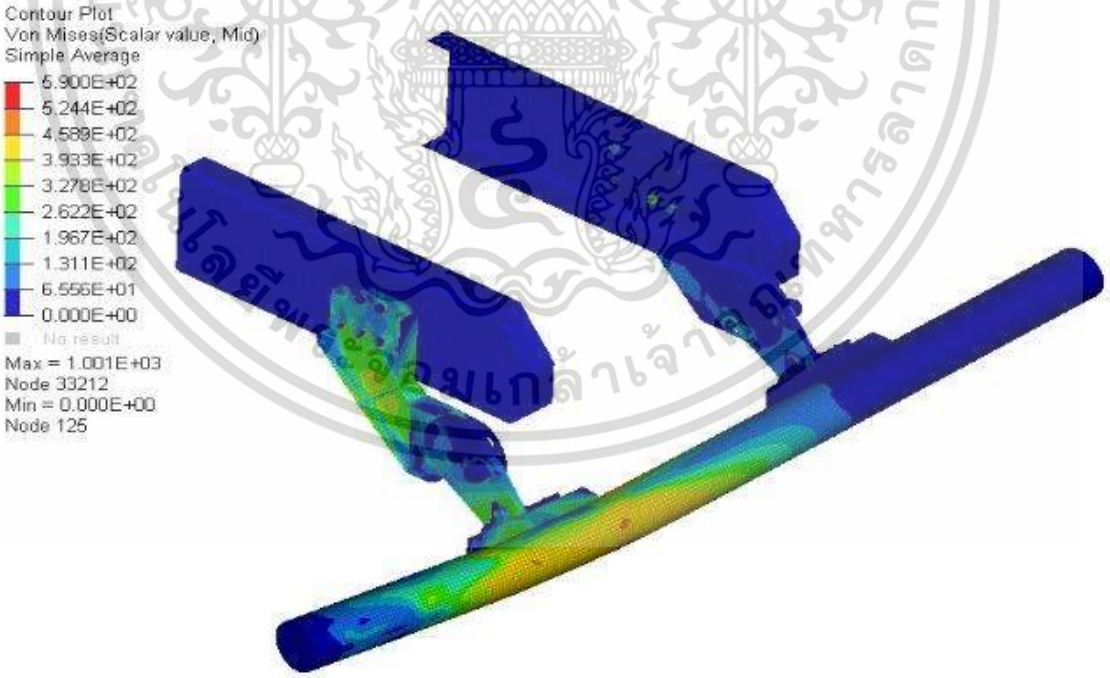

Figure 4.22 Result of design case 2 testing point P1.

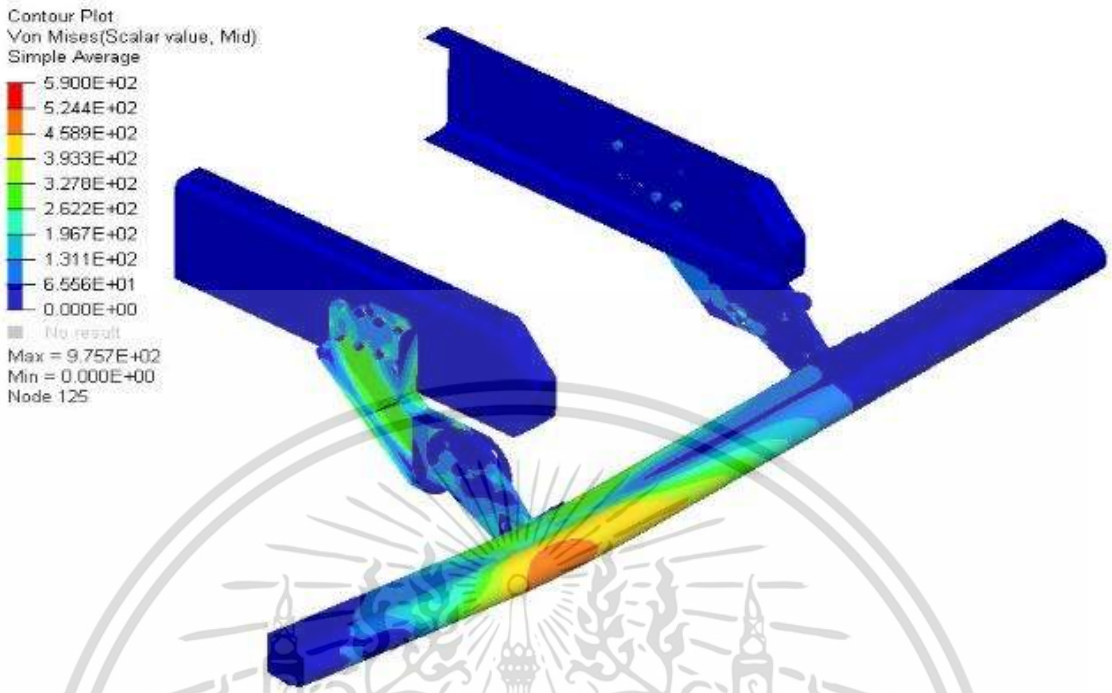

Figure 4.23 Result of design case 3 testing point P1.

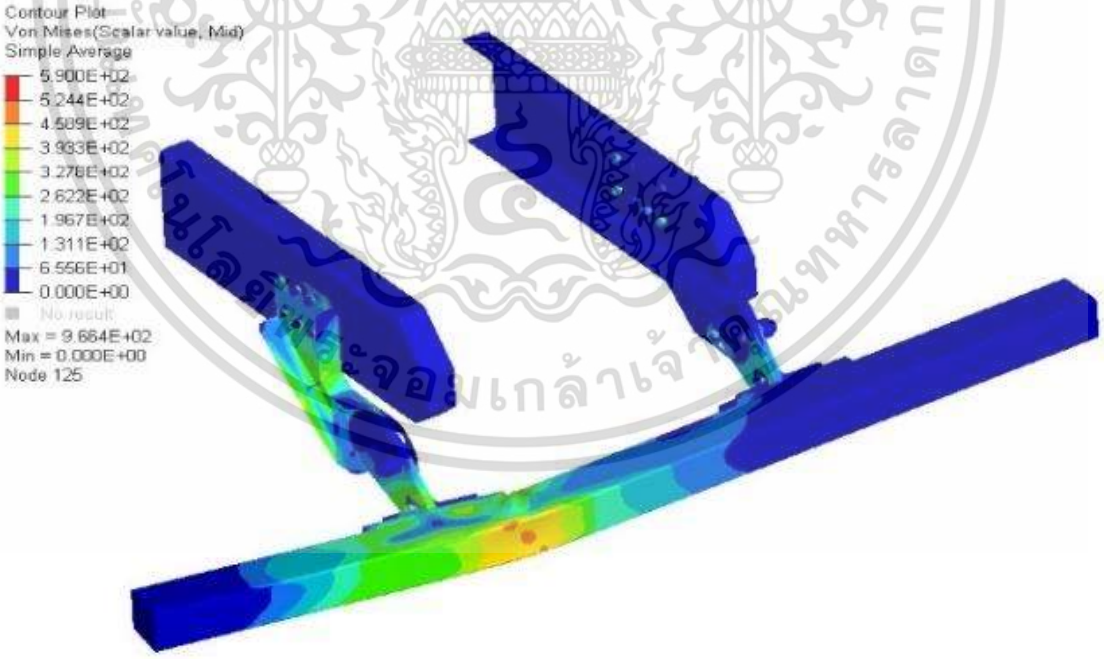

Figure 4.24 Result of design case 4 testing point P1.

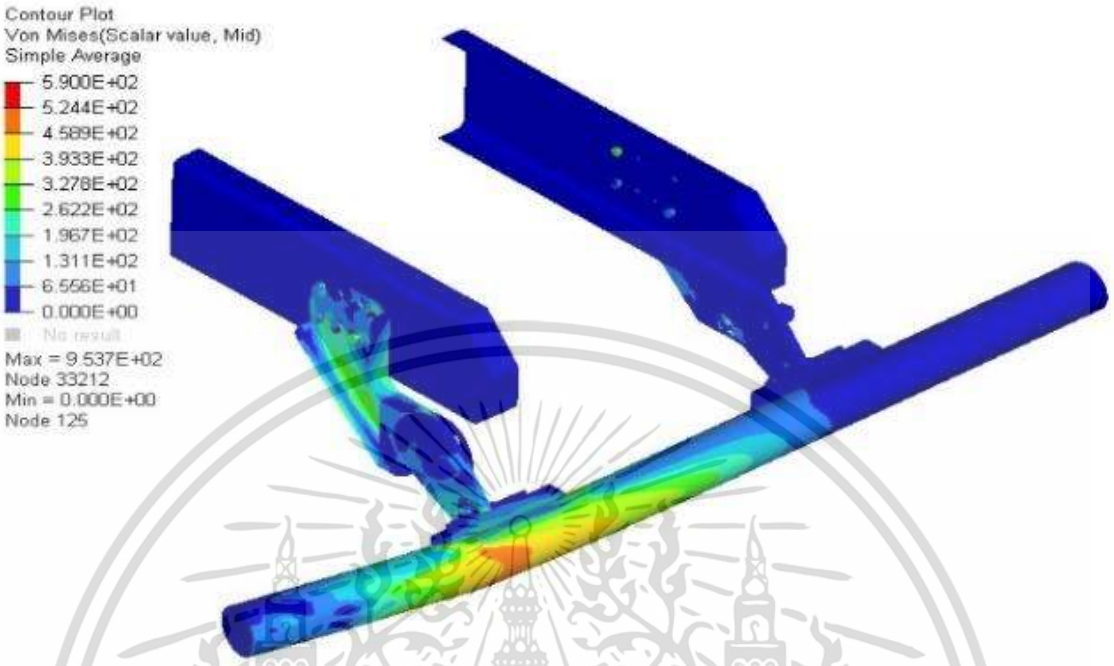

Figure 4.25 Result of design case 5 testing point P1.

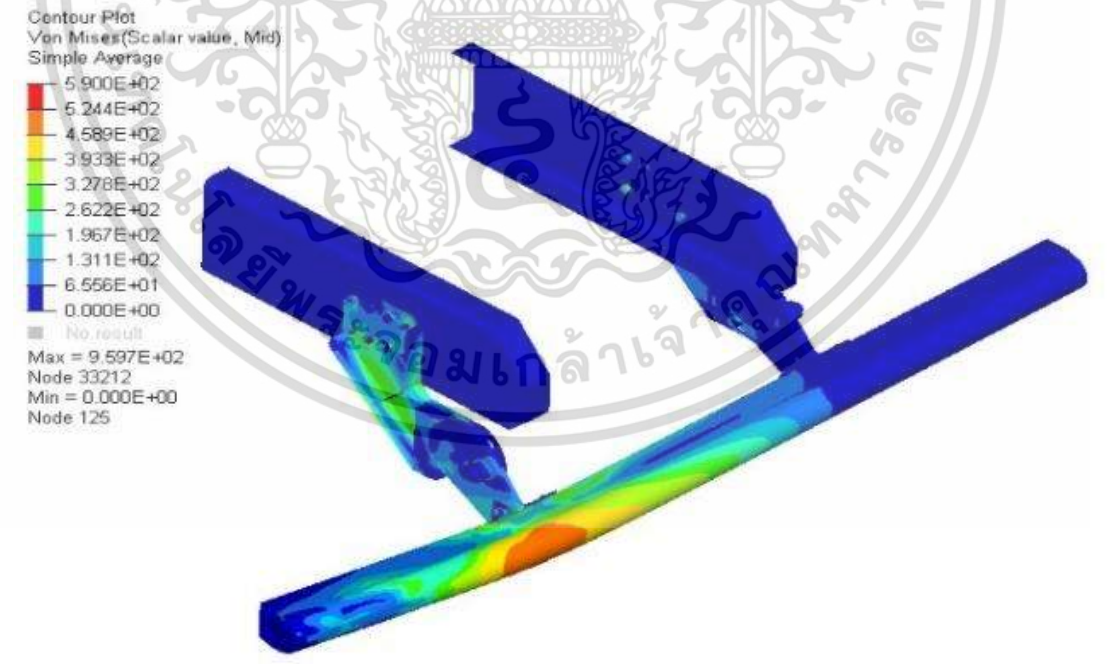

Figure 4.26 Result of design case 6 testing point P1.

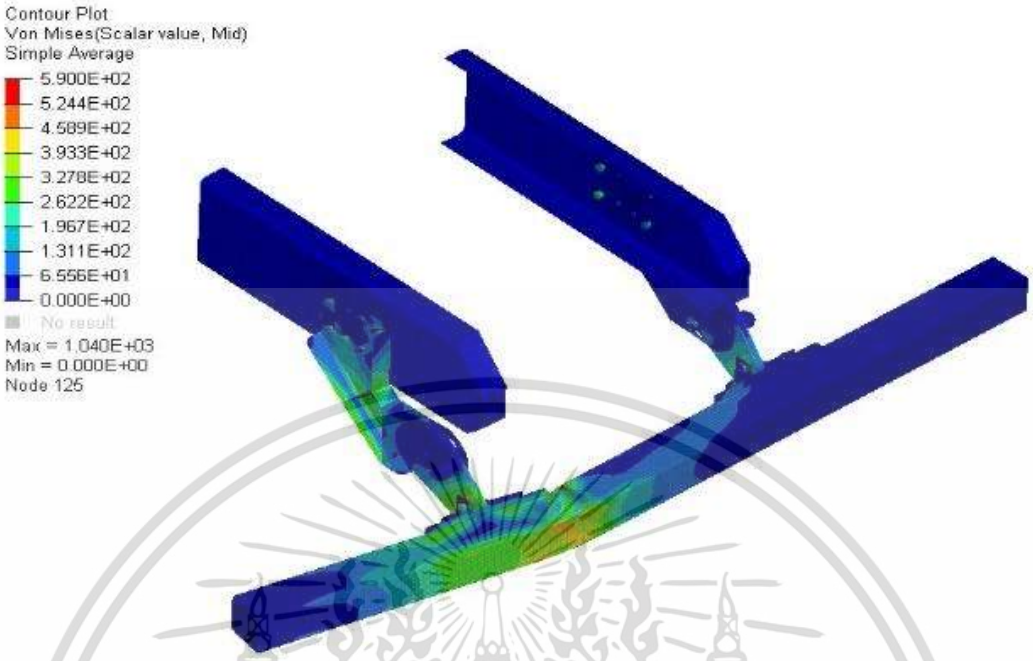

Figure 4.27 Result of design case 7 and case 8 testing point P1.

Figure 4.28 Result of design case 7 and case 8 testing point P1.

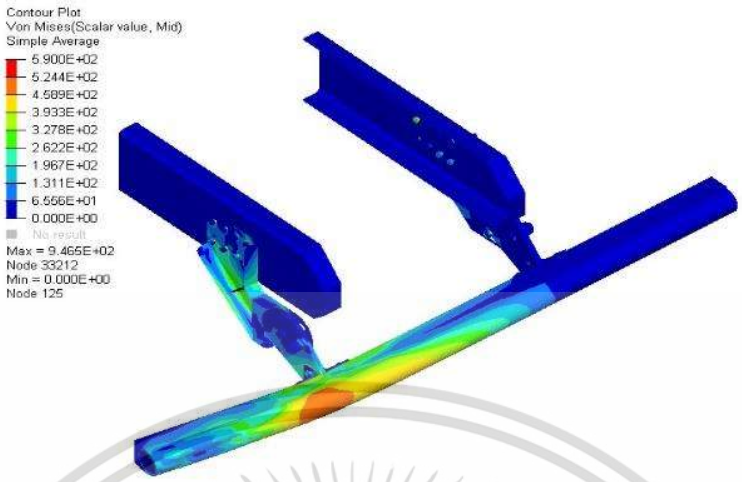

Figure 4.29 Result of design case 9 testing point P1

Table 4.4 Foldable RUPD design case 1-9 finite element analysis result.

Design case	Maximum Reaction Force P1	Maximum Reaction force P1 to weight ratio	UN Regulation No.58
	kN	kN/kg	
1	145	1.20	pass
2	139	1.17	pass
3	118	0.94	pass
4	106	0.98	pass
5	102	0.95	pass
6	107	0.92	pass
7	71	0.72	not pass
8	65	0.67	not pass
9	89	0.82	not pass

When considering the load-carrying capacity and force-to-weight ratio, the round tube was found to withstand fewer loads than the square tube, and the square tube had a higher force-to-weight ratio. Therefore, it was concluded that the cross-section of a square tube protective beam with a thickness of 4.5 mm or design case 4 is the best choice.

After analyzing the results of the previous design cases, the weight of design case 4 is still heavy, even though it is an improvement from design case 1. Therefore, there is a need to continue optimizing the design of the RUPD by varying the thicknesses of the mounting brackets, swing arms, and other critical components. For this purpose, design cases 10 - 21 have been developed, with a focus on testing points P1 and P2. The square tube with a thickness of 4.5 mm is still used as the protective beam, but the mounting brackets and swing arms are now made of different thicknesses, as shown in Table 4.5. These design cases aim to identify the optimal combination of material thicknesses that will result in the lightest weight RUPD while still meeting the requirements of UN Regulation No. 58.

Table 4.5 Properties of foldable RUPD design case 10 - 21.

Design case	Mounting brackets		Swing arms thickness	weight
	fully	without center rib		
	thickness			
	mm	mm	mm	kg
10	12	-	20	109
11	9	-	20	101
12	-	12	20	106
13	-	9	20	98
14	12	-	15	105
15	9	-	15	97
16	-	12	15	102
17	-	9	15	94
18	12	-	12	102
19	9	-	12	94
20	-	12	12	99
21	-	9	12	92

Among the design cases tested, it was found that all the design cases at testing point P2 exceeded the minimum force requirement. This finding meant that other factors needed to be considered in selecting the optimal design case. After a comprehensive evaluation of the design cases, the criteria to choose the best design case was based on the total weight and force-to-weight ratio of testing point P1.

Table 4.6 Foldable RUPD design case 10 - 21 finite element analysis result.

Design case	Maximum reaction force P1	Maximum reaction force P2	Maximum reaction force P1 to weight ratio	Maximum Reaction force P2 to weight ratio	UN Regulation No.58
	kN	kN	kN/kg	kN/kg	
10	106	254	0.98	2.33	Pass
11	102	215	1.01	2.13	Pass
12	103	244	0.97	2.30	Pass
13	98	202	0.99	2.06	not pass
14	103	253	0.98	2.41	Pass
15	100	215	1.03	2.22	pass
16	100	244	0.99	2.40	Pass
17	96	198	1.02	2.10	not pass
18	102	252	1.00	2.46	Pass
19	99	213	1.05	2.26	not pass
20	100	238	1.00	2.40	pass
21	96	194	1.04	2.11	not pass

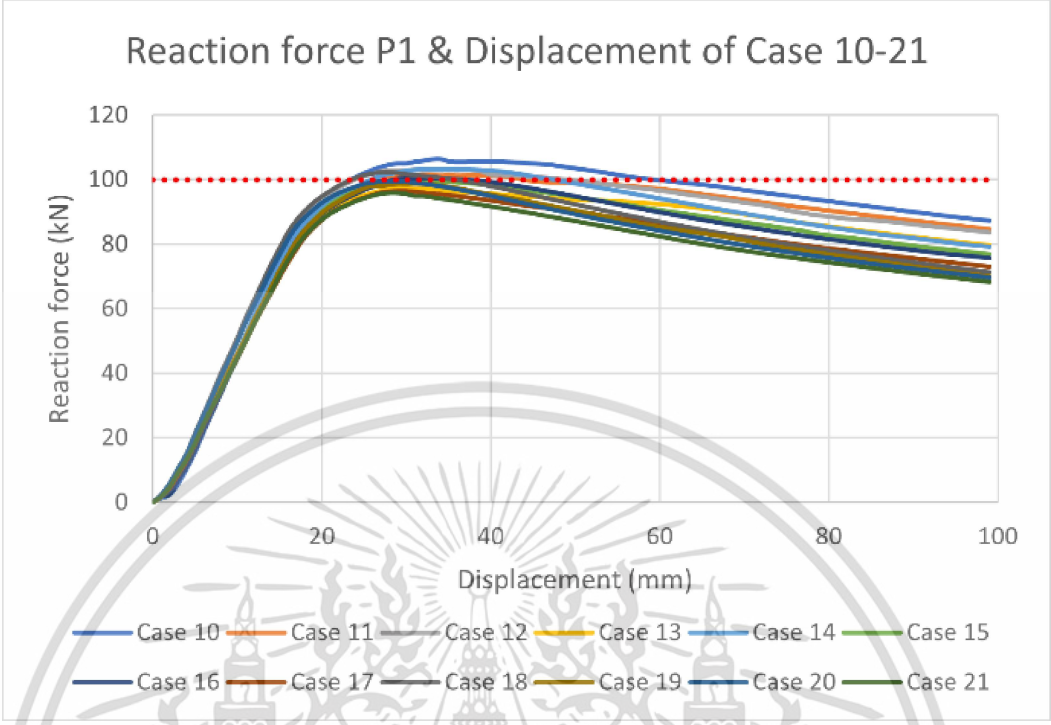

Figure 4.30 Reaction force P1 & displacement of cases 10-21.

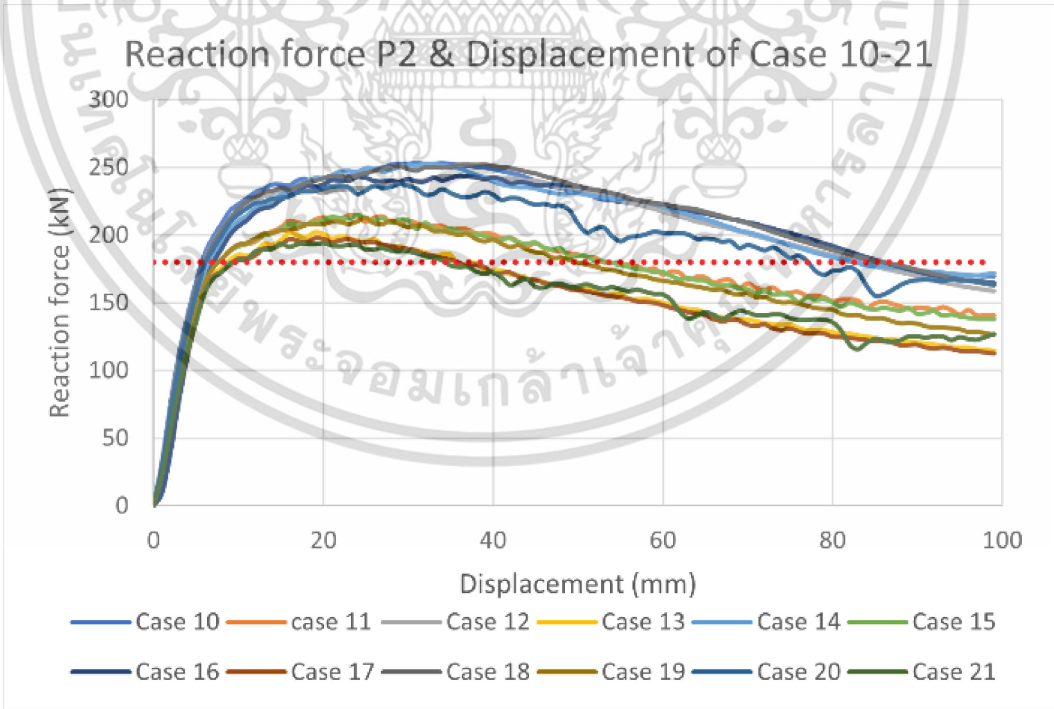

Figure 4.31 Reaction force P2 & displacement of cases 10-21.

The maximum stress from testing point P1 and P2 on the front surface of the protective beam near the support of the swing arm and on the rear side of the mounting bracket. The maximum stress in design cases 10 - 21 is higher than the yield stress leading to nonlinear material behavior as shown in Figure 4.32 – 4.55. The deformation following these tests is permanent. Displacements of design cases 10 - 21 at maximum reaction force at testing points P1 and P2 mostly are about 20 - 40 mm which does not exceed the requirement of UN regulation No.58 of 300 mm as shown in Figure 4.30 – 4.31.

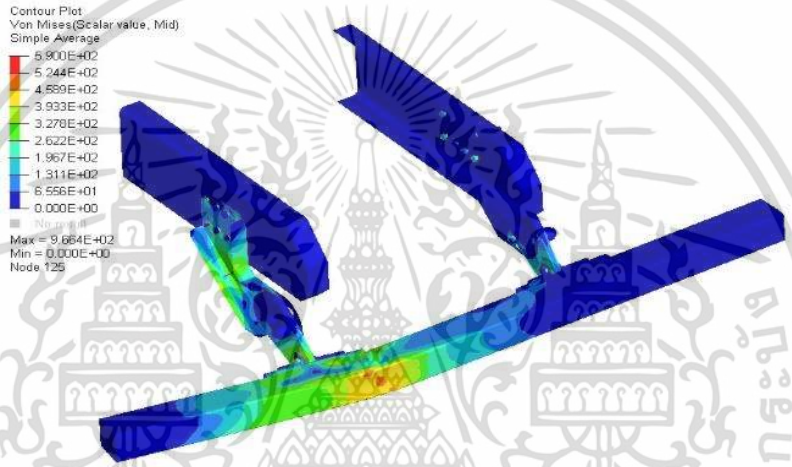

Figure 4.32 Result of design case 10 testing point P1.

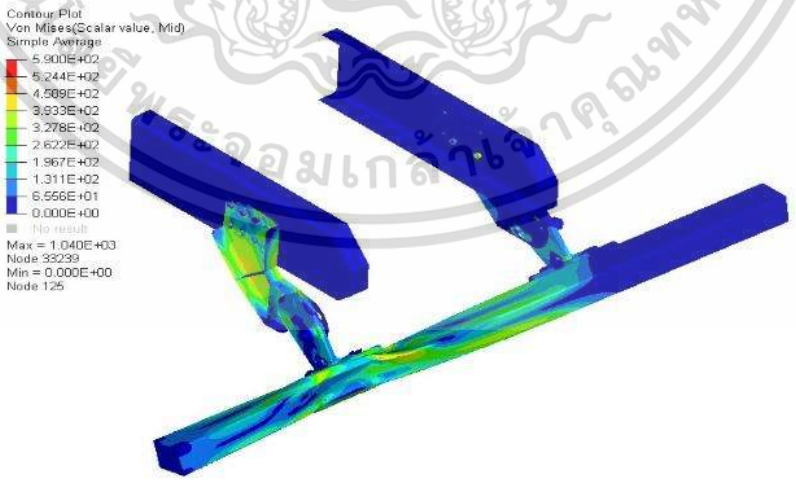

Figure 4.33 Result of design case 10 testing point P2.

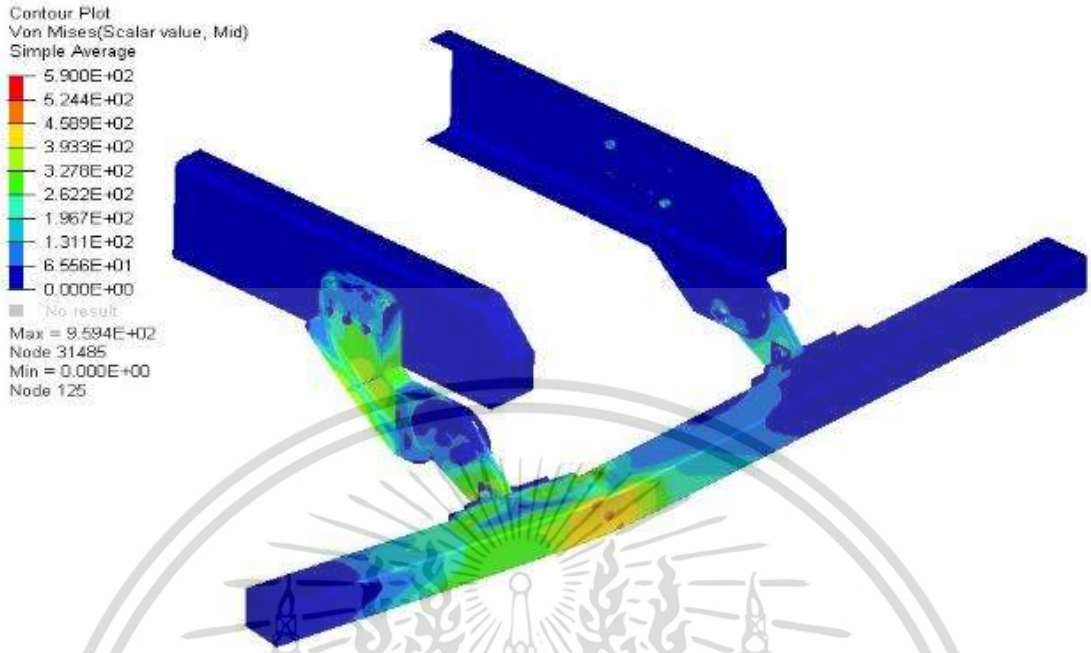

Figure 4.34 Result of design case 11 testing point P1.

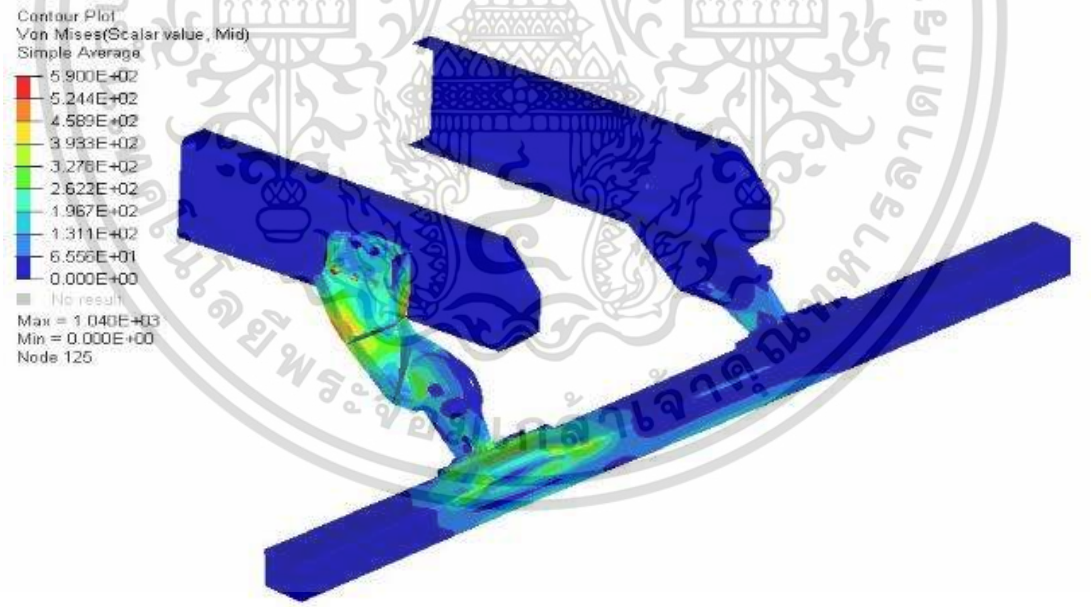

Figure 4.35 Result of design case 11 testing point P2.

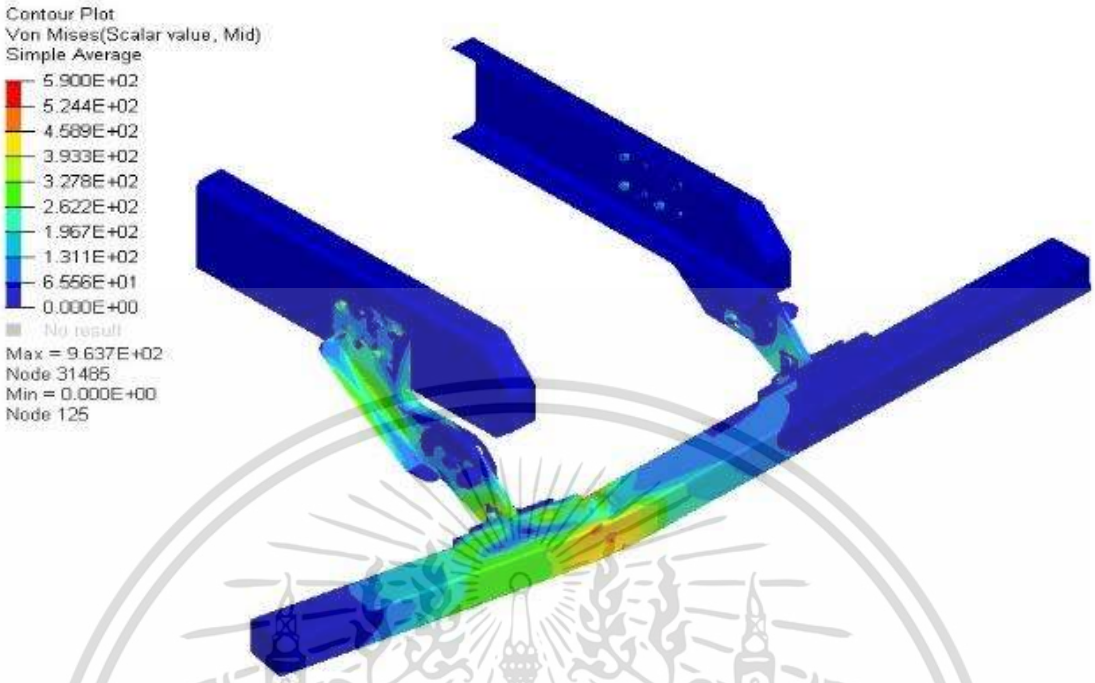

Figure 4.36 Result of design case 12 testing point P1.

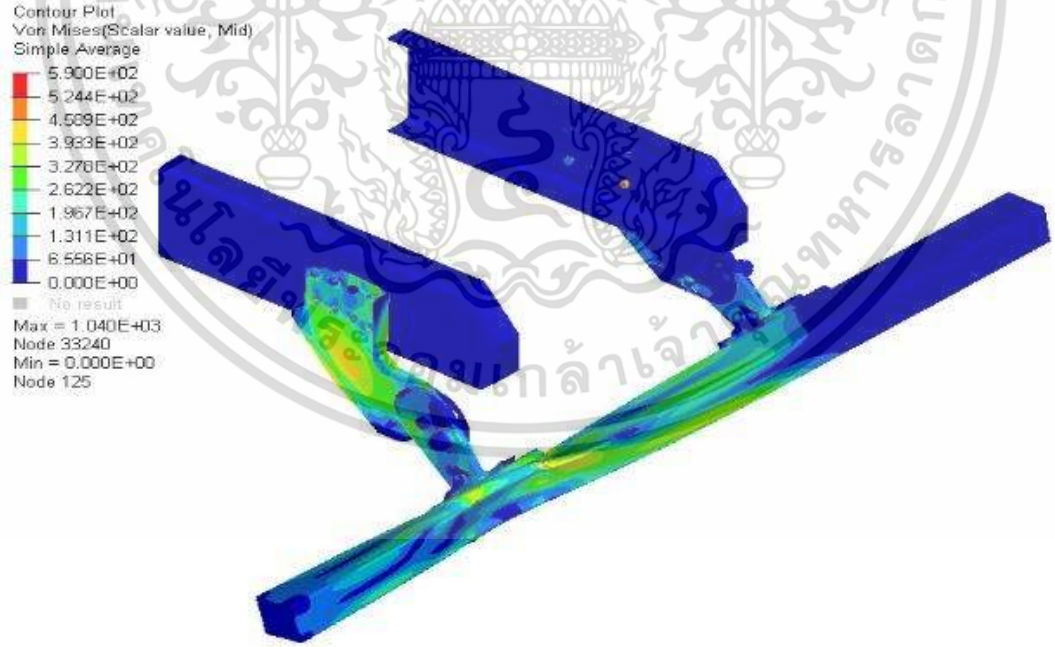

Figure 4.37 Result of design case 12 testing point P2.

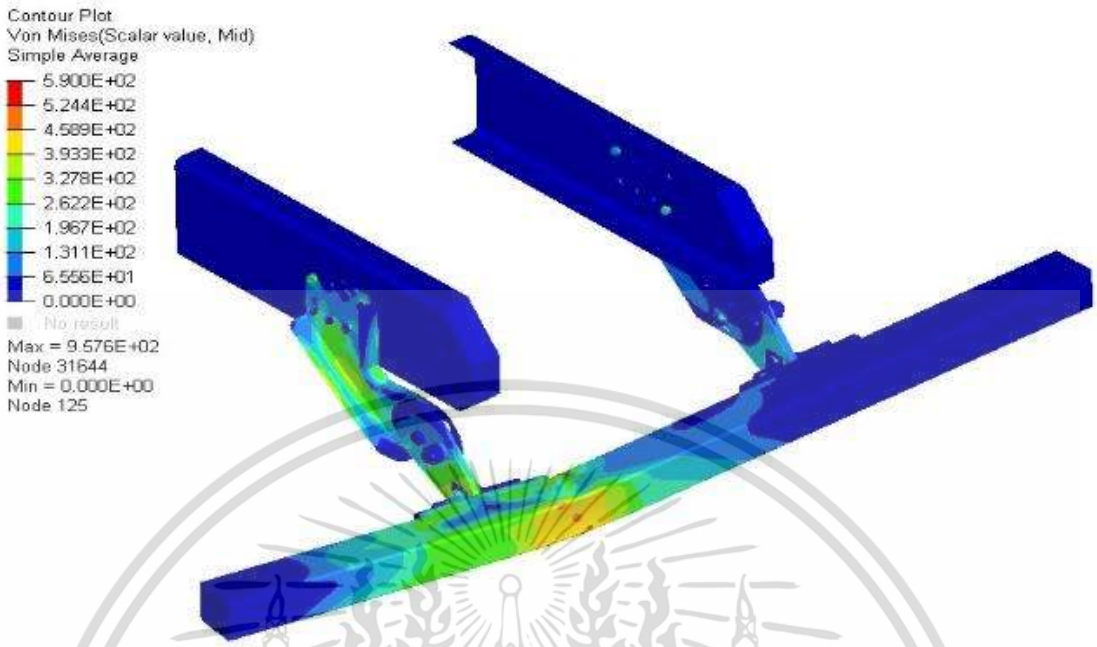

Figure 4.38 Result of design case 13 testing point P1.

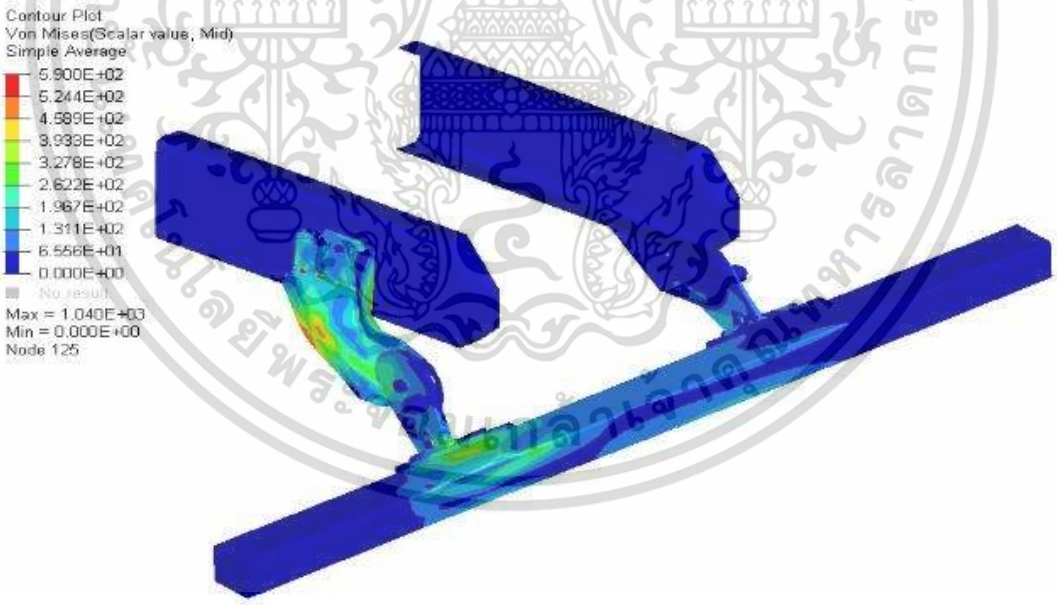

Figure 4.39 Result of design case 13 testing point P2.

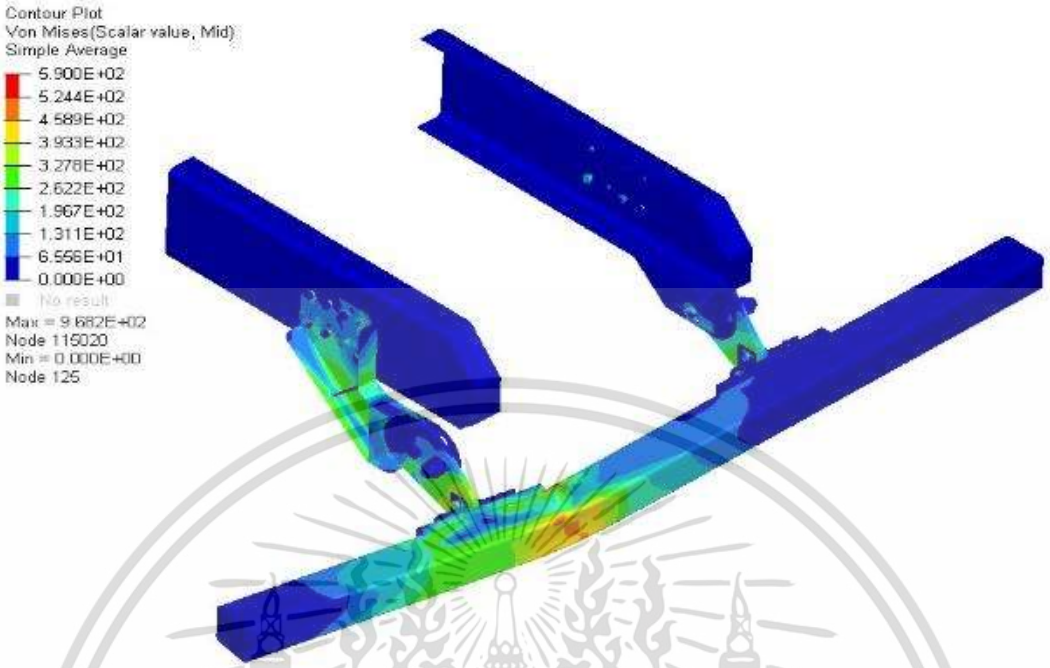

Figure 4.40 Result of design case 14 testing point P1.

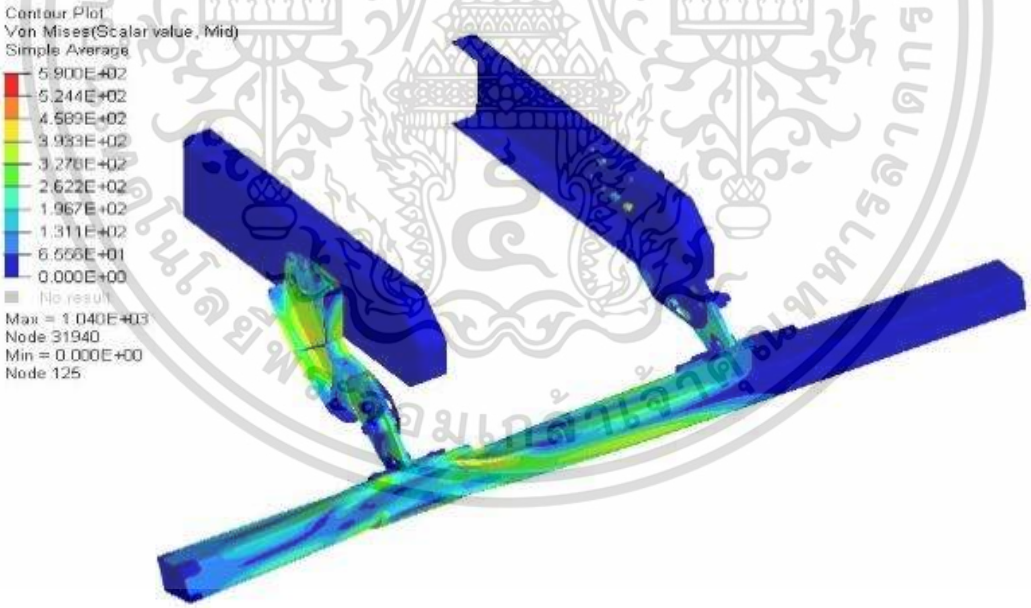

Figure 4.41 Result of design case 14 testing point P2.

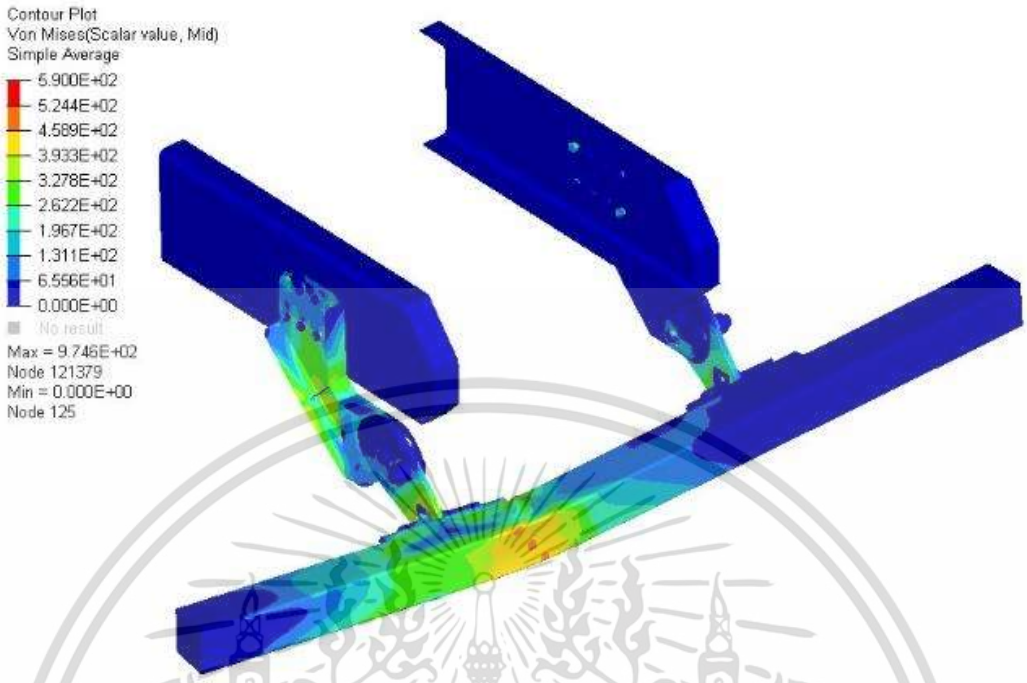

Figure 4.42 Result of design case 15 testing point P1.

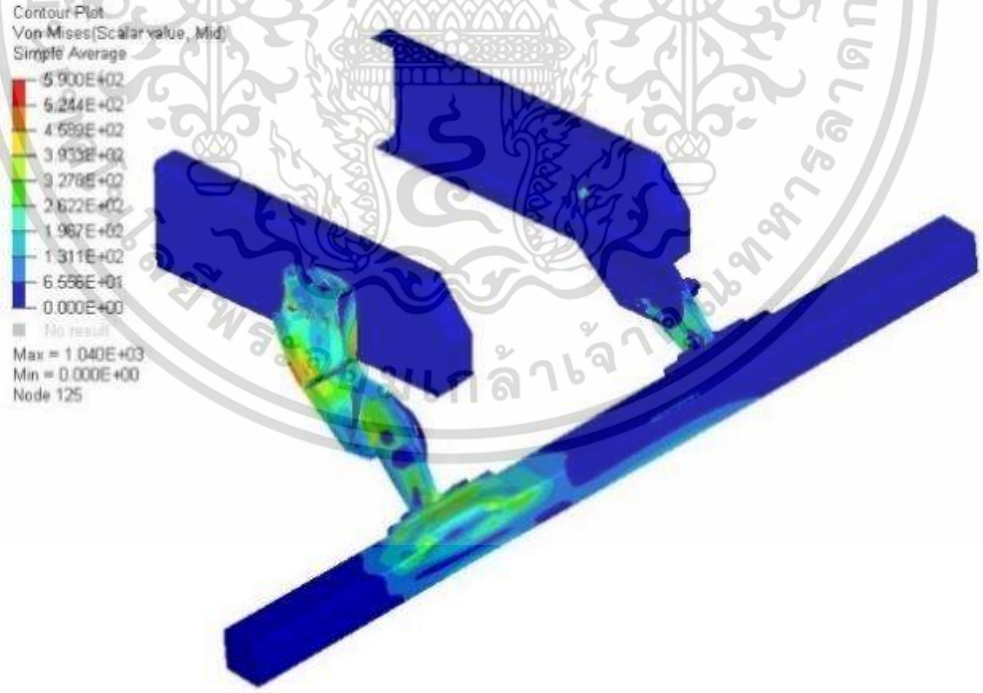

Figure 4.43 Result of design case 15 testing point P2.

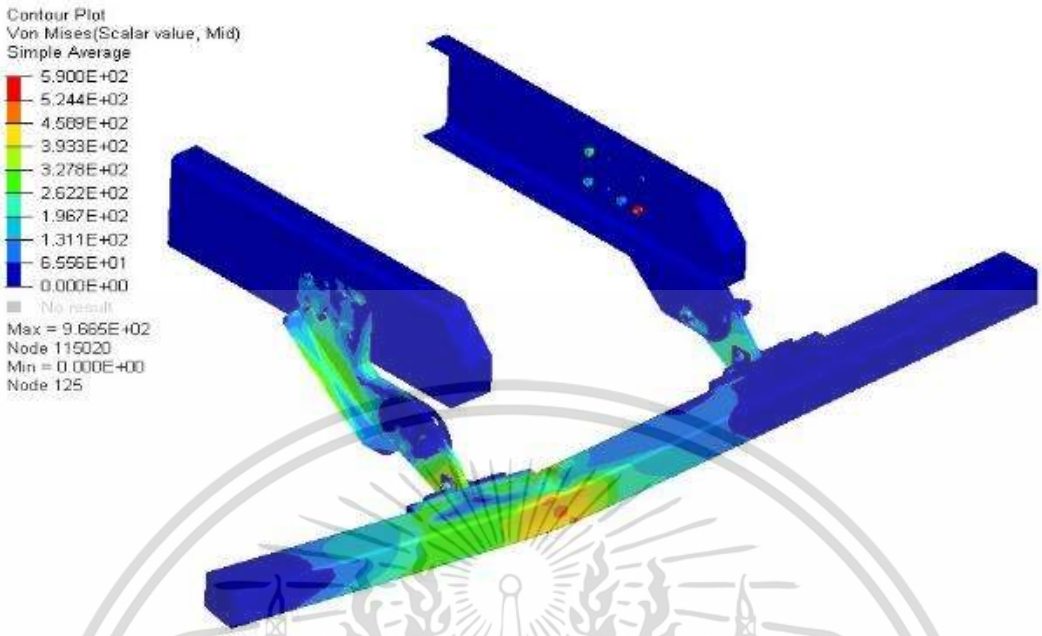

Figure 4.44 Result of design case 16 testing point P1.

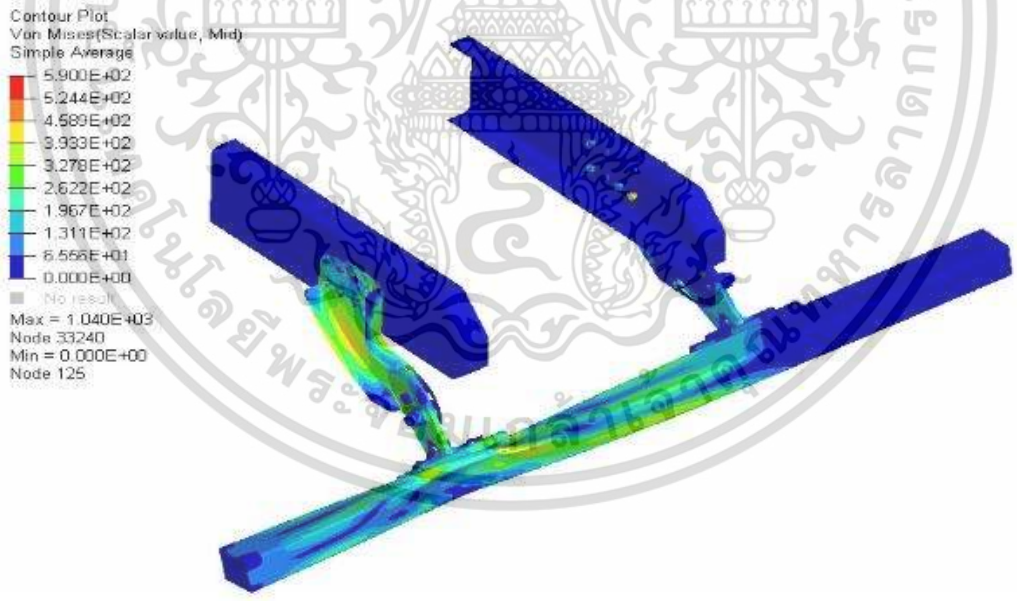

Figure 4.45 Result of design case 16 testing point P2.

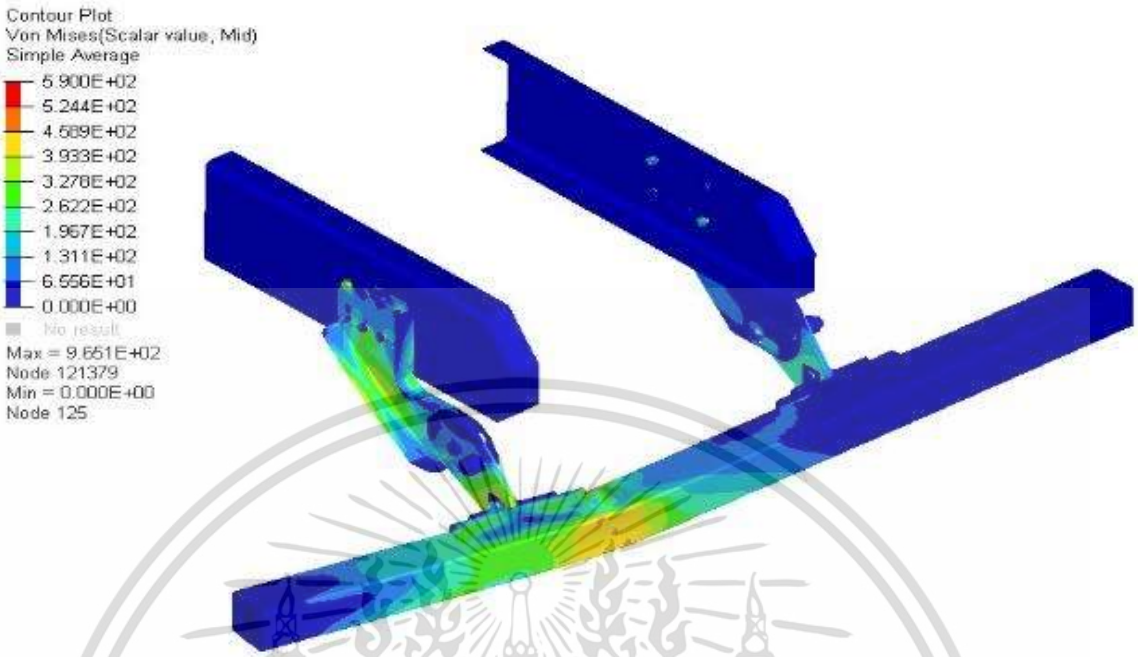

Figure 4.46 Result of design case 17 testing point P1.

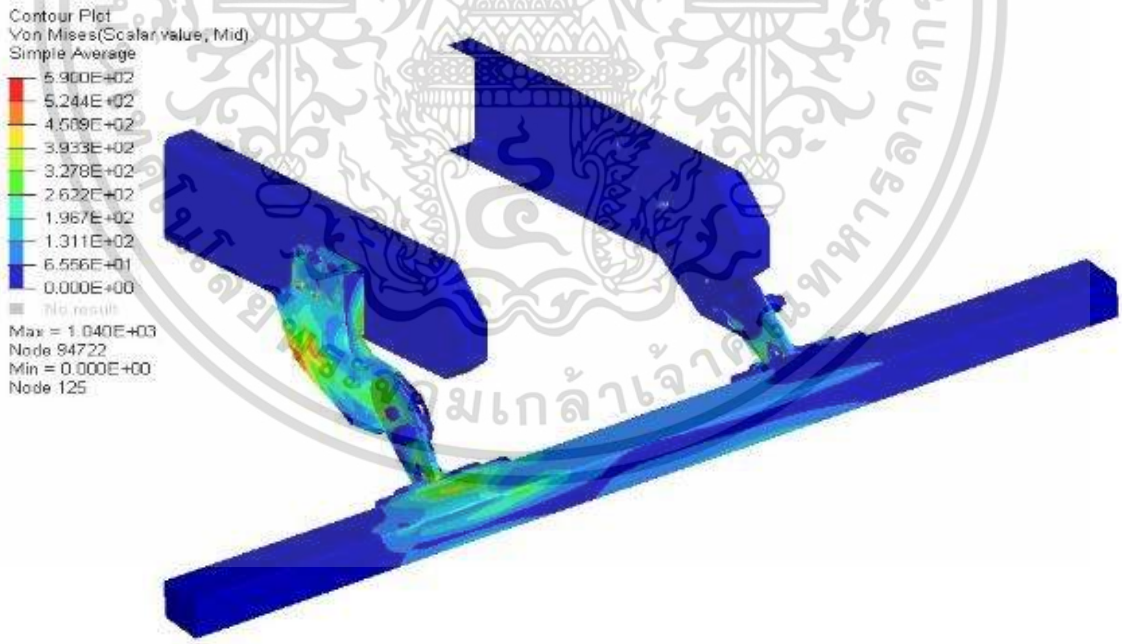

Figure 4.47 Result of design case 17 testing point P2.

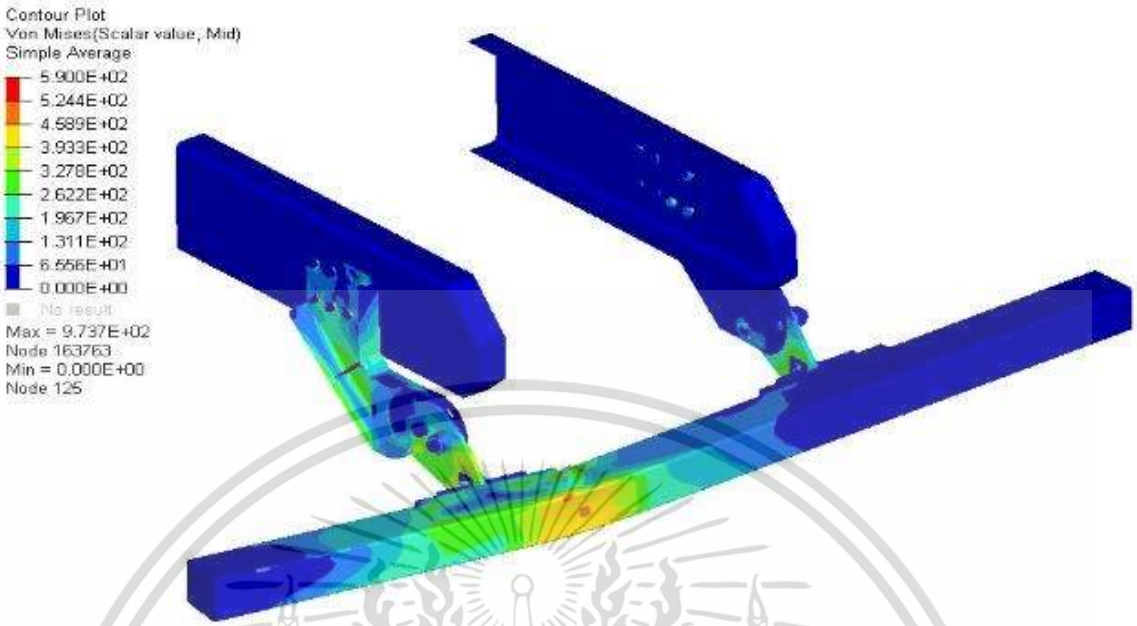

Figure 4.48 Result of design case 18 testing points P1.

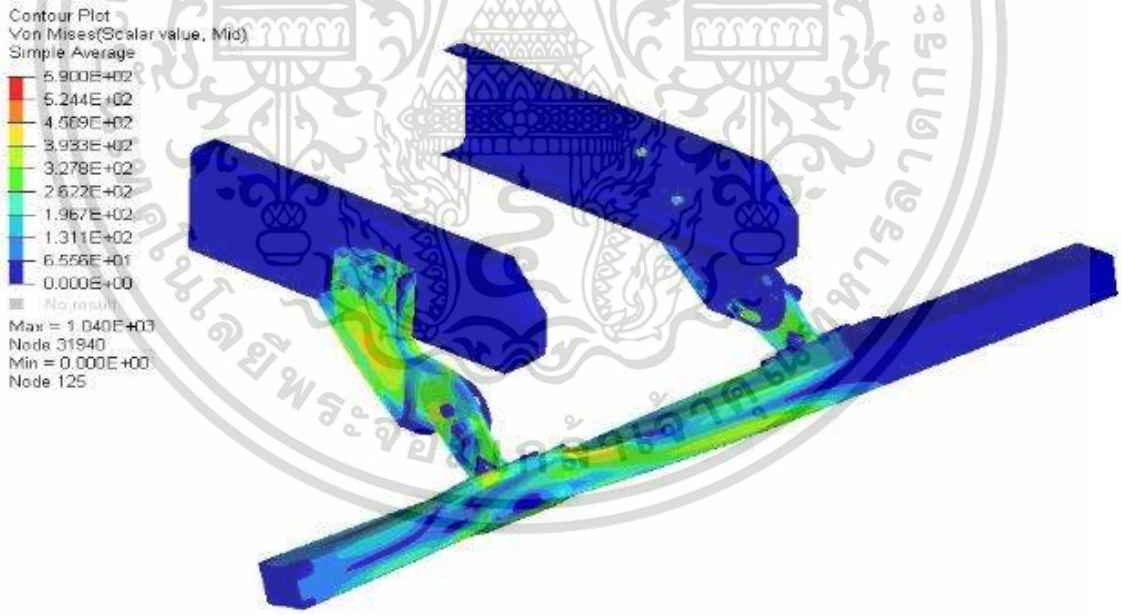

Figure 4.49 Result of design case 18 testing points P2.

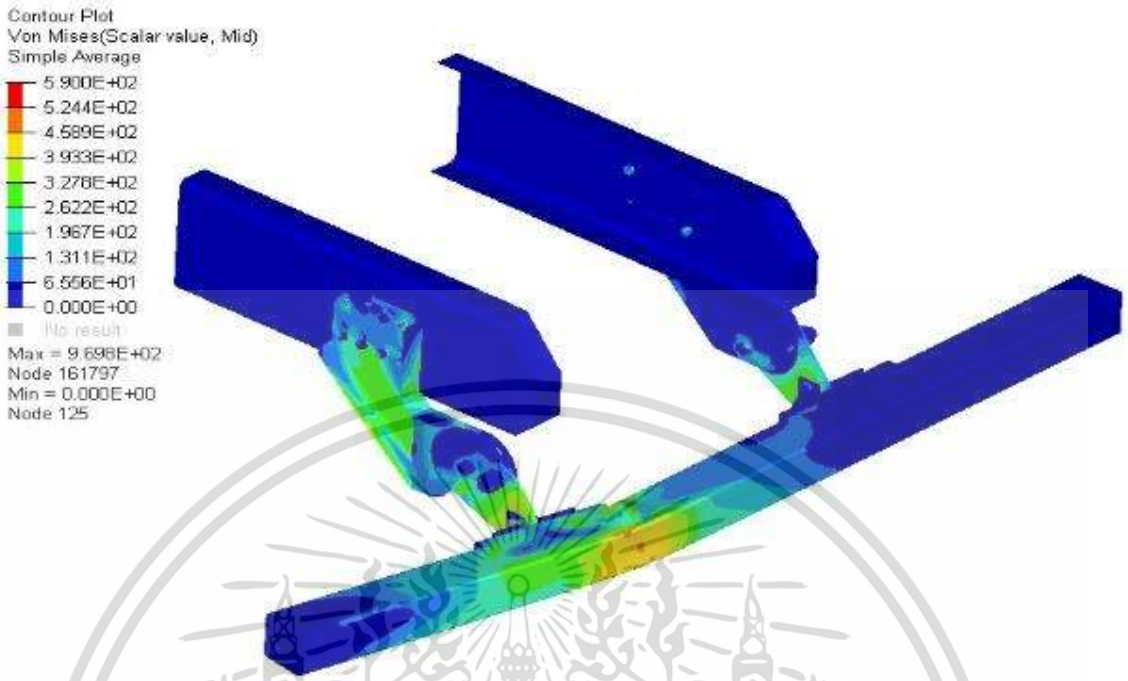

Figure 4.50 Result of design case 19 testing point P1.

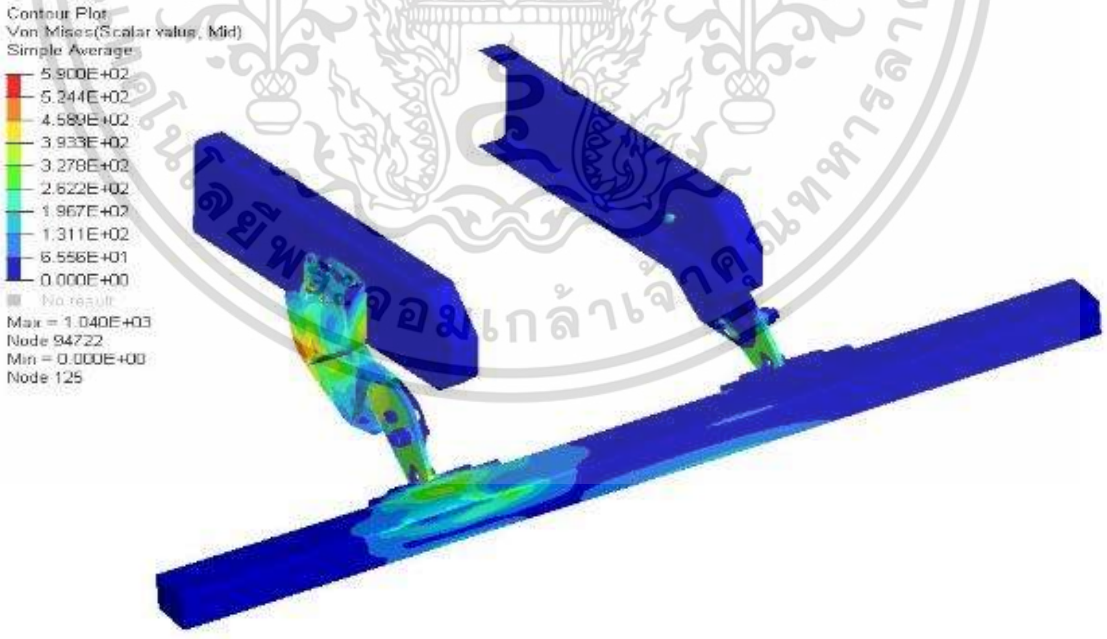

Figure 4.51 Result of design case 19 testing point P2.

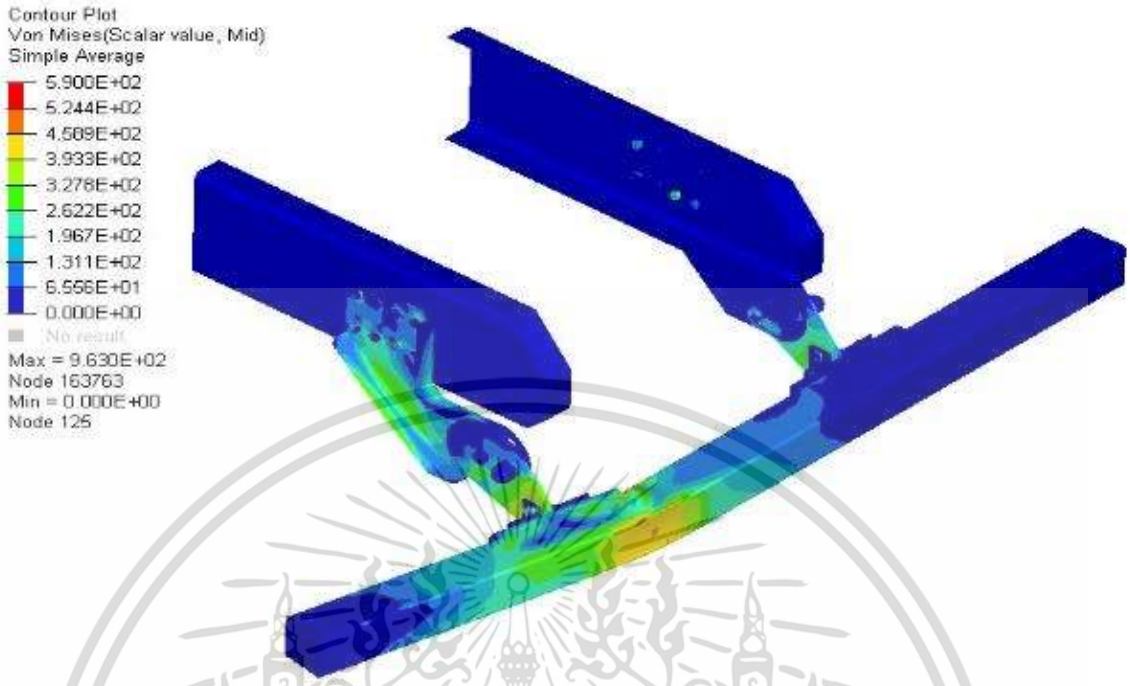

Figure 4.52 Result of design case 20 testing point P1.

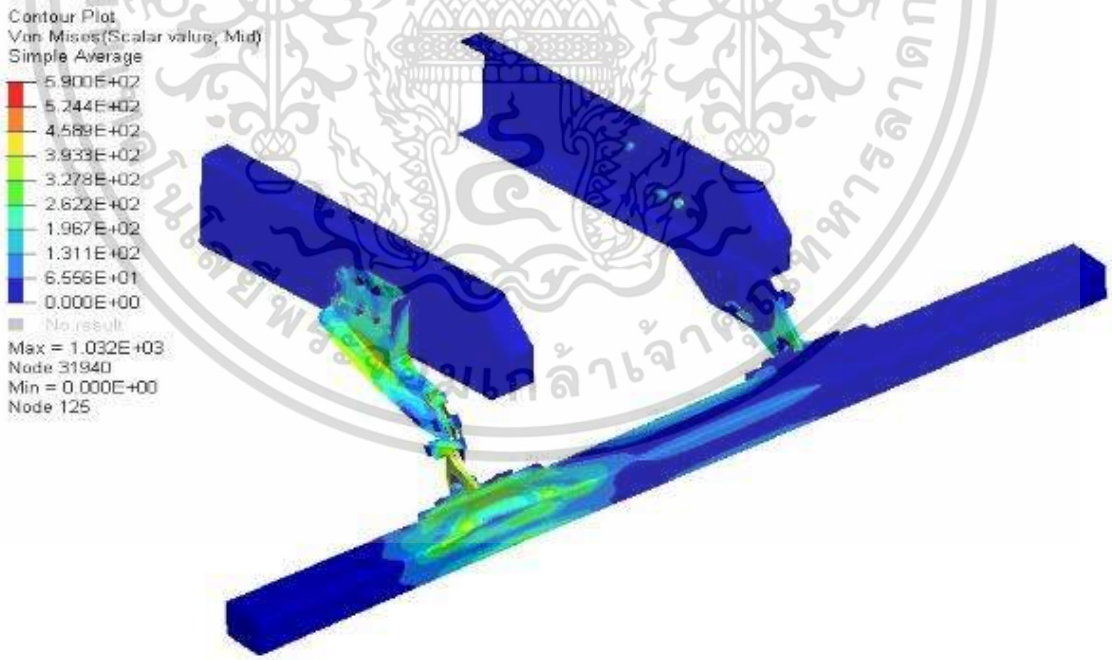

Figure 4.53 Result of design case 20 testing point P2.

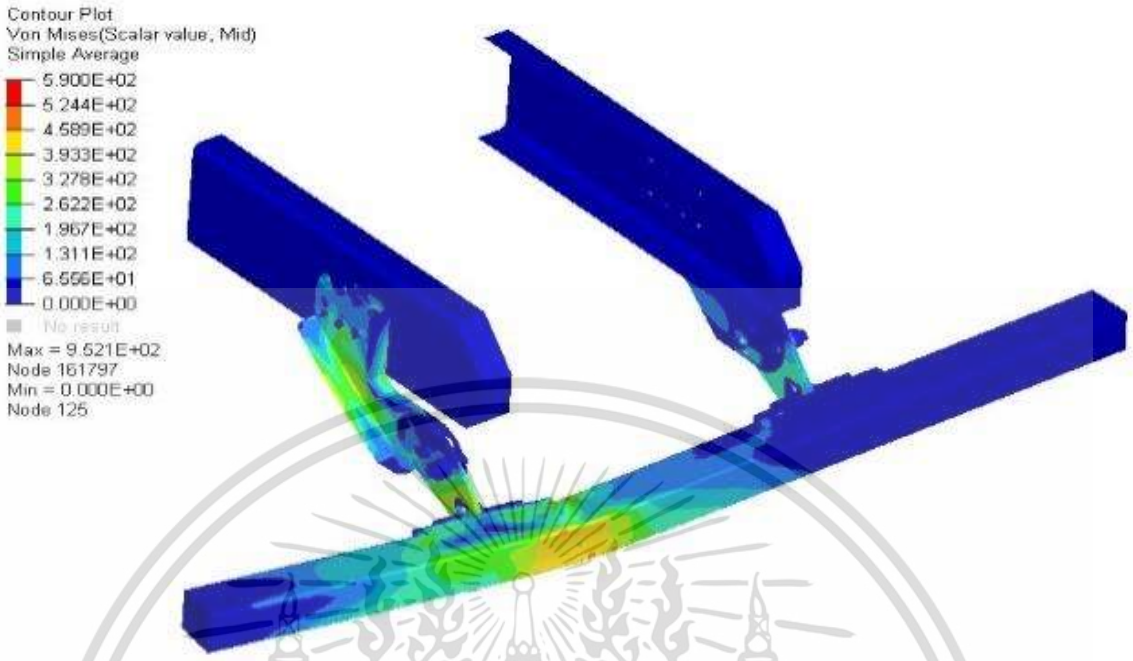

Figure 4.54 Result of design case 21 testing point P1.

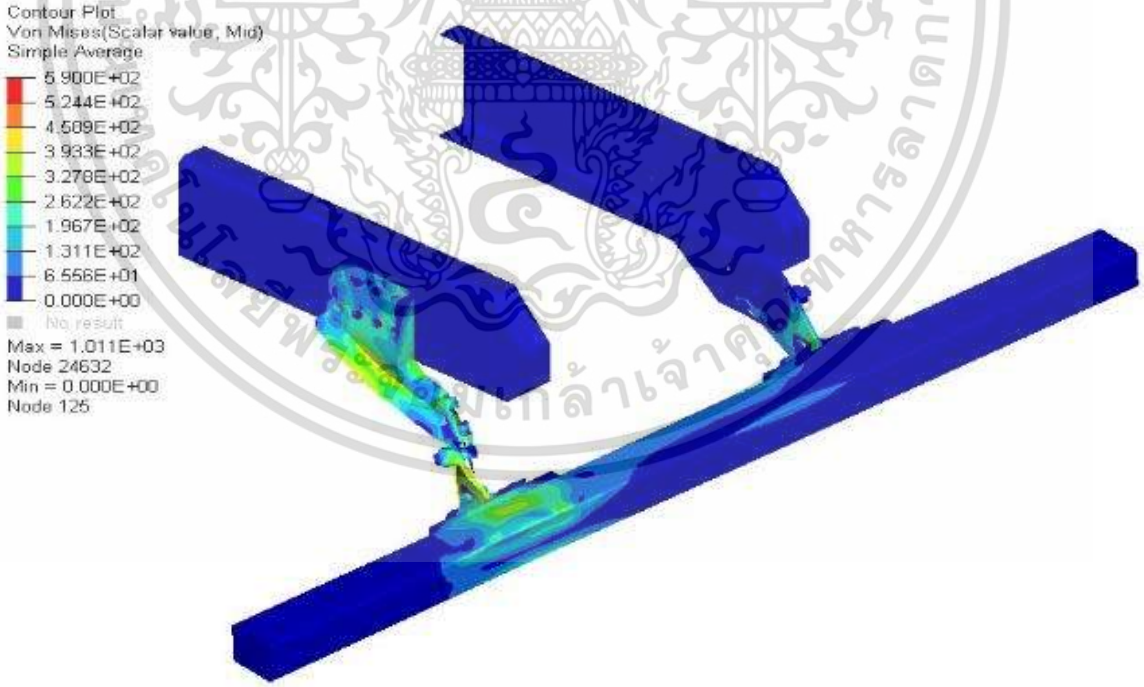

Figure 4.55 Result of design case 21 testing point P2.

Among the different design cases evaluated for the foldable RUPD, design case 15 proved to be the most promising parameter. This design case comprised a protective beam square tube thickness of 4.5 mm, mounting brackets thickness of 9 mm, and swing arm thickness of 15 mm, resulting in a weight of 97 kg, which was the lightest among all the design cases tested.

Furthermore, design case 15 satisfied both the minimum force requirement of testing point P1 at 100 kN and UN regulation No.58. It also exhibited the highest reaction force P1-to-weight ratio of 1.03, which is a critical factor for ensuring the RUPD's stability and performance during an impact. As shown in Table 4.6, these factors made design case 15 the most suitable parameter for a foldable RUPD design.

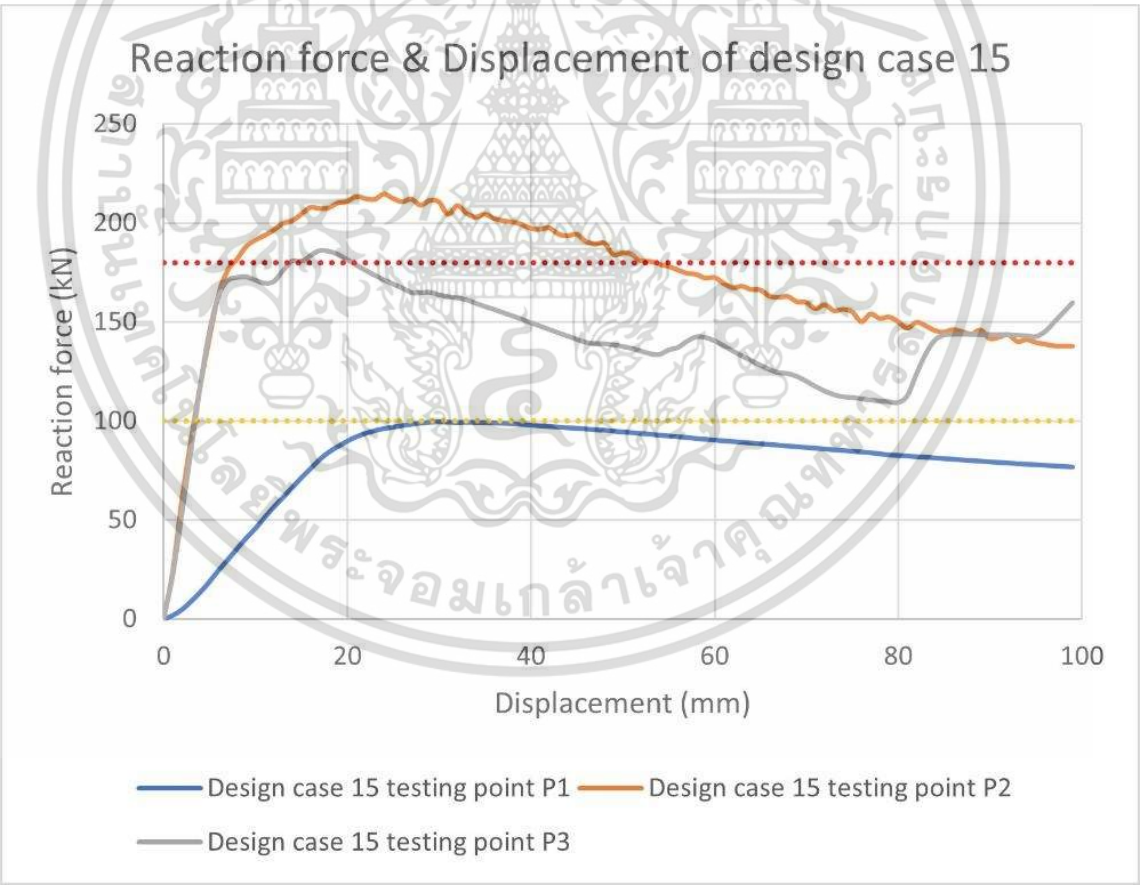

Figure 4.56 Reaction force and displacement of design case 15.

Moreover, comparing the weight of design case 15 to the weight of design case 1, which was the first design evaluated at 121 kg, showed a significant reduction in weight of around 20 percent. This reduction in weight highlights the potential of design case 15 to contribute to the development of safer and more efficient foldable RUPDs for use in various vehicles. In conclusion, design case 15 demonstrated outstanding performance in terms of weight, force requirements, and stability, making it the most appropriate parameter for a foldable RUPD design. Its ability to significantly reduce the weight of the RUPD while maintaining its performance and safety levels shows great promise for the future of RUPD design.

At testing point P1, the maximum reaction force recorded was 100kN, which exceeded the minimum requirement of the standard that was set at 100kN, as shown in Figure 4.56. This performance was a testament to the efficacy of design case 15, which incorporated a protective beam square tube thickness of 4.5 mm, mounting brackets thickness of 9 mm, and swingarm thickness of 15 mm. However, the test did result in some damage to the front of the protective beam near the swing arm, as shown in Figure 4.57.

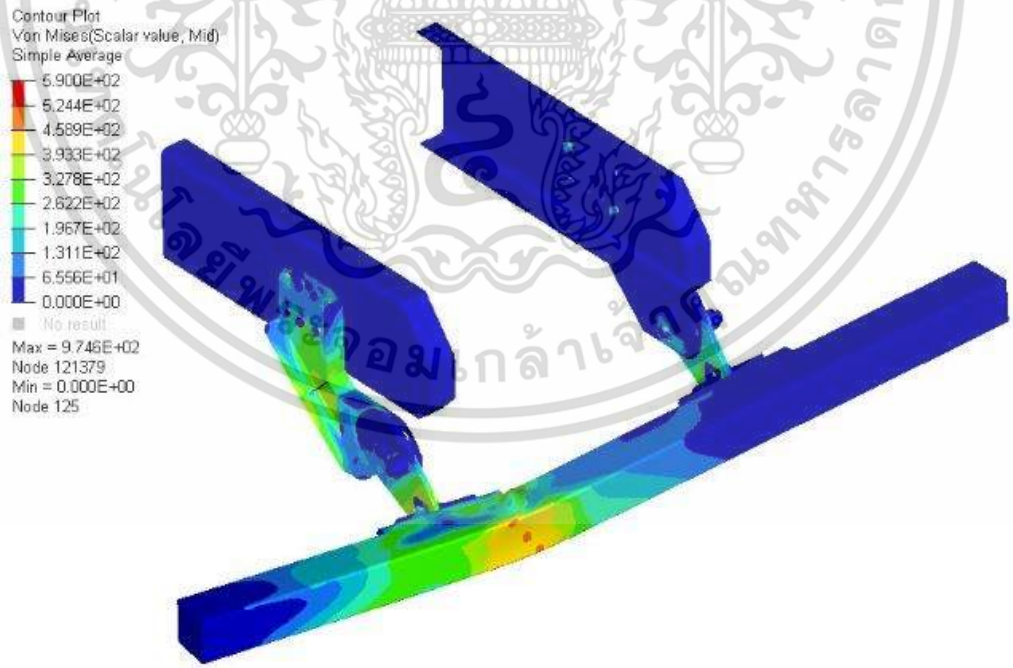

Figure 4.57 Result of design case 15 testing point P1.

Moving on to testing point P2, the maximum reaction force recorded was 215kN, and the performance met the minimum requirement of the standard that was set at 180kN, as shown in Figure 4.56. However, the test resulted in damage to the fasteners used to attach the chassis, the swing arm, the mounting bracket, the mechanisms, and the protective beam, as depicted in Figure 4.58.

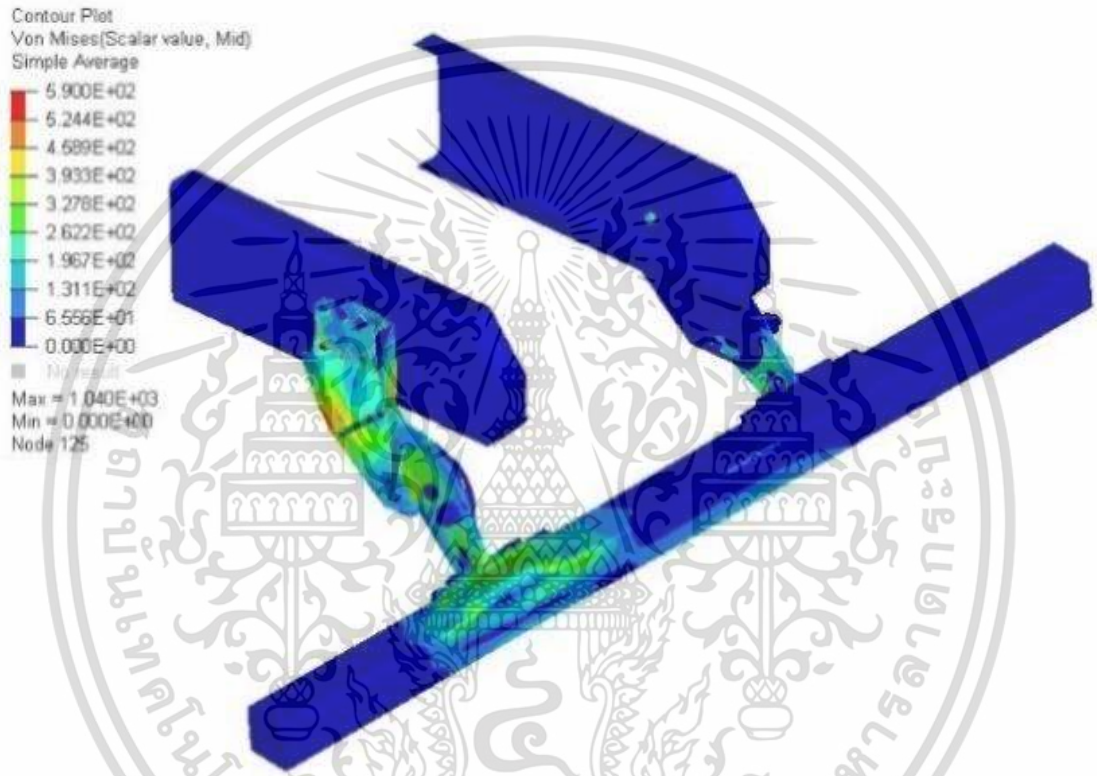

Figure 4.58 Result of design case 15 testing point P2.

Finally, during testing at point P3, the maximum reaction force recorded was 186kN. The performance of both models met the minimum requirement of the standard that was set at 100kN, as shown in Figure 4.56. The deformation was concentrated mainly at the center of the protective beam, as depicted in Figure 4.59. However, minimal deformation occurred around both swing arms, as force could transfer from the center of the protective beam to both brackets.

Overall, the testing results demonstrated that design case 15 was the most suitable parameter for a foldable RUPD design. Despite some damage during testing, the design met the minimum force requirements and satisfied UN regulation No. 58. The findings of this study can be used to further optimize the design of foldable RUPDs and improve their overall performance.

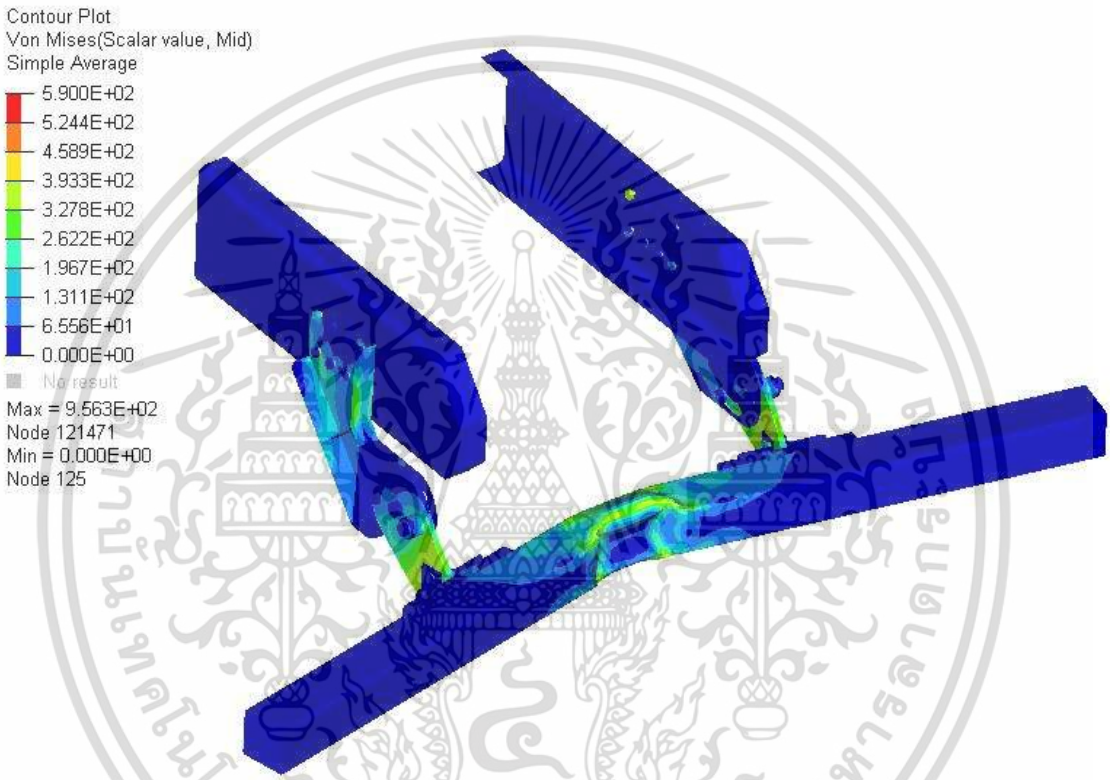

Figure 4.59 Result of design case 15 testing point P3.

To achieve further weight reductions in the design of bumpers, one approach is to explore the use of high-strength materials. These materials have the advantage of being able to maintain the same strength as the original material while reducing the thickness of the material. This approach offers a potential solution for manufacturers to meet the customer demand for lightweight designs that do not compromise performance.

However, the use of high-strength materials comes at a higher production cost, which may have implications for the manufacturing company. The increased cost may result in higher prices for customers or reduced profit margins for the company. Therefore, a balance needs to be struck between the use of high-strength materials and the costs associated with their production.

From the customer's perspective, a lighter bumper offers several benefits, including lower energy consumption and higher payload. With a lighter bumper, the overall weight of the vehicle is reduced, which translates to improved fuel efficiency and reduced emissions. Additionally, a lighter bumper allows for a higher payload capacity, which can be advantageous for commercial vehicles that need to carry heavy loads.

CHAPTER 5
CONCLUSION AND RECOMMENDATIONS

The objective of this research is to develop a design guideline for validating the structural strength analysis method of a foldable rear underrun protective device (RUPD), following the UN regulation No.58 standard, using both experimental and finite element analysis methods. Additionally, this study seeks to identify the significant design parameters of the RUPD. The design of the foldable RUPD follows UN Regulation No. 58, considering the availability of materials in Thailand. The selection of the most significant parameters is based on three criteria: the lowest weight, the greatest force-to-weight ratio, and the satisfaction of the minimum requirement of UN Regulation No. 58.

In this study, experimental testing using a full-scale model of the protective beam and hydraulic actuator pressing, as well as finite element analysis using explicit dynamics by RADIOSS and UN regulation No.58 standard, were compared. The results demonstrated good agreement between the two methods, indicating that finite element analysis using RADIOSS with quasi-static loading is an acceptable representation of experimental testing. Moreover, commercial models I and II, which meet UN regulation No.58 standards, were investigated to ensure the validity of the finite element analysis method and to analyze the damaged characteristics of the RUPD. The results of both models showed that the strength of the commercial models met all the minimum requirements of the UN regulation No.58 standard. Therefore, local materials in Thailand and finite element analysis parameters used in this study can be employed to design the RUPD.

The testing points P1, P2, and P3 were found to significantly affect the protective beam and swing arm system, respectively. These results, along with the finite element analysis of the previous models, were used as a guideline for designing the proposed model. However, the results at testing point P2 showed that the resulted in maximum reaction force was still greater than the minimum requirement of the standard. Nevertheless, the proposed design model satisfied all the minimum requirements of the UN regulation No.58

standard and has the potential for future weight reduction by applying the process presented in this study as a design guideline for the RUPD.

Furthermore, the significant parameters in reducing the weight of the foldable RUPD were determined based on cross-section type and component thicknesses in 21 cases, using non-linear dynamic RADIOSS analysis. As a result, the design case with a square tube protective beam of 4.5 mm, mounting brackets of 9 mm, and a swing arm of 15 mm satisfied the minimum requirement of UN Regulation No. 58 in all testing points, while having the lightest weight and highest force-to-weight ratio. Therefore, this RUPD design is recommended as a foldable RUPD for dumping trucks, with a weight reduction potential of approximately 20 percent or 24 kg. Furthermore, the proposed process can be used as a future design guideline for the RUPD, enhancing the road safety of other vehicles by ensuring compliance with international standards.

REFERENCES

[1] Blowel, D. and Woodrooffe, J. 2012. **Survey of The Status of Truck Safety: Brazil, China, Australia, and The United States.**

[2] World Health Organization. 2018. **Global Status Report on Road Safety 2018.**

[3] United Nations Economic Commission for Europe (UNECE). 2017. **Addendum 57: UN Regulation No. 58 Revision 3.**

[4] Joseph, G., Shinde, D. and Patil, G. 2013. "Design and Optimization of the Rear Under Run Protection Device Using LS-DYNA." **International Journal of Engineering Research and Applications (IJERA).** 3(4) : 152-162.

[5] Balta, B., Erk, O. and Solak, H.A. 2014. "Pareto Optimization of Heavy Duty Truck Rear Underrun Protection Design for Regulative Load Cases." **SAE International Journal of Commercial Vehicles.** 7(2) : 726-735.

[6] Lerspalungsanti, S., Pitaksapsin, N., Viriyarattanasak, P., Wattanawongsakun, P. and Suebnunta, S. 2021. "Design approach of heavy goods vehicle underrun protection using morphological analysis." **Proceedings of the Institution of Mechanical Engineers, Part D: Journal of Automobile Engineering**.

[7] Gogte, S. and Vijendran, N. 2014. "Conceptual design and development of movable rear underrun protection." master's thesis in the Department of Product and Production Development Chalmers University of Technology Gothenburg, Sweden.

[8] Brumbelow, L.M. and O'Malley, S.P. 2020. "A proposed quasi-static test for improving the crash performance of trailer rear underride guards." **Int. J. of Crashworthiness.**

[9] Rechnizer, G. Powell, and C. Seyer, K. 2001. "Performance Criteria, design and crash tests of effective rear underride barrier for heavy vehicle." **Int. Conf. on Enhanced Safety of Vehicle.**

[10] ASTM E8. 2013. **Standard Test Method for Tension Testing of Metallic Materials, American Society for Testing and Materials.**

[11] **"Folding Systems."** [Online]. Available: https://www.vbg.eu/en/products/underrun protection/hinged. [Accessed 14 Sep 2020].

[12] **“Under Run Bars / Tow Bar.”** [Online]. Available: https://www.marcar.co.uk/product_category/transport-products/under-run-bars-towbars. [Accessed 14 Sep 2020].

[13] Thai Industrial Standards Institute (TISI). 2018. **TIS 107-2561 Carbon steel tubes for general structure**.

[14] Thai Industrial Standards Institute (TISI). 2015. **TIS 1479-2558 Hot rolled flat steel for general structure.**

[15] Govardhan, R., Waykar, V., Patel, M., Rajaraman, R. and Padmanaban, J. 2020. “Effectiveness of rear underrun protection devices in trucks for reducing passenger car fatalities and serious injuries in India” **IRCOBI conference.** : 100-110.

[16] Altair University. 2018. **Introduction to Explicit Analysis using RADIOSS.**

[17] Liang, C. and Le, G. 2010. “Analysis of Bus Rollover Protection Under Legislated Standards Using LS-Dyna Software Simulation Techniques” **Int. J. of Automotive Technology.** 11(4) : 495-506.

[18] Hu, Y., Shen, L., Nie, S., Yang, B. and Sha, W. 2016. “Fe Simulation and Experiment Tests of High-strength Bolts Under Tension” **Int J. of Construction Steel Research.**

APPENDIX A

Proceedings of the 11th International Conference on Materials Science and Technology, 29-31 August 2022

Analysis of Rear Underrun Protective Device Using Real-Life Test and Finite Element Techniques

Narongrit Suebnunta[1,2*], Sarawut Lerspalungsanti[2], Preechar Karin[1], Kazuaki Inaba[3]
[1] Department of Mechanical Engineering, School of Engineering, King Mongkut's Institute of Technology Ladkrabang, Bangkok, 10520, Thailand
[2] National Metal and Material Technology Center, National Science and Technology Department Agency, Pathum Thani, 12120, Thailand
[3] School of Engineering, Tokyo Institute of Technology, Tokyo 152-8550, Japan

*Corresponding author e-mail address: narongrit.sue@mtec.or.th

Abstract

One of the most fatal accidents on the road occurs due to the rear underrun, i.e., a passenger car crashing into the rear of a truck. One solution to reduce injury and death from this type of accident is installing a rear underrun protective device (RUPD) on the truck, which should meet safety standards. This research aims to establish a design guideline to validate the structural strength analysis method of the RUPD using a quasi-static test and finite element analysis according to the UN R58 standard, in which the minimum required forces applied at a cross-section of the protective beam and the corresponding deformation limits are given. Significant design parameters such as the cross-sectional area, section height, and thickness are investigated. As an example, a benchmark study of two models of commercial RUPDs satisfied the UN R58 regulation and the proposed RUPD design was carried out following the presented design guideline which all models were based on domestically available materials, such as SS400. The finite element analysis to demonstrate the structural strength of all RUPD models is achieved using RADIOSS. These findings provide performances of all models and can be used as guidelines for other RUPD types, such as foldable or slidable RUPD.

Keywords: UN R58 (Economic Commission for Europe Regulation 58) RUPD (Rear Underrun Protective Device); Heavy Truck; Finite Element Analysis

Introduction

In 2016, 1.35 million people worldwide and 22,491 people in Thailand were killed by road traffic accidents [1]. 2004 – 2008 in the USA, people have killed involving truck traffic accidents 16.5 percent in the truck and 74.7 percent in other vehicles [2]. One of the most fatal accidents on the road that occurs due to the rear underrun is a passenger car crashing into the rear of a truck.

One solution to reduce injury and death from this type of accident is installing a rear underrun protective device (RUPD) on the truck. The RUPD is used to prevent a passenger car's cabin room from crashing into the rear-end truck directly. The RUPD must be strong enough to stop a passenger car and be able to absorb the energy of a collision. Generally, the crumple zone, airbag, and seatbelt of the passenger car are designed to absorb energy and reduce the severity of a collision Thus, combining these functions of a passenger car with the function of the RUPD is safer.

The standard related to this accident and widely used in the world is the UN R58 standard concerning rear underrun protective devices that contains requirements for the static testing load in each position, the height of the cross-section, and the location of the device. Depending on the factory's requirements, the tests in this standard can be tested by real-life testing and by the finite element method [3].

The finite element analysis was widely used for studying the RUPD. Joseph et.al [5] have studied RUPD by using LS-DYNA according to the UN R58 rev2 regulation. They have developed by using 3 materials and six models of the RUPD and selected the best model. Balta et.al [6] have studied the RUPD by comparing the experimental testing result and the finite element analysis by using RADIOSS result and found good agreement between both methods. After that, they used materials, thickness, support position, and beam type factors to generate sixteen finite element models and used those results to optimize the best parameter using an optimizer program. Lerspalungsanti et.al [7] presented the design approach of RUPD by using morphological analysis with finite element analysis using RADIOSS and they used strength weight ratio to consider the decision criteria for the RUPD.

This research aims to establish a design guideline to validate the structural strength analysis method of the RUPD using a real-life test method according to the UN R58 standard and finite element method and identify the significant design parameters.

Materials and methods

The materials involved in this study are TIS 107-2561 carbon steel tubes, TIS 107-2561 carbon square steel tubes, TIS 1479-2558 hot-rolled steel plate (SS400), TIS 1228-2561 lip channel steel, bolts and nuts grade 10.9. Specimens of the material used for material properties are cut from the parts of the protective beam model referring to dimensions according to ASTM E8 [4] by a wire-cut process of five pieces each, to obtain properties that are similar to those from general metal shops. The engineering stress-strain curve of each material is determined using a standard tensile testing machine, as shown in Figure 1. The engineering stress-strain curve is converted into the true stress-strain curve and the smoothing of the data curve is performed as RADIOSS requires. The material card in RADIOSS M36_PLAS_TAB is used which is given a density of 7,850 kg per cubic meter, Poisson ratio of 0.3, young modulus. yield stress, and plasticity table curve. Elastic material stress-strain curve defined by Poisson's ratio and young modulus. The stress exceeds more than the yield stress the material properties are switched to nonlinear material instead by this function. All material properties are defined for all models in this study.

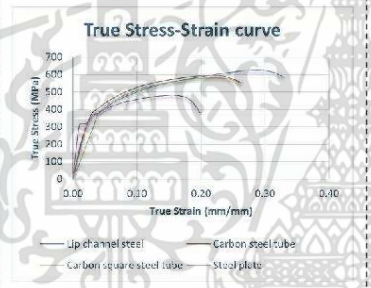

Figure 1 True Stress-Strain curves of material.

Requirements on RUPD regarding dimension and strength

According to UN R58 standard, the ground clearance to the underside of the RUPD shall not exceed 500 mm. The horizontal distance between the rear side of the RUPD to the most rearward point of the vehicle shall not exceed 300 mm. The width of the RUPD shall be smaller than the width of the rear axial measured outside of each wheel and shall not be shorter than 100 mm per side. the height of the cross member shall be more than 120 mm.

The requirement of the force for tests via surface shall not be more than 250 mm in height and 200 mm wide with a radius of 5 mm at the vertical edge. Testing points P1 shall be applied to two points at 300 mm from the outer edges of the rear axial wheel with a horizontal force of 100kN. Testing points P2 shall be applied to two points at the symmetrical line of the RUPD to another point 700 – 1000 mm with a horizontal force of 180kN. Testing point P3 shall be applied at the center of the vehicle with a horizontal force of 100kN [3].

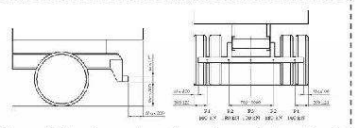

Figure 2 Requirement on dimension and strength of RUPD according to UN R58 regulation.

Finite element analysis and experimental testing

These finite element models of the RUPD are used for simulation. The finite element meshing is done using Hypermesh. Finite element analysis is performed with non-linear explicit dynamic in RADIOSS. Finite element analysis post-processing is utilized by Hyperview. The finite element mesh for parts that are made from steel plate is modeled to shell surface by mid-surface and defined as a 4-node shell element. For parts made from thick steel plate and machined process defined as the 3D solid 8-node element. Bolts and nuts are modeled to the simple 3D model and defined as the 3D solid 8-node element. Almost all the finite meshing element is defined as 10 mm in all parts except the chassis is defined as 20 mm. The interaction contract between each contracting surface is defined as a type7 multi-purpose interface, which is the node-to-surface contract. The friction coefficient between each part is defined as 0.2. The chassis is cut at 1000 mm from the rear end of the chassis and fixed constraints in all translations and rotations. The loading plate is defined as rigid by a 1D rigid element and fixed constraints in all directions and rotations except the x direction and y rotation at the center point of the 1D rigid element thus the loading plate can move in a normal direction, rotate around the center point, and always attend with the protective beam at during loading process. The loading condition is defined using the displacement-time function to represent the quasi-static loading test. The mass scaling of analysis is limited to around 5 %. The outputs of finite element analysis are the reaction force of RUPD, displacement of the loading plate, and the von-mises stress contour plot.

The finite element models in this study have 4 models, the protective beam model, the commercial model I, the commercial model II, and the purposed design.

The protective beam model is specially designed to validate the method by comparing the finite element analysis results with experimental test results. In this case, the protective beam model is made from steel plates, steel tubes, and lip channels

that are available use materials in Thailand as shown in Figure 3. To ensure both results the real material thickness and material properties are important. Pieces of structural and plate steel are cut to find the material properly and the real thickness to define in the finite element analysis.

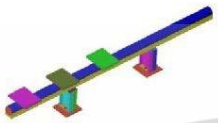

Figure 3 Finite element model of the protective beam.

To improve the confidence of the finite element analysis method commercial models I and II are studied. Commercial models I and II are modeled as well as possible close to the following two models of foldable RUPD that are available on the market and claimed to meet the UN R58 revision 3 standards. Therefore, the finite element analysis result of both models should also meet the standard. the protective beam of the commercial model I is made of a tube outer diameter of 120 mm with a thickness of 6 mm. But the protective beam thickness of the commercial model II is made of a square tube cross-section of 125 x 125 mm with a thickness of 6 mm. Fasteners and mechanisms are modeled by 3D simple models. The same chassis is used for both models as shown in Figures 4 and 5.

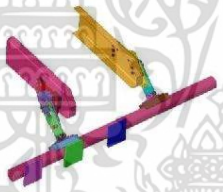

Figure 4 Finite element model of the commercial model I.

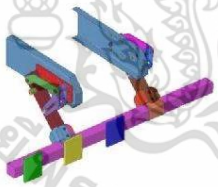

Figure 5 Finite element model of the commercial model II.

The purposed RUPD design is designed for the dump truck. It can be folded up to avoid the material flowing out of the truck during the dumping process and the departure angle of the road sometimes where the previous two models are not suitable. The finite element analysis result of two previous models is used to be the guideline design for this model. The protective beam of this model uses a square tube of 4.5 mm thickness. the mounting brackets that use for mounting the chassis use plates of 12 mm thickness. The swing arms use plates of 20 mm thickness. Mechanisms and fasteners are modeled by 3D simple models. The chassis is used in the same previous model as shown in Figure 6.

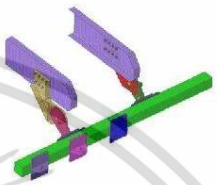

Figure 6 Finite element model of purposed design.

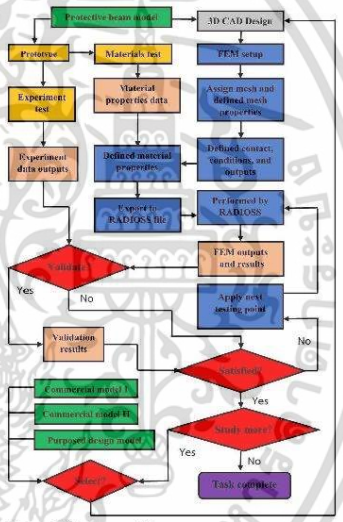

Figure 7 Study workflow.

The prototype of the protective beam model is installed on the test bench and connected by bolts and nuts. The loading test is applied to the protective beam using a hydraulic actuator pressing on the loading plate. The reaction force and displacement of the protective beam are measured carefully by a load cell and string potentiometer as shown in Figure 8. The test is performed by applying the load to the RUPD by controlling the loading distance and stopping the test when RUPD cannot withstand the loading force more.

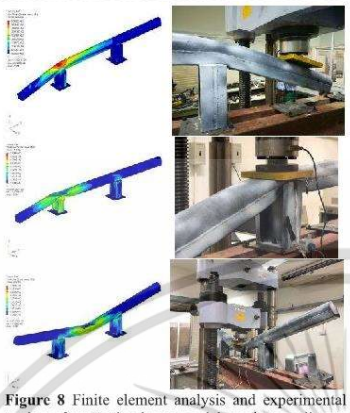

Figure 8 Finite element analysis and experimental testing of protective beam model result regarding to load applied at point P1, P2, and P3.

Validation of the protective beam model

To validate experimental testing and finite element analysis results, reaction force and displacement curves are mainly compared and focused on the reaction force. In the case of testing point P1, the maximum reaction from experimental testing and finite element analysis are 59kN and 60kN as its error is 1.8%. In the case of testing point P2, the maximum reaction from experimental testing and finite element analysis are 224kN and 215kN as its error is 4.0%. In the case of testing point P3, the maximum reaction from experimental testing and finite element analysis are 93kN and 102kN as its error is 10.0% as shown in Figure 9.

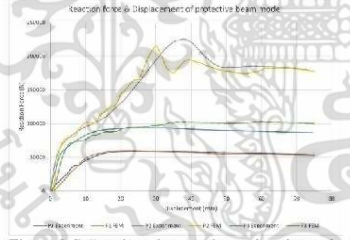

Figure 9 Comparison the experimental testing and the finite element analysis of simple model.

However, the maximum reaction force of the protective beam model in testing points P1 and P3 does not meet the requirements of the standard. The average of all testing points is 5.4%. It can mention that the maximum reaction force from experimental testing and finite element analysis are good correlated. The trend of the curve from both methods was the same way. For this reason, the finite element analysis using a non-linear explicit dynamic in RADIOSS with quasi-static loading is acceptable to represent the experimental testing.

Strength analysis results of the commercial model I and II

In the case of testing at point P1, the maximum reaction forces of commercial models I and II are 114N and 114N as shown in Figures 13, and 14. The performance of both models in this testing meets the minimum requirement of the standard of 100kN. In this test, the end of the protective beam deforms. The most damage is on around the front of the protective beam close to the left swing arm as shown in Figure 10. This testing point is the worst case for the protective beam. To specifically determine the strength of the protective beam, this testing point might be used.

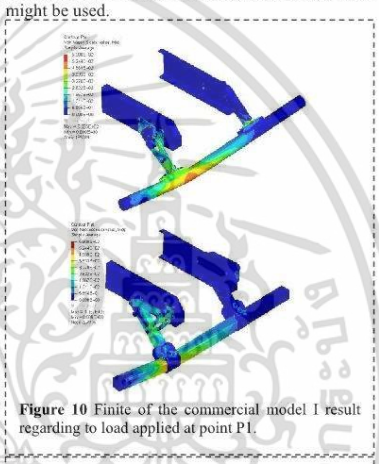

Figure 10 Finite of the commercial model I result regarding to load applied at point P1.

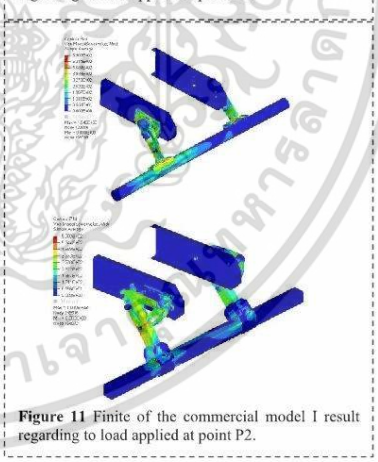

Figure 11 Finite of the commercial model I result regarding to load applied at point P2.

In the case of testing at point P2, the maximum reaction force of commercial models I and II are 232kN and 269kN as shown in Figures 13, and 14. The performance of both models in this testing meets the minimum requirement of the standard of 180kN. In this case, fasteners that use to attach the chassis, mounting bracket, and swingarms are directly affected by this test as shown in Figure 11. Even though the swing arm deformed quite severely in this test, it is still able to withstand high loads. To specifically determine the strength of mounting brackets, swingarms, and fasteners this testing point might be used.

In the case of testing at point P3, the maximum reaction forces of commercial models I and II are 147kN and 245kN as shown in Figures 13, and 14. The performance of both models in this testing meets the minimum requirement of the standard of 100kN. The protective beam and swing arm in this test are directly affected. There is significant deformation in the center of the protective beam and little deformation around both swing arms as shown in Figure 12. The result is much more than the standard. Therefore, this test is the least harmful to the RUPD.

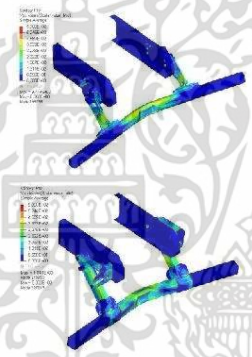

Figure 12 Finite of the commercial model II result regarding to load applied at point P3.

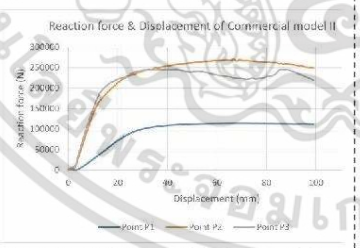

Figure 13 Reaction force and displacement of the commercial model II.

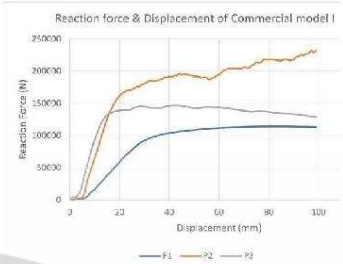

Figure 14 Reaction force and displacement of the commercial model I.

Strength analysis results of purposed design.

In the case of testing at point P1, the maximum reaction forces at testing at point P1 of the purposed design model is 106N. The performance in this testing meets the minimum requirement of the standard of 100kN as shown in Figure 18, in this test, most of the damage occurs on the front of the protective beam near the swing arm as shown in Figure 15. To reduce the weight of the protective beam the thickness is reduced to 4.5 mm.

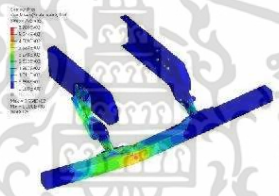

Figure 15 Finite of the purposed design result regarding to load applied at points P1

In the case of testing at point P2, the maximum reaction force is 253kN. The performance in this testing meets the minimum requirement of the standard of 180kN as shown in Figure 18. the damage occurs directly to fasteners for attaching the chassis, the swing arm, mounting bracket, mechanisms, and protective beam. Several parts of the model were deformed but the maximum reaction force was still much greater than the minimum requirement of the standard as shown in Figure 16. It may be possible to lose the weight of these parts in the future by reducing the thickness of the mounting bracket and the moving arm and re-analyzing testing points P1 and P2.

In the case of testing at point P3, the maximum reaction force was 181kN. The performance of both models in this test meets the minimum requirement of the standard of 100kN as shown in Figure 18. The most deformation occurred at the center of the protective beam and little deformation occurred

around both swing arms as shown in Figure 17. The reaction force in this test is much higher than the minimum requirement of the standard because force can transfer from the center of the protective beam to both brackets. Therefore, it is sufficient to mainly focus on simulated results at points P1 and P2

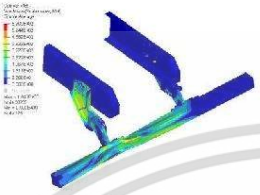

Figure 16 Finite of the purposed design result regarding to load applied at points P2

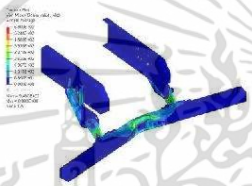

Figure 17 Finite of the purposed design model result regarding to load applied at points P3.

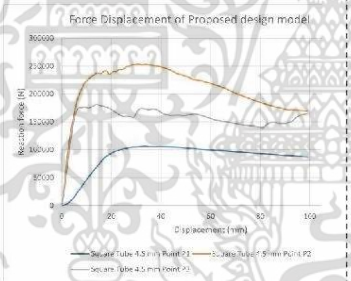

Figure 18 Reaction force and displacement of the purposed design model.

Conclusion

This research aims to establish a design guideline to validate the structural strength analysis method of the RUPD using a real-life test method according to the UN R58 standard and finite element method and identify the significant design parameters.

In this study, the experimental testing using the full scale of the protective beam model and testing by the hydraulic actuator pressing and the finite element of the protective beam model using explicit dynamics by RADIOSS, according to the UN R58 standard were compared. The comparing results found good agreement between both methods. For this reason, the finite element analysis using a RADIOSS with quasi-static loading is acceptable to represent the experimental testing.

Commercial models I and II that are available on the market and meet the UN R58 standards were studied to ensure the finite element analysis method and study the damaged character of the RUPD. The result of both models found that the strength of commercial models I and II meet all the minimum requirements of the UN R58 standard which means the local material in Thailand and finite element analysis parameter in this model can use to design the RUPD. The result found that testing point P1 most affects the protective beam, testing point P2 most affects the swing arm system, and testing point P3 most affects the protective beam.

The finite element analysis result of all previous models was used to be the guideline design for the purposed design model. To reduce the weight, the protective beam thickness was reduced to 4.5 mm by using testing point P1 to study. However, testing point P2 found that the maximum reaction force was still much greater than the minimum requirement of the standard.

As a result, the purposed design model meets all minimum requirements of the UN R58 standard. It could be possible to lose the weight of these parts and apply the process in this study to be the guideline for the design of the RUPD in the future.

References

1. Global Status Report on Road Safety 2018. Geneva: World Health Organization (2018).
2. D. Blowel, J. Woodrooffe, Survey of The Status of Truck Safety: Brazil, China, Australia, and The United States, Report No. UMTRI-2012-13 (2012).
3. UN Regulation No.58, Rear Underrun Protective Devices, (2017).
4. ASTM E8, Standard Test Method for Tension Testing of Metallic Materials, American Society for Testing and Materials (2013).
5. G. Joseph, D. Shinde, G. Patil, Design and Optimization of the Rear Underrun Protection Device Using LS-DYNA, International Journal of Engineering Research and Applications (IJERA), Vol.3, Issue 4, 152-162 (2013).
6. B. Balta, O. Erk, H. Solak, N. Durakbasa, Pareto Optimization of Heavy-Duty Truck Rear Underrun Protection Design for Regulative Load Cases, SAE Int. J. Commer. Veh. 7 (2014).
7. S. Lerspalungsanti, N. Pitaksapsin, P. Viriyarattanasak, P. Wattanawongsakun, N. Suebnunta, Design approach of heavy goods vehicle underrun protection using morphological analysis, Proceedings of the Institution of Mechanical Engineers, Part D: Journal of Automobile Engineering (2021).

APPENDIX B

The 12th TSME International Conference on Mechanical Engineering
13th – 16th December 2022
Phuket, Thailand

CST0022

New Design Guideline of Foldable Rear Underrun Protective Device for Heavy Goods Vehicle Using Finite Element Analysis

N Suebnunta[1,2*], S Lerspalungsanti[2], P Karin[1] and K Inaba[3]

[1] Department of Mechanical Engineering, School of Engineering, King Mongkut's Institute of Technology Ladkrabang, Bangkok 10520, Thailand
[2] National Metal and Materials Technology Centre, National Science and Technology Department Agency, Pathum Thani 12120, Thailand
[3] School of Engineering, Tokyo Institute of Technology, Tokyo 152-8550, Japan

* Corresponding Author: narongrit.sue@mtec.or.th

Abstract. One kind of accident on the road is a passenger car colliding with the rear end of a heavy goods vehicle (HVG). Installing rear underrun protective devices (RUPD) in the rear of trucks can greatly reduce the severity of accidents. This study proposes a novel design guideline for a foldable RUPD, design inputs are determined based on the set of requirements. They are vehicle structural strength according to UN Regulation No.58 standard, the capability of local motor vehicle manufacturers, lightweight components, and widely used materials. Based on the given design inputs and proposed design guidelines, significant design parameters such as the type of cross-section and thickness of the RUPD are investigated. For example, a foldable RUPD for HGV is designed, and the resulting structural strength is determined using non-linear explicit dynamic finite element (FE) analysis in RADIOSS. The results show that the deformations and load-bearing performance of several foldable RUPD models satisfied UN Regulation No.58 regulation. Finally, the RUPD model with the highest performance in terms of reaction force-to-weight ratio has been selected and proposed for production.

Keywords: RUPD (Rear Underride Protective Device); UN Regulation No.58 (Economic Commission for Europe Regulation 58); Heavy Goods Vehicle; Non-linear explicit dynamic finite element analysis

1. Introduction

In 2016, WHO reported that 22,491 or 32.7 per 100,000 population of Thailand died from road accidents [1]. One kind of accident on the road is a passenger car colliding with the rear end of a heavy goods vehicle (HVG). This accident is very severe because their geometry, size, and mass are different. The high of the passenger car is lower than the truck's body so that it can move to underride. The passenger car can be protected by installing a rear underrun protective device system on the truck's rear. This device is specifically designed against the crumple zone of the passenger crash into the device. Typically, the crumple zone of the passenger car is designed to absorb a lot of the impact energy. Therefore, passengers in the passenger car can be more secure. However, this bumper must meet the standard to prevent accidents and reduce injuries and fatalities effectively.

One of the standards in this accident and widely enforced worldwide is UN regulation No.58 rear underrun protective device. This standard concerns the cross-section high, the location of the protective beam, and the strength and deformation of each testing point on the protective beam surface. Actual tests or simulations can do the static test [2]. In the real test, the researcher [3] studied five models of RUPD attached to the trailer chassis using a quasi-static test, and the researcher [7] studied using sedan cars with a speed of 48 km/h crash into RUPD attached to the fixed barrier. It requires a suitable test site, the cost of prototyping, and the cost of testing, which is a considerable cost. In the simulation test, the RUPD was simulated using finite element analysis by the researcher [4] using LS-DYNA and the researcher [5-6] using RADIOSS. Consequently, finite element analysis can reduce the cost and time of testing, and it is also possible to repeat the test on many different designs. The researcher [4-6] mostly studied fixed RUPD and used several techniques example trial and error, Pareto optimization, and morphological analysis to design an optimal model depending on each researcher. The researcher [8] investigated the process to design foldable RUPD to solve the problem of trucks such as avoiding interference during tripping and being able to vary departure angle.

This study aims to design a foldable RUPD for a dump truck that passes UN Regulation No.58, is low weight, uses widely used local material, the local motor vehicle manufacturers can produce, avoid the material flowing out of the truck during the dumping process, and avoid the departure angle of the road. The given design constraint, proposed design guidelines, and the significant design parameters of the RUPD are investigated.

2. Requirements on rear underrun protective device and proposed design

2.1 Rear underrun protective device test standard

UN Regulation No.58. requirements are shown in figure 1 and are described as follows:

- The ground clearance from the underside of the RUPD to the ground shall not exceed 500 mm.
- The distance between the endpoint of the vehicle to the end of the RUPD shall not exceed 300 mm.
- The height of the cross member shall not be less than 120 mm.
- The length of the RUPD shall not be less than 100 mm on the outside of each wheel.
- The force requirement for tests using a surface must not exceed 250 mm in height, 200 mm in width, and 5 mm in radius at the vertical edge.
- Horizontal force of 100kN shall be applied to two places located 300 mm from the outer of each wheel in testing point P1.
- Horizontal force of 180kN shall be applied to two points at the symmetrical line of the RUPD to another point 700 – 1000 mm in testing points P2.
- Horizontal force of 100kN shall be applied at the center of the RUPD in testing points P3 [2].
- The deformation of each testing point shall not exceed 400 mm.

According to UN Regulation No.58, the minimum force is therefore a force that can properly stop a passenger car. In addition, the RUPD position in this regulation is designed for the crumple of a passenger car crash into the RUPD of a truck to prevent passengers from crashing directly into the rear of the truck. The crumple zone of passenger car and airbag systems can also absorb a lot of energy, resulting in much less shock from this event being transmitted to the passenger. Therefore, in this design, minimum force and geometry shape are used as criteria for designing RUPD.

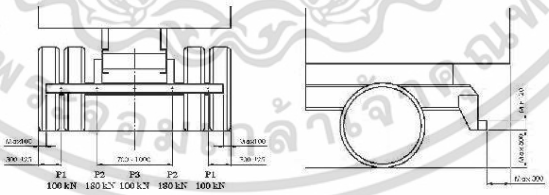

Figure 1. UN Regulation No.58 geometry and strength requirements [2].

2.2 RUPD constraints

The RUPD in this study is designed for a dump truck. Generally, the dump truck unloads materials from the truck body by lifting the truck bed using hydraulics. In this process, the materials flow out in a triangular pile at about 90 degrees, as shown in figure 2. The constraints for installing the rear underrun protective device are two problems. The first effect occurs when the material flows down onto the rear underrun protective device, causing damage. The second effect occurs when this car drives up very slope roads or departure angles such as piers, mountains, and truck weighbridge weighing scales. This rear underrun protective device may be scratched on the road surface, as shown in figure 2.

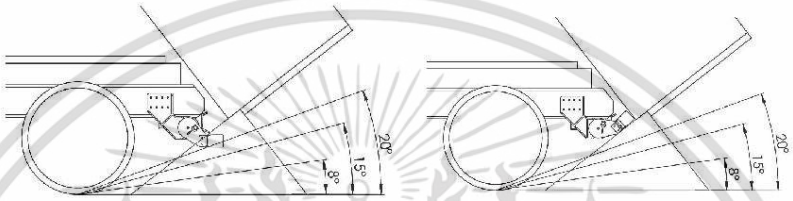

Figure 2. The constraints of installing RUPD on the dump truck.

3. Material and Method

3.1 Proposed Foldable RUPD design guideline

The main components of foldable RUPD are three groups, as shown in figure 3(a). The mounting brackets are used for mounting with chassis by using fasteners. The swing arms are used for folding the protective beam to avoid material slide and departure angle, and it can adjust the position by manual foldable function and lock work by the pin-lock system. The protective beam is used for protecting the underrun case.

The protective beam is designed following the geometry of UN Regulation No.58. The ground clearance in this design is 464 mm. not exceeding 500 mm. The distance between the endpoint of the vehicle to the end of the RUPD is 288 mm, not exceeding 300 mm. the protective beam cross-section uses a square tube 125 x 125 mm higher than 120 mm. the length of the protective beam is shorter than the distance of each outside wheel 100 mm. so that, the foldable RUPD meets the geometry of UN Regulation No.58 as shown in figure 3(b). Moreover, this rear underrun protective device solved RUPD constraints by designing to be the foldable RUPD to avoid material flow out and departure angle by fold up, as shown in figure 2.

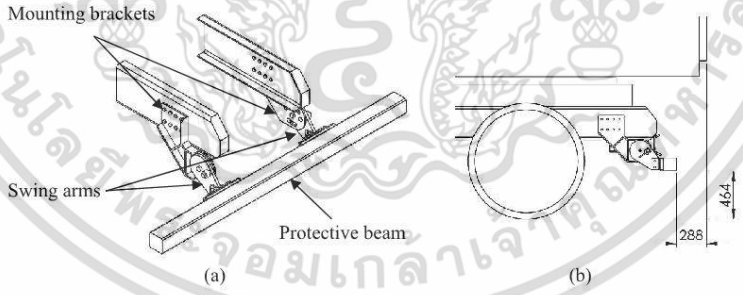

Figure 3. (a) The component of foldable RUPD, (b) Protective beam position.

The weight of foldable RUPD is an essential factor of the design, resulting in a reduced allowable payload and increased power consumption. Therefore, the lightweight design of the foldable RUPD while still meeting the standards and using locally available materials is the best choice.

The variables and significant parameters involved in this study affecting strength and weight are protective beam cross-sections, mounting brackets, and swingarms. There are three types of protective beam cross-sections: round tube OD 139.8 mm, square tube 125 x 125 mm, and round tube OD114.3 mm mixed with C-folded steel plates 4.5 mm with thicknesses of cross section 3.2mm, 4.5mm, and 6mm, as shown in figure 4(a). There are two mounting brackets, mounting brackets and mounting brackets without center ribs with thicknesses of 12 mm and 9 mm, as shown in figure 4 (b-c). The swingarm is available in thicknesses of 20 mm, 15 mm, and 12 mm, as shown in figure 4(d). The criteria for selecting the best foldable RUPD for this study are the lightest weight, strength close to the minimum strength requirement of UN Regulation No.58, and strength-to-weight ratio. The strength of the foldable RUPD is focused only on the maximum reaction force of each testing case.

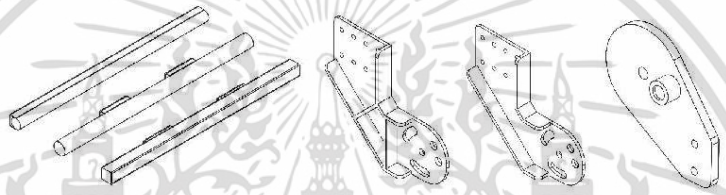

Figure 4. (a) protective beam type, (b) Mounting bracket, (c) Mounting bracket without center rib, (d) Swing arm.

3. Finite element analysis and material

The finite element meshing is done using Hypermesh. The analysis is performed with explicit non-linear dynamics in RADIOSS. Hyperview utilizes post-processing. The meshing in this study was mixed. Parts made from steel plates are defined as shell elements 24K elements. Part is made from thick steel plate combined with a machined process and all fasteners are represented as 3D solid elements 16K elements. Mesh size is defined as 10 mm for all deformable components. The total number of nodes and elements of the whole model is around 48k and 40k.

The constraint condition is defined by fixed chassis with all degrees of freedom. The loading condition is determined by the plate as rigid by the 1D rigid element, fixed all degrees of freedom except translation direction and vertical rotation at the center hole, and imposed displacement with a ramp function to solve in quasi-static testing as shown in figure 5(a). Nodes define the contact of each part to surfaces with the friction of 0.2. The reaction force between the loading plate and protective beam, the loading plate displacement, and the von-mises stress contour plot is determined to analyze the output.

The Materials used to design the foldable RUPD are chosen from the TIS standard that manufacturers can buy in Thailand, such as Carbon round steel tubes, carbon square steel tubes, and hot-rolled steel plates. The material properties of these materials are obtained by cutting a piece of material with a wire-cut machine to make specimens referring to the ASTM E8 standard. After that, the specimens are tested by a standard universal test machine. Finding the properties of these materials increases the confidence that they are consistent with those consumed from a general material store. To assign material properties for finite element analysis, all engineering stress-strain of materials are converted to true stress-strain and reduced data points to be smooth data curves, as shown in figure 5(b). After that, assign non-linear material properties data, young modulus, passion ratio, and material density in the M36 PLAS TAB module in RADIOSS.

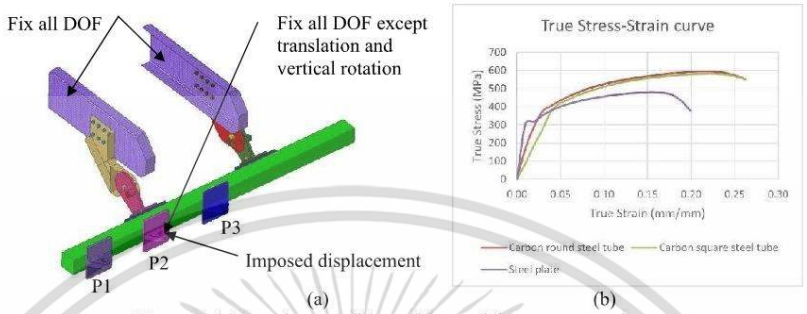

(a) (b)

Figure 5. (a)Boundary conditions, (b) material true stress-strain curve.

4. Result and discussion

Design case 1 uses the parameters according to table 1, which is the design using the maximum thickness of all materials. Design case 1 is used to study the behavior of each testing point. Testing point P1 had the most effect on the protective beam and a little on mounting brackets and swing arms, the maximum stress is 459 MPa. Testing point P2 had the most impact on mounting brackets and swing arms, the maximum stress is 393 MPa. Testing point P3 had the most effect on the center of the protective beam and a little on the pair of swing arms, the maximum stress is 393 MPa. as shown in figure 6(a-c).

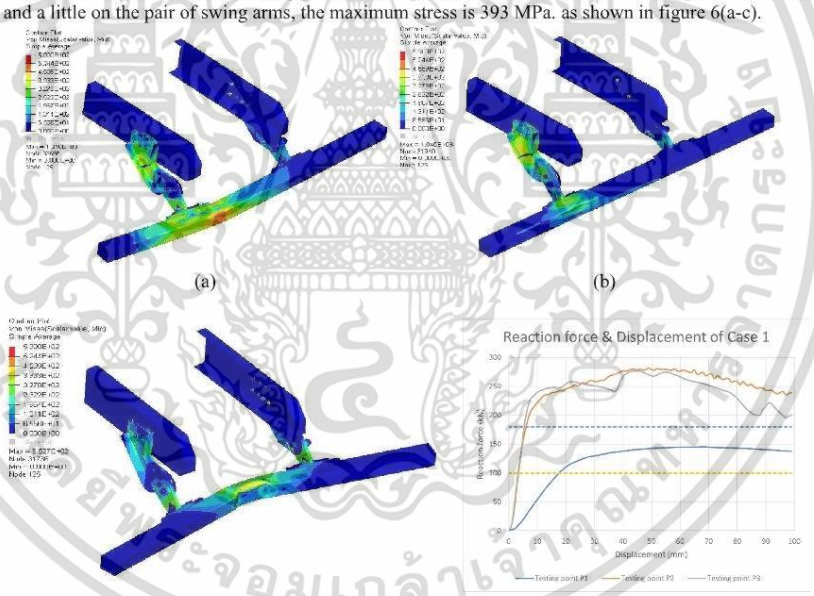

(a) (b)

(c) (d)

Figure 6. (a) Result of the case 1 testing point P1, (b) Result of the case 1 testing point P2, (c) Result of the case 1 testing point P3, (d) Reaction force & displacement of case 1

Table 1. Foldable RUPD design case 1 finite element analysis result.

case	Protective beam type	Mounting brackets thickness	Swing arms thickness	weight	Reaction force P1	Reaction force P2	Reaction force P3	UN R58 regulation
		mm	mm	kg	kN	kN	kN	
1	Square tube 125 x 125 t = 6 mm	12	20	121	145	282	277	pass

Figure 6(d) show the reaction force versus displacement of design case 1 at testing point P1, P2, and P3. The maximum reaction of testing points P1 and P3 as shown in table 1 is higher than the requirement of UN regulation No.58 of 100 kN and testing point P2 of 180 kN. The result of displacement at the maximum reaction force of all testing points does not exceed the requirement of UN regulation No.58 of 400 mm. The result showed that all testing points passed quite a lot. Therefore, Design case 1 is still overdesigned and the weight of design case 1 is 121 kg and still too heavy.

The tests in testing point P1 and testing point P3 most affected the protective beam. But the testing point P3 position can handle a much higher load than the regulation. Therefore, this study is not the focus at this point. The testing point P1 is used to select the appropriate protective beam cross-section type and thickness to achieve the lightest weight and pass UN Regulation No.58. Different protective beam cross-sections and tube thicknesses are used to design nine test cases, as shown in Table 2.

Table 2. Foldable RUPD design case 1-9 finite element analysis result.

Case	Protective beam type	Thickness	weight	Reaction Force P1	Reaction force P1 to weight ratio	UN Regulation No.58
		mm	kg	kN	kN/kg	
1	Square tube	6	121	145	1.20	pass
2	Round tube	6	119	139	1.17	pass
3	Round tube & C plate	6	125	118	0.94	pass
4	Square tube	4.5	109	106	0.98	pass
5	Round tube	4.5	108	102	0.95	pass
6	Round tube & C plate	4.5	116	107	0.92	pass
7	Square tube	3.2	98	71	0.72	not pass
8	Round tube	3.2	98	65	0.67	not pass
9	Round tube & C plate	3.2	108	89	0.82	not pass

Figures 7(a-c) show the contour plot of high stress on 3 types of protective beams. The maximum stress is on the front surface of the protective beam near the support point of about 459 MPa. Mostly, the maximum stress in this study is greater than the yield stress of materials but lower than the ultimate strength of materials and becomes nonlinear material behavior. Therefore, the deformation after these tests is permanent.

The result of displacement at the maximum reaction force of design cases 1-9 is around 50 – 60 mm which does not exceed the requirement as shown in Figures 7(d). As a result of Table 2, the tube thickness of 6 mm can withstand too much load, making it too heavy. But the tube thickness of 3.2 mm cannot resist the standard load. Therefore, the tube thickness of 4.5 mm is most suitable for this foldable RUPD design. The round tube mixed with a C-folded plate cross-section is the heaviest, followed by the square tube cross-section, and the round tube cross-section is the least weight. But when focusing

on the load-carrying capacity and the force-to-weight ratio, the round tube can withstand fewer loads than the square tube, and the square tube has more force-to-weight ratios than one. Therefore, the cross-section of a square tube protective beam with a thickness of 4.5 mm or design case 4 is the best choice.

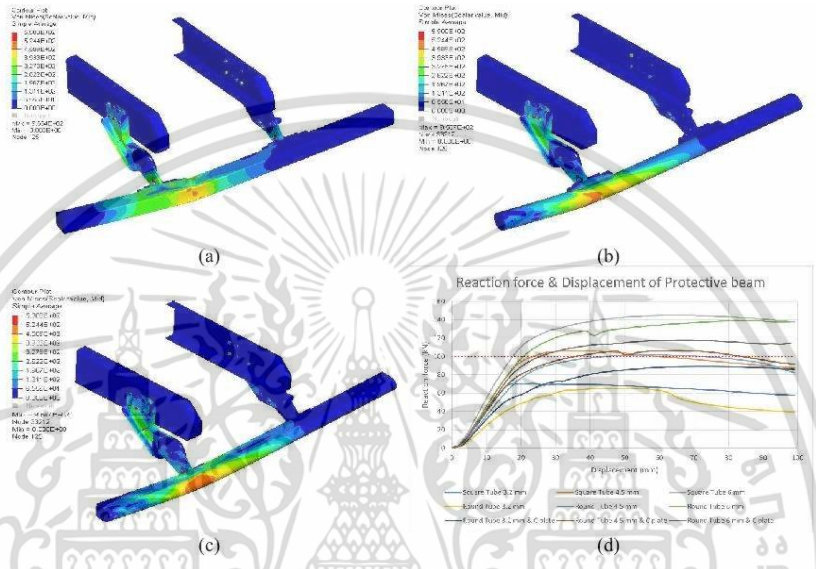

Figure 7. (a) Result of the case 4 testing point P1, (b) Result of the case 5 testing point P1, (c) Result of the case 6 testing point P1, (d) Reaction force & displacement of case 1-9

Based on the previous design, the weight of design case 4 is 109 kg and still heavy which can still be reduced further. The square tube of 4.5 mm thickness combined with mounting brackets, mounting brackets without center ribs, and swingarms of various thicknesses are used to be a significant parameter for study and select the best parameter for RUPD. Design cases 10-21 are designed. Testing points P1 and P2 are assigned to analyze this case.

As a result, in testing point P2, all the design cases a much higher than the minimum force requirement. Therefore, the Criteria to choose the best design case use total weight and the force-to-weight ratio of testing point P1 as deciding factors. Design case 15 consists of the protective beam square tube thickness of 4.5 mm combined with mounting brackets thickness of 9 mm and swingarm thickness of 15 mm. It is the most lightweight at 97 kg, passes the minimum force requirement of testing point P1 at 100 kN meets the minimum requirement of UN regulation No.58, and has the highest reaction force P1-to-weight ratio of 1.03, as shown in Table 3. Therefore, this case is the best parameter to use in foldable RUPD design.

The maximum stress is about 459 MPa from testing point P1 and about 393 MPa from testing point P2 on the front surface of the protective beam near the support of the swing arm and on the rear side of the mounting bracket as shown in figure 8(a-b). The maximum stress in design case 15 is higher than the yield stress leading to nonlinear material behavior. The deformation following these tests is permanent.

Table 3. Foldable RUPD design case 10-21 finite element analysis result.

case	Mounting brackets thickness: fully	Mounting brackets thickness: without center rib	Swing arms thickness	weight	Reaction force P1	Reaction force P2	Reaction force P1 to weight ratio	Reaction force P2 to weight ratio	UN Regulation No.58
	mm	mm	mm	kg	kN	kN	kN/kg	kN/kg	
10	12	-	20	109	106	254	0.98	2.33	Pass
11	9	-	20	101	102	215	1.01	2.13	Pass
12	-	12	20	106	103	244	0.97	2.30	Pass
13	-	9	20	98	98	202	0.99	2.06	not pass
14	12	-	15	105	103	253	0.98	2.41	Pass
15	9	-	15	97	100	215	1.03	2.22	pass
16	-	12	15	102	100	244	0.99	2.40	Pass
17	-	9	15	94	96	198	1.02	2.10	not pass
18	12	-	12	102	102	252	1.00	2.46	Pass
19	9	-	12	94	99	213	1.05	2.26	not pass
20	-	12	12	99	100	238	1.00	2.40	pass
21	-	9	12	92	96	194	1.04	2.11	not pass

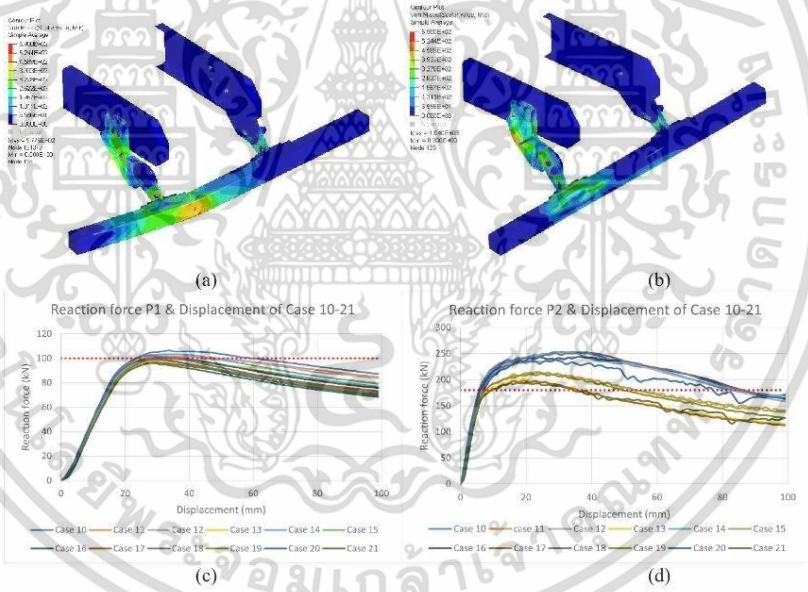

Figure 8. (a) Result of the case 15 testing point P1, (b) Result of the case 15 testing point P2, (c)Reaction force P1& displacement of case 10-21, (d)Reaction force P1& displacement of case 10-21

Displacements of design cases 10-21 at maximum reaction force at testing points P1 and P2 mostly are about 20 - 40 mm which does not exceed the requirement of UN regulation No.58 of 400 mm as shown in figure 8(c-d).

Comparing the weight of design case 15 of 97 kg to design case 1 which is the first design of 121 kg reduces the weight by around 20 percent. For future weight reductions, using high-strength materials can reduce the thickness of the material while maintaining the same strength as the original. Using that material comes at higher production costs, affecting the manufacturing company. But from the customer's point of view, the lighter the bumper, the lower the energy consumption and the higher the payload.

5. conclusion

The foldable RUPD is designed following UN Regulation No.58, considering the material available in Thailand. It is designed to be able to fold avoiding material flow out on RUPD and the required departure angle. The design criterion used to select the best significant parameters in this study is the lightest weight, has the greatest force-to-weight ratio, and passes the minimum requirement of UN Regulation No.58. Cross-section type and component thicknesses are used to be significant parameters in creating a design study in 21 cases to reduce the weight of foldable RUPD as much as possible and use Non-linear dynamic RADIOSS to analyze the problem. As a result, designs case 15 satisfied the minimum requirement of UN Regulation No.58 in all testing points, has the lightest weight, and has the highest force-to-weight ratio. Therefore, designs case 15 with a square tube protective beam of 4.5 mm, mounting brackets of 9 mm, and swing arm of 15 mm are optimal parameters for designing a foldable rear underrun protective device. It can reduce the weight of the first design case by around 20 percent or 24 kg. It could reduce the weight of the foldable RUPD more by using high-strength steel in the future. The process presented in this study is proposed as a future design guideline for the RUPD. In addition, the lightweight RUPD meets international standards that greatly enhance the road safety of other vehicles.

5. References

[1] World Health Organization 2018 *Global Status Report on Road Safety*.
[2] United Nations Economic Commission for Europe 2017 *UN Regulation No.58, Rear Underrun Protective Devices*.
[3] Brumbelow M L and O'Malley S P 2020 *Int. J. of Crashworthiness*.
[4] Joseph G, Shinde D, and Patil G 2013 *Int. J. of Engineering Research and Applications*.
[5] Balta B, Erk O, Solak H and Durakbasa N 2014 *SAE Int. J. Commer. Veh.*
[6] Lerspalungsanti S, Pitaksapsin N, Viriyarattanasak P, Wattanawongsakun P, and Suebnunta N 2021 *Int. J. of Automobile Engineering*.
[7] Rechnizer G, Powell C, Seyer K 2001 *Int. Conf. on Enhanced safety of Vehicle.*
[8] Gogte S, Vijendran N 2014 Conceptual Design and Development of Moveable rear underrun protection.

AUTHOR BIOGRAPHY

Author: Mr. Narongrit Suebnunta

Date of Birth: 25th Feb 1991

Place of Birth: Chiang Rai, Thailand

Undergraduate and Graduate Education:

Bachelor's degree in automotive engineering technology,
King Mongkut's University of Technology North Bangkok, Bangkok, 2013

Major: Automotive Engineering

Presentations and Publications:

[1] Narongrit Suebnunta, Sarawut Lerspalungsanti, Preechar Karin and Kazuaki Inaba "Analysis of Rear Underrun Protective Device Using Real-Life Test and Finite Element Techniques", 2022, Proceedings of the 11th International Conference on Material Science and Technology, 29-32 Aug 2022, Bangkok, Thailand

[2] Narongrit Suebnunta, Sarawut Lerspalungsanti, Preechar Karin and Kazuaki Inaba "New Design Guideline of Foldable Rear Underrun Protective Device for Heavy Good Vehicle Using Finite Element Analysis", 2022, The 12th TSME International Conference on Mechanical Engineering, 13-16 Dec 2022, Phuket, Thailand